Navigation of guidewires and catheters during interventional procedures

A computer-based simulation

Sharei Amarghan, Hoda

DOI
10.4233/uuid:078e8cff-d9bb-417a-b80e-8fcac19c3b9a

Publication date
2019

Document Version
Final published version

Citation (APA)
Sharei Amarghan, H. (2019). *Navigation of guidewires and catheters during interventional procedures: A computer-based simulation*. [Dissertation (TU Delft), Delft University of Technology]. https://doi.org/10.4233/uuid:078e8cff-d9bb-417a-b80e-8fcac19c3b9a

Important note
To cite this publication, please use the final published version (if applicable).
Please check the document version above.

Navigation of Guidewires and Catheters during Interventional Procedures

A Computer-based Simulation

Hoda Sharei Amarghan
Ph.D. Thesis

Navigation of Guidewires and Catheters during Interventional Procedures

A Computer-based Simulation

Dissertation

for the purpose of obtaining the degree of doctor

at Delft University of Technology

by the authority of the Rector Magnificus prof.dr.ir. T.H.J.J. van der Hagen
chair of the Board for Doctorates
to be defended publicly on
Wednesday 30 January 2019, at 10:00 o'clock

by

Hoda SHAREI AMARGHAN

Master of Science in Electrical Engineering, Shiraz University, Iran
Born in Mashhad, Iran

This dissertation has been approved by the promotors:

Prof. dr. J. Dankelman
Dr. J.J. van den Dobbelsteen

Composition of the doctoral committee:

Rector Magnificus,	Chairperson
Prof. dr. J. Dankelman,	Delft University of Technology, promotor
Dr. J.J. van den Dobbelsteen,	Delft University of Technology, promotor

Independent members:

Prof. dr. A.G.J.M. van Leeuwen,	Amsterdam University
Prof. dr.ir. R. Dekker,	Delft University of Technology, EWI
Prof.dr.ir. J.L. Herder,	Delft University of Technology, 3ME
Dr. A. Moelker,	Erasmus MC
Dr.ir. T.H. van Walsum,	Erasmus MC

Reserve member:

Prof.dr.ir. P. Breedveld,	Delft university of technology, 3ME

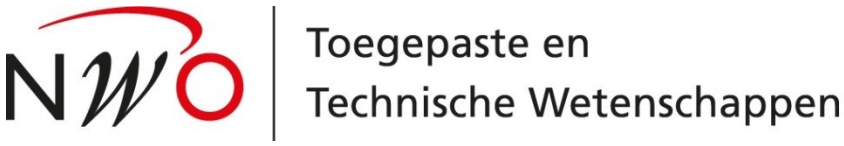

This work is part of the research program CONNECT project (Grant Nr. 12705) within the research program interactive Multi-Interventional Tools (iMIT), which is supported by the Netherlands Organization for Scientific Research (NWO).

Printed by: Gildeprint - The Netherlands

Summary

Endovascular interventions include a variety of techniques, chiefly involving guidewires and catheters, that give access to the vascular system through small incisions. It is imperative to reach the place of interest quickly and safely. By considering the fact that the composition of guidewires and catheters differ (e.g., in material, diameter, length, tip shape, stiffness, and coating), each one shows a different behavior based on its structure, and therefore the choice of instruments becomes challenging. Currently, the choice of the instruments in each procedure is often based solely on a specialist's experience, which is not sufficient and does not always result in a successful procedure. Therefore, in this thesis, we focus on the performance of the guidewires and catheters with considering their structure.

Since the newly developed instruments with improved capacity for measuring physical quantities, such as flow, pressure, vessel diameter, and arterial wall thickness, are becoming more popular, this thesis starts with reviewing the available proximal connectors of such guidewires. The connector plays an important role in these instruments as it relays the measured data from the distal side of the guidewire, which is placed inside the body, to the monitoring devices. They are classified according to the types of connections found including physical (e.g. electrical, optical, magnetic.), wireless and combinations of them.

Next, we focused on pre-intervention planning, specifically, the selection of the guidewires and catheter. Therefore, by considering different compositions of each instrument in the distal side, we concentrated on the performance of the guidewires and catheters and their behavior inside the vascular system. Given that using computer models has become increasingly popular to investigate the behavior of these instruments, we performed an extensive literature review and surveyed different techniques used for instrument modelling and identified their strengths and weaknesses. The results show that the main techniques used in the modelling are FEM, MSM, and Rigid Multibody Links. FEM and MSM are not suitable for modelling a rigid object, such as the guidewire and catheter, due to the complexity and high computational effort. On the contrary, the Rigid Multibody Links technique has a simple structure, which makes it easy to understand and interpret the results. Additionally, this method is relatively faster than the first two methods and can be used for real time applications.

We used the multibody approach for modelling the motion of these instruments. A computer model was developed, to evaluate the performance of different instruments for a specific vasculature geometry. In particular, we sought to predict the behavior of guidewires and catheters by considering the mechanical properties of these instruments and of the relevant vasculature. This information plays an even more decisive role for the newly developed instruments, which are constantly coming to the market and their performance is not fully known even to the experienced specialists.

In our model, first, the effect of bending stiffness of the instrument and of the friction between the instrument and vasculature on its behavior were investigated by modelling the

motion of guidewires in 2D space while only a translational motion was applied. We validated the model with actual movement of different guidewires in a phantom model. An average error of 0.56*mm* and 0.87*mm* for a flexible and a stiff guidewire, respectively, were calculated.

Then, as guidewires and catheters are always used together, we added a catheter to the model to mimic the way they interact. Moreover, we extended our simulation to a 3D version and had not only a translation motion but also a rotation motion applied to the proximal side to propagate the instrument. The sensitivity of the model to different factors was examined. The results show that the applied forces increase when the friction increases; on the other hand, a higher friction causes less fluctuation of the instrument's tip. Therefore, the friction coefficient needs to be optimized to strike a balance between the increase in the applied forces and the performance of the instrument. Moreover, investigating instruments of different bending stiffness show that the higher flexibility of the tip causes more contact points with the artery's wall. This can be explained by the fact that the flexible tip deflects easier than the stiff one, and thus, it needs less force to navigate.

As we implemented a discretized model of the instrument, the total number of segments (n) to define the length of the instrument in the simulation model had a significant effect on the behavior and the computation time; a lower number of segments results into bigger error. On the other hand, increasing the number above a certain threshold does not change the behavior anymore, but the computation time increases.

In the current model, we focused on the modelling of the instrument itself, and the radii and centerline data of the vasculatures were used as geometry information. Therefore, in future studies, a dynamic centerline instead of a static one has to be considered.

As explained above, during our research, we endeavored to evaluate the simulation results by comparing them with experimental data, obtained from phantom models. Therefore, in the appendix, we presented an overview of phantoms we developed. The phantoms were used to validate our simulation model. The first validation experiment is done on a simple 2D phantom model which includes branches with diameters between 2 and 8 mm, and bifurcation angels between 60 and 120 degree. The results show that the mean error between simulated trajectories and validation experiments for different instruments was smaller than 1*mm*. Then, considering the used design criteria, e.g., similar mechanical properties to vascular walls and being transparent for the purpose of video tracking, a phantom made of a PVA-H and DSMO mixture was chosen. The data of the right coronary artery (RCA) of a real patient served as an example of vascular geometry. Despite of having a well-developed phantom, the experimental set-up and tracking method need improvements in order to measure the exact error between the simulation and validation experiment.

It is foreseen that pre-interventional application of the simulation model will provide information about the possible taken trajectory based on the instrument tip angle, stiffness and the coefficient of friction of the instrument, as well as based on the elasticity and friction coefficient of the vasculature walls and the vascular geometry. Additionally, the amount of

applied forces to the vascular wall will be predicted in order to avoid rupturing the vascular walls. These information will give insight to specialists in the expected behavior of the instruments and help them to select a proper instrument in each specific vasculature geometry, which may increase the success rate of the procedure.

The developed model is generic and allows for evaluation of a large variety of instruments and vascular geometries. Therefore, despite of the limited variety of vasculatures and instruments used in this study, the model can easily be adopted to other ones.

Samenvatting

Endovasculaire interventies omvatten een verscheidenheid aan technieken, waarbij voornamelijk gebruik wordt gemaakt van voerdraden en katheters, die via kleine incisies toegang geven tot het vasculaire systeem. Het is noodzakelijk om het doelgebied snel en veilig te kunnen bereiken. In beschouwing nemend dat de samenstelling van voerdraden en katheters verschilt (bijvoorbeeld qua materiaal, diameter, lengte, vorm van de punt, stijfheid en coating), vertoont elk instrument een ander gedrag, afhankelijk van de structuur, hetgeen de instrumentkeuze bemoeilijkt. Momenteel is de keuze van de instrumenten voor elke procedure alleen gebaseerd op de ervaring van een specialist, hetgeen niet altijd resulteert in een succesvolle procedure. In dit proefschrift focussen we daarom op de prestaties van de voerdraden en katheters, hun samenstelling in beschouwing nemend.

Nieuw ontwikkelde instrumenten met verbeterde mogelijkheden voor het meten van fysieke grootheden, zoals stroming, druk, vatdiameter en wanddikte van de slagader, worden steeds populairder. De connector van deze instrumenten speelt een belangrijke rol, omdat deze de gemeten gegevens van de distale zijde van de voerdraad, die in het lichaam wordt geplaatst, doorstuurt naar het bewakingsapparaat. Daarom zijn we begonnen met het beoordelen van de beschikbare proximale connectoren van voerdraden; de connectoren zijn geclassificeerd op basis van verbindingstype, zoals fysieke connectie (bijvoorbeeld elektrisch, optisch, magnetisch), draadloze connectie of combinaties daarvan.

Na deze literatuurstudie hebben we ons gericht op pre-interventieplanning, met name de selectie van de voerdraad en de katheter. Door de verschillen in samenstelling van elk instrument aan de distale zijde te analyseren, zijn we de prestaties van de voerdraden en katheters en hun gedrag in het vaatstelsel gaan voorspellen. Omdat het gebruik van computermodellen steeds gangbaarder is geworden om het gedrag van deze instrumenten op een efficiënte wijze te onderzoeken, hebben we een uitgebreide literatuurstudie uitgevoerd. We hebben verschillende technieken voor instrumentmodellering bestudeerd en hun sterke en zwakke punten geïdentificeerd. De resultaten laten zien dat FEM, MSM en Rigid Multibody Links de belangrijkste technieken zijn die voor modellering gebruikt worden. FEM en MSM zijn niet geschikt voor het modelleren van een stijf object, zoals de voerdraad en katheter, vanwege de complexiteit en hoge rekenkracht. De Rigid Multibody Links-techniek daarentegen heeft een eenvoudige structuur, waardoor het gemakkelijk is om de resultaten te begrijpen en te interpreteren. Bovendien is deze methode relatief sneller dan de eerste twee methoden en kan deze gebruikt worden voor real-time toepassingen.

We hebben de multibody-benadering gebruikt om de beweging van voerdraden en katheters te modelleren. Er is een computermodel ontwikkeld om de prestaties van verschillende instrumenten voor een specifieke geometrie te evalueren. In het bijzonder hebben we getracht het gedrag van voerdraden en katheters ,voorspeld door de mechanische eigenschappen van deze instrumenten, en de relevante delen van het vaatstelsel in beschouwing te nemen. De informatie over de prestaties van de instrumenten speelt vooral een bepalende rol bij pas ontwikkelde instrumenten, die voortdurend naar de markt worden

gebracht, waarvan het gedrag en de prestaties nog niet bekend zijn, zelfs niet bij ervaren specialisten.

In ons model is allereerst het effect van de buigingsstijfheid van het instrument en de wrijving tussen het instrument en de vaatwand op het gedrag onderzocht door de beweging van de voerdraden in twee dimensies te bestuderen, waarbij enkel een translatiebeweging wordt uitgeoefend. We hebben het model gevalideerd met experimenten waarbij verschillende voerdraden in een fantoom model zijn gemaneuvreerd. Als gemiddelde fout zijn 0.56 *mm* en 0.87 *mm* voor respectievelijk flexibele en stijve voerdraden gevonden.

Omdat voerdraden en katheters altijd samen worden gebruikt, hebben we daarna een katheter aan het model toegevoegd om te simuleren hoe deze elkaar beïnvloeden. Bovendien hebben we onze simulatie uitgebreid naar een 3D-versie waarin niet enkel de translatiebeweging is meegenomen, maar waarbij ook een rotatiebeweging wordt uitgeoefend op de proximale zijde om de voerdraad voort te bewegen.

De gevoeligheid van het model is onderzocht onder verschillende omstandigheden. Uit de resultaten blijkt dat indien de wrijving toeneemt, de opgelegde krachten ook toenemen. Echter, een toegenomen wrijvingskracht resulteert ook in een kleinere fluctuatie van de tip. De frictiecoëfficiënt zal daarom moeten worden geoptimaliseerd zodat er een balans ontstaat tussen de opgelegde kracht en de prestatie van het instrument. Daarnaast toont het onderzoek, waarbij instrumenten met verschillende buigstijfheden werden gebruikt, aan dat een grotere flexibiliteit van de tip resulteert in meer frequent contact met de slagaderwand. Dit kan worden verklaard door het feit dat een flexibele tip gemakkelijker buigt. Hierdoor is het mogelijk te navigeren onder kleine krachten.

Het totale aantal segmenten (n) en daarmee de lengte van het instrument in het simulatie model, heeft een significant effect op de het gedrag en de berekeningstijd van het model, omdat er gebruik is gemaakt van een discreet model. Een kleiner aantal segmenten resulteert vaker in grotere fouten. Echter, het gedrag van het model blijft onveranderd na een zekere drempelwaarde van het aantal segmenten. Meer segmenten resulteert slechts in hogere berekeningstijden.

In het huidige model hebben we ons gericht op het modelleren van het instrument op zich, waarbij de geometrische informatie werd behaald uit de radii en middellijnen van vatenstelsels. In toekomstige studies zou men kunnen overwegen om in plaats van statische, dynamische middellijnen te gebruiken.

Zoals hierboven beschreven, hebben we in dit onderzoek getracht de simulatieresultaten te evalueren doormiddel van een vergelijking met experimentele gegevens. Hiervoor hebben wij gebruik gemaakt van fantoommodellen. In de bijlage vindt men een overzicht van de ontwikkelde fantoommodellen. Het eerste validatie-experiment werd uitgevoerd met behulp van een eenvoudig 2D-fantoommodel met aftakkingen tussen de 2 en 8mm onder hoeken van 60 tot 120 graden. Uit de resultaten blijkt dat de gemiddelde fout tussen de gesimuleerde trajecten en de validatie-experimenten kleiner was dan 1 mm. Tijdens een tweede

experiment werd gebruik gemaakt van een fantoommodel, bestaande uit een mix van PVA-H en DSMO, dat voldoet aan de ontwerpcriteria, zoals de overeenkomende mechanische eigenschappen en de transparantie ter gebruik van videovalidatie. Het model werd ontwikkeld met behulp van de geometrie van de rechter kransslagader (RCA) van een echte patiënt. Hoewel het fantoommodel goed is ontwikkeld, dienen de experimentele set-up en trackingmethode te worden verbeterd, zodat de verschillen tussen het simulatie- en validatie-experiment nauwkeurig kunnen worden gemeten.

Het simulatiemodel kan dienen als een pre-interventionele informatiebron over het mogelijke traject van het instrument op basis van de hoek van de tip, de stijfheid en de wrijvingscoëfficiënt van het instrument, evenals de elasticiteit en wrijvingscoëfficiënt van de wanden van het vaatstelsel en de vasculaire geometrie. Bovendien zal de hoeveelheid uitgeoefende kracht op de vaatwand kunnen worden voorspeld ter voorkoming van scheuren in vaatwanden. Deze informatie zal specialisten inzicht kunnen geven in het verwachte gedrag van verschillende instrumenten en met kennis van de geometrie van de vaten hen kunnen ondersteunen tijdens het selecteren van het juiste instrument. De kans op slagen van de procedure kan hierdoor worden vergroot.

Het ontwikkelde model is generiek en kan worden gebruikt ter evaluatie van een verscheidenheid aan instrumenten en vasculaire geometrieën. Om deze reden kan het model, ondanks dat in deze studie slechts een beperkte variëteit aan geometrieën en instrumenten is gebruikt, gemakkelijk op andere situaties worden toegepast.

1. Introduction

1.1 Endovascular interventions

Vascular disease is one of the leading causes of morbidity and mortality worldwide [1-2]. Some examples of vascular disease include heart attacks, strokes, lower extremity occlusive disease, and aneurysmal disease; atherosclerosis, which is hardening and narrowing of the vasculatures, is the main cause of these diseases [2]. Endovascular interventions, which have evolved over the last several decades to diagnose and treat vascular diseases, include a variety of techniques that give access to the vascular system through small incisions. This access is mainly via guidewires and catheters, which are flexible and elongated instruments (~1 to 2 meter) with small diameters (a few millimeters).

Endovascular intervention, compared to conventional open vascular surgery, is of great interest because it offers several advantages, including decreased surgical trauma and accelerated recovery due to small incisions [3-5]. However, it also imposes new challenges on the specialists. For example, they lose the direct access and visual feedback, and instead their access is via long instruments (i.e., guidewires and catheters) from outside the body; they have to manipulate the instruments by applying a translation and rotation motion at their proximal side.

As the instrument traverses inside the vascular system, its structure and mechanical properties play an important role in accessing the desired location. For this reason, there are a wide variety of guidewires and catheters available in the market which have different structures and mechanical properties (see Figure 1, which shows the different catheters made by only one manufacturer). Therefore, another complicating factor of endovascular interventions is that a high degree of expertise is required to select a proper instrument for a particular blood vessel geometry. Considering the fact that in every intervention, frequent guidewire or catheter exchanges are required to gain access [6], having additional exchanges due to a wrong choice makes the procedures even more expensive, both in cost and time. Moreover, the comfort of the patient will also decrease.

Some of the newly designed guidewires and catheters are equipped with sensors at the distal tip to measure different physical quantities (e.g., flow and pressure) [7]. Having these information might reduce the number of wire exchanges. However, considering the small diameter of guidewires and catheters (less than a few millimeters), transmitting the data from the sensor at the distal tip to an external device via a connector at the proximal tip of the instrument is a challenging issue. In this thesis, we presented a literature study and provide essential input for the development of novel solutions to have proper communication from the proximal side of a guidewire to the external device.

Recently, using computer models to predict the behavior of guidewires and catheters has become increasingly popular [8-10]. Although these models are mainly used for training purposes [11-15], they can also be developed in other areas such as pre-intervention planning and designing new instruments [10]. In this thesis, we focus on pre-intervention planning; specifically, we develop a computer model to evaluate the performance of

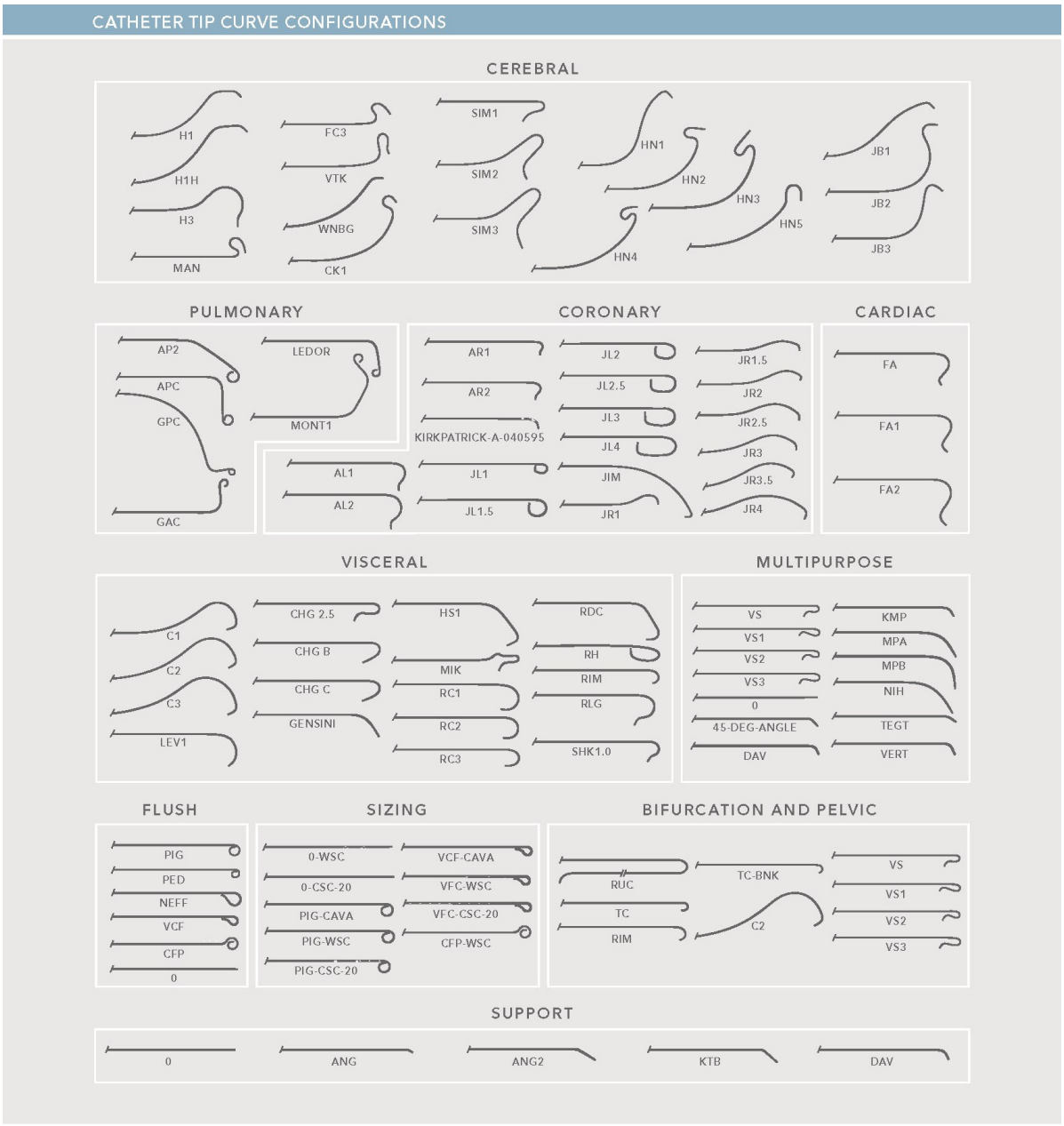

Figure 1: Catheters for different vessel anatomy (Permission for use granted by Cook Medical, Bloomington, Indiana)

different instruments for a particular blood vessel structures. Until now, selecting the instrument has often been based on a specialist's experience or the experience of his or her superior, which does not always result in a successful procedure [16]. With our developed model, we aim to predict the performance of the instrument prior to the procedure by evaluating its probable trajectory inside the vasculature and the amount of force applied to the vasculature's wall. These information plays even more decisive role for the newly developed instruments, which are constantly coming to the market and their performance is not fully known even to the experienced specialists.

1.2 Research questions and approach

In this thesis, we seek to predict the behavior of guidewires and catheters by considering the mechanical properties of these instruments and of the relevant vasculature. Therefore, we will develop a 3D multibody model that simulates the propagation of the instrument inside the vascular system. We endeavor to make the model generic in a way that allows for evaluation of a large variety instruments and vascular geometries. The results will lend insight to the specialists and help them in selecting a proper instrument in each specific case, thus, the success rate of the procedure may increase.

1.3 Outline of this thesis

The goal of this thesis is to present the developed model and investigate its accuracy and applicability. Each chapter is based on published or submitted articles and is self-contained. Therefore, there will be some overlap between chapters. The thesis is organized as follows:

Chapter 2: Guidewires consist of multiple components (core, distal tip and outer covering), and variation in each component influences the properties and performance of the guidewire (Figure 2). In guidewires with a sensor (e.g., flow or pressure) on the distal tip, the proximal connector is also an important part. Although it does not influence the mechanical properties, it is very important to ensure a secure signal transmission. Therefore, in the first part of this thesis, we review the available proximal connectors for guidewires and possible ways of relaying data from the distal side of the guidewire, which is placed inside the body, to the monitoring devices.

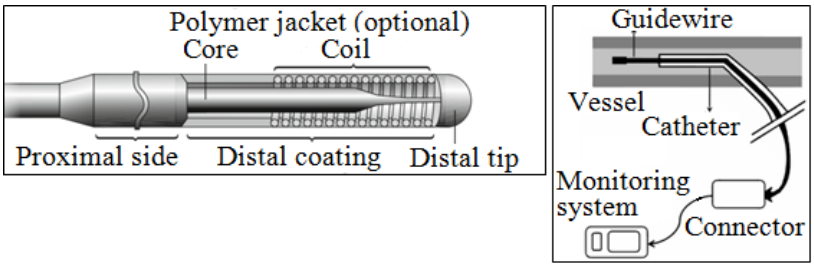

(a) (b)

Figure 2: Guidewire structure: a) guidewire components at the distal tip (adopted from [17]), b)guidewire with a sensor at the distal tip and a connector at the proximal tip

Chapter 3: In this chapter, we concentrate on the main body of the guidewires and catheters, along with their performance. In order to investigate the behavior of these instruments inside the vascular system, different modelling techniques are presented in the literature. Therefore, we first explain the purposes of guidewire and catheter modelling. We then survey different approaches used for instrument modelling and identify their strengths and weaknesses. Moreover, we study the important factors that affect the interaction between the instrument and the vascular wall. Finally, we give recommendations about what methods for modelling would be most appropriate for each domain purpose.

Chapter 4: In Chapter 4, we introduce a 2D multibody model of a guidewire traversing a simple vascular geometry. We consider the guidewire as a set of small rigid segments connected to each other by revolute joints. These joints have one degree of freedom to allow rotation. Linear torsional springs and dampers are applied in each joint to account for the elastic properties of the guidewire. To evaluate the performance of the model, we measure these elastic properties for two commercially available guidewires (Hi-Torque Balance Middleweight Universal II sold by Abbot and Amplatz Super Stiff sold by Boston Scientific) and use them in the model. We investigate the effect of the bending stiffness of the guidewire and of the friction between guidewire and vasculature on its behavior. Finally, we validate the results with actual movement of the guidewires in a simple phantom model and calculate the error to examine the accuracy of the model.

Chapter 5: In a continuation of the previous chapter, we extend the 2D developed model to a 3D model. Moreover, we add a catheter to the model, as guidewires and catheters are always used together; in this way, the applicability of the model is increased. The ways in which the instruments interact with each other and with the vascular wall are considered. The right coronary artery (RCA) is implemented as an example of vascular geometry, although our model is generic and we can readily adopt the simulation to a new geometry. As in the previous chapter, we measure the elastic properties of the real guidewires and one multi-purpose catheter to be used in the model.

Chapter 6: In the previous chapter, we have developed a computer model to investigate the behavior of guidewires and catheters by considering the mechanical properties of the instrument, and of the vasculature such as bending stiffness and friction. In this chapter, we use the developed model to investigate the effect of geometry properties such as the tip angle of guidewires, and the narrowed cross section of the arteries, due to vascular disease, on the behavior of the guidewire.

Appendix: In this thesis, the trajectory of guidewires and catheters were simulated and the amount of applied forces to the vascular walls were estimated. During our research, we endeavored to evaluate the simulation results by comparing them with experimental data, obtained from phantom models. Therefore, the objective of this appendix is to develop phantoms which can be used in our validation experiments. We will suggest an experimental set-up and tracking method which can be used to analyze the trajectory, and the amount of applied forces of the instruments inside the phantom models. The results of these experiments can be used to validate the accuracy of our developed model.

References

1. World Health Organization — Who | The top 10 causes of death, http://www.who.int/mediacentre/factsheets/fs310/en/ [Accessed: Nov-2017].

2. Fogarty, Thomas J., and Rodney A. White, eds. Peripheral endovascular interventions. New York: Springer, 2010.

3. Dankelman, Jenny, Cornelis A. Grimbergen, and Henk G. Stassen, eds. Engineering for patient safety: issues in minimally invasive procedures. CRC Press, 2004.

4. Kaufman, John A., and Michael J. Lee. Vascular and interventional radiology. Elsevier Health Sciences, 2013.

5. Aklog, Lishan, David H. Adams, Gregory S. Couper, Reuben Gobezie, Samuel Sears, and Lawrence H. Cohn. "Techniques and results of direct-access minimally invasive mitral valve surgery: a paradigm for the future." The Journal of thoracic and cardiovascular surgery 116, no. 5 (1998): 705-715.

6. Peter A. Schneider, ”Endovascular Skills: Guidewire and Catheter Skills for Endovascular Surgery”, Third Edition, Ch. 5, ISBN: 1-4200-6937-3 (Hardcover), 2008.

7. Sharei, Hoda, Ronald Stoute, John J. van den Dobbelsteen, Maria Siebes, and Jenny Dankelman. "Data Communication Pathway for Sensing Guidewire at Proximal Side: A Review." Journal of Medical Devices 11, no. 2 (2017): 024501.

8. Badash, Ido, Karen Burtt, Carlos A. Solorzano, and Joseph N. Carey. "Innovations in surgery simulation: a review of past, current and future techniques." Annals of Translational Medicine 4, no. 23 (2016).

9. Kunkler, Kevin. "The role of medical simulation: an overview." The International Journal of Medical Robotics and Computer Assisted Surgery 2, no. 3 (2006): 203-210.

10. Sharei, Hoda, Tanja Alderliesten, John J. van den Dobbelsteen, and Jenny Dankelman. "Navigation of guidewires and catheters in the body during intervention procedures: a review of computer-based models." Journal of Medical Imaging 5, no. 1 (2018): 010902.

11. M. K. Konings, E. B. van de Kraats, T. Alderliesten, W. J. Niessen, “Analytical guide wire motion algorithm for simulation of endovascular interventions”, Medical and Biological Engineering and Computing 2003, Volume 41, Issue 6, pp 689-700.

12. Cotin, Stephane, S. Dawson, Dwight Meglan, D. Shaffer, M. Ferrell, R. Bardsley, F. Morgan et al. "ICTS, an interventional cardiology training system." Studies in health technology and informatics (2000): 59-65.

13. Ursino, Michele, Joseph L. Tasto, Binh H. Nguyen, Richard Cunningham, and Gregory L. Merril. "CathSim: an intravascular catheterization simulator on a PC." Studies in health technology and informatics 62 (1998): 360-366.

14. Rebholz, Philipp, Carsten Bienek, Dzmitry Stsepankou, and Jürgen Hesser. "CathI–training system for PTCA. A step closer to reality." In Medical Simulation, pp. 249-255.

Springer Berlin Heidelberg, 2004.

15. Wu, Xunlei, Vincent Pegoraro, Vincent Luboz, Paul F. Neumann, Ryan Bardsley, Steven Dawson, and Stéphane Cotin. "New approaches to computer-based interventional neuroradiology training." Studies in health technology and informatics 111 (2005): 602-607.

16. M Al-Moghairi, Abdulrahman, and Hussein S Al-Amri. "Management of retained intervention guide-wire: a literature review." Current cardiology reviews 9, no. 3 (2013): 260-266.

17. C. A Thompson,. Textbook of cardiovascular intervention. Springer (2016): 92-93.

2. Data Communication Pathway for Sensing Guidewires

Hoda Sharei, Ronald Stoute, John J van den Dobbelsteen, Maria Siebes, Jenny Dankelman

Published in the Journal of Medical Devices, ASME (2017)

Background: As the connection at the proximal tip plays an important role for sensing guidewires, we compared various sensing guidewires with regard to their proximal connectors. The strengths and weaknesses of each are discussed and recommendations for future development are provided.

Method: A literature search limited to the English language for the time period from the 1960s to the 2010s has been performed on the USPTO database, Espacenet and Web of Science. The results have been categorized on the basis of the connector design.

Results: A comprehensive overview and classification of proximal connectors for sensing guidewires used for cardiovascular interventions is presented. The classification is based on both the type of connector (fixed or removable) and the type of connection (physical, wireless, or a combination).

Conclusion: Considering the complexity of the currently prototyped and tested connectors, future connector development will necessitate an easy and cost effective manufacturing process that can ensure safe and robust connections.

2.1 Introduction

A guidewire is a long, thin and flexible wire used to introduce and position interventional devices (e.g., catheter, stent) during intravascular procedures [1]. Fig. 1 gives a schematic overview of guidewire and catheter placement in a vessel; the guidewire tracks through the vessel to access the lesion, which is usually guided under fluoroscopy (real time x-ray imaging). When the distal[1] tip of the guidewire has crossed the lesion atraumatically, it steers into or away from side branches and provides device delivery support [2–4].

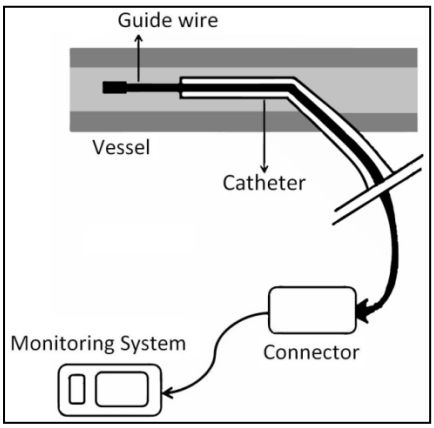

Figure 3: Guidewire and catheter placement in a vessel.

In the current trend the guidewire is not limited to lead other instruments, but can also be used to measure physical quantities such as flow, pressure, vessel diameter and arterial wall thickness. Moreover it can even be used to visualize the place of interest [4–13]. To detect changes in the physical quantities, major efforts have been made to integrate sensors at the distal tip of the guidewire. The measured data are sent via wires (copper or optical fibers) through the guidewire to the proximal tip, and subsequently via a connector to an external device [5, 6, 7].

The goal of this study is to review the state-of-the-art in relation to existing guidewires with a focus on their connectors, and is motivated by the important role of the connection in the proximal tip in sensing guidewires. This includes both the currently employed connectors in clinical practice and the patented literature. The strengths and weaknesses of each are discussed and recommendations for future development are provided.

2.2 Review method

A literature search was performed on the USPTO, Espacenet and Web of Science database which was limited to the English language for the time span from the 1960s to the 2010s. Overall, more than 50 patents and scientific papers were reviewed and categorized on the basis of the connector design. All databases were explored using the

[1] The term distal refers to the tip of the guidewire situated away from the user (inside the vessel) and the term proximal refers to the tip of the guidewire situated closest to the user (outside the body).

following keywords for all fields: sensor, guidewire, catheter, proximal side, intervention, connector, optical fiber, electrical contacts, magnetic connector, hybrid connector. The search terms were connected with either "AND" or "OR". For the sake of coherence, the patent search results constitute the most recent up-to-date one by a given patent assignee.

2.3 Results

2.3.1 Design requirements for the male/female connector on the proximal side of a guidewire

A sensing guidewire requires one or more cables for signal transmission purposes. These serve for either carrying the signals of the sensor at the distal tip or to distribute the power. Thus, the guidewire must be connected at the proximal tip to an external device via a connector to transmit the signals. In this section, we discuss some of the important features to be taken into account when designing a connector.

Intravascular procedures often result in the deposit of some blood or other bodily fluids on the guidewire. Therefore, minimizing the entering of fluids or other contamination into the female[2] connector is the first challenge to be addressed [14]. One approach is to use a wiper [15] or a seal [14] at the opening. A hydrophobic surface makes the guidewire itself more compatible in such an environment [16].

A connection is either fixed or removable. In a fixed configuration, both male and female parts need to be adapted to allow the catheter or other medical devices to be placed over them. This type of connection might limit the exchange or removal of the other instruments. In a removable connector the male part is limited to the size of the guidewire whereas the female part has no restrictions. One of the advantages of a removable connector is its allowance for device exchange without the need of removing the guidewire from the patient [15, 17]. However, the frequent connecting and disconnecting requires a quick disconnect design.

To prevent any torsion in the guidewire, a rotation free connector with respect to the mated connector can be employed [4, 15-17].

A locking mechanism should be applied to avoid any kind of axial or rotational motion of the guidewire relative to the connector. A connection detector can detect simultaneously whether an unintentional disconnection of the guidewire from the interface circuit has occurred [18].

The female connector is either disposable or reusable. In case of reusable, by making the female part of the connector relatively more complicated than the male part, the price of the male part reduces whereas the manufacturing costs of a reusable female connector raises. The disposal of the male part together with the guidewire and the frequent use of the female connector result in a decrease of the total price. However, a reusable female

2 In this review, we refer to the proximal tip of the guidewire as the "male connector" and to the receptacle as the "female connector".

connector should be designed to facilitate sterilization, and to prevent infection a reliable cleaning process is necessary before the subsequent use [19-20].

Regarding the power supply, it can be either a battery placed in the female part or an external source. The former is an essential requirement when a wireless connection is employed. In such cases, the sensor loses its physical connection for powering which results in a demand of a battery holder in the female part [9, 10].

2.3.2 Existing guidewires and their connectors

Sensing guidewires differentiate on various aspects. One can think of varying the sensor type at the distal tip, changing the communication manner of the distal tip and the proximal tip, or employing a different manufacturing process for the proximal tip as a male connector. Diverse guidewires are manufactured by a number of companies employing in-house connectors on the proximal side. Some of these are listed here.

❖ **Volcano Corporation [21]**

- Flowire Doppler Guidewire (Fig. 3.a): This guidewire which measures flow velocity is equipped with a Doppler transducer tip. At the proximal tip, as a male connector, there are three ring-contacts to provide electrical connection (Fig. 2.a and 2.b). The female counterpart contains three conductive members as well. The ring-contacts transfer the signals to the matching conductive members inside the female connector whenever it meets its female counterpart.
- Combowire XT Guidewire (Fig. 3.b): This guidewire measures simultaneous intravascular pressure and Doppler flow and is equipped with a combined miniature pressure and flow sensor at the distal tip. To transfer an electrical signal, three electrical conductors are required for the pressure sensor and two for Doppler signal. Hence the total number of conductors is five. Similar to the previous one, it has ring-contacts at the proximal tip for electrical connection with the female connector [4].
- Verrata Pressure Guidewire (Fig. 3.c): This guidewire which has a pressure sensor uses the same principle of ring-contacts for the male connector. For the female connector, there is a clip connector providing multiple back up contact points for a secure signal. This type of connector resists kinks while allowing free wire rotation when connected. Additionally, it repels moisture [22].

❖ **Jude Medical Corporation (St. Jude) [16]**

- Pressurewire Certus: This guidewire has a pressure sensor at the distal tip and is equipped with a protective hydrophobic male connector. The hydrophobic surface prevents the electrical connector from short-circuiting (on the hydrophobic surface, fluid is not absorbed but individual droplets do form). Similar to the concept of Volcano guidewires, the electrical connection uses ring-contacts at the proximal tip.
- Pressurewire Aeris: This guidewire employs the same design as the previous one and differs in that the female connector is wireless.

❖ **Boston Scientific Corporation [23]**

- TruePath CTO Device: This device has all the functionality of a guidewire in terms of steering and guidance, along with an increased ability to cross difficult vascular occlusions [24, 25]. It has a diamond-coated distal tip that rotates at 13,000 rpm on a 460µm guidewire to create a micro-dissection through the occlusion. The female part of the device consists of a disposable battery and an operative control unit. It has audio-visual feedback indicators that monitor the tip when navigates within the lumen.
- COMET Pressure Guidewire [20]: This is a workhorse FFR guidewire equipped with a pressure sensor. Its design is very similar to Pressurewire Certus which is introduced above. However is employs an optical fiber is connected to the pressure sensor and extends to the proximal side. Thus, a removable optical connector is used.

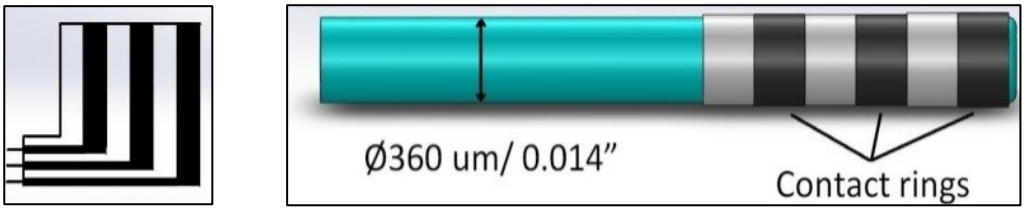

(2.a) (2.b)

Figure 2: The concept of a male connector for electrical connection: a) the electrical contacts on a flexible material before rolled into cylindrical shape, b) the electrical contacts after rolled around the proximal tip of the guidewire. Adopted from [26].

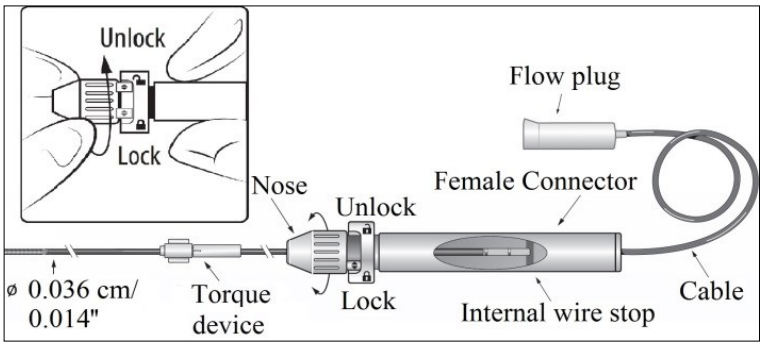

(3.a)

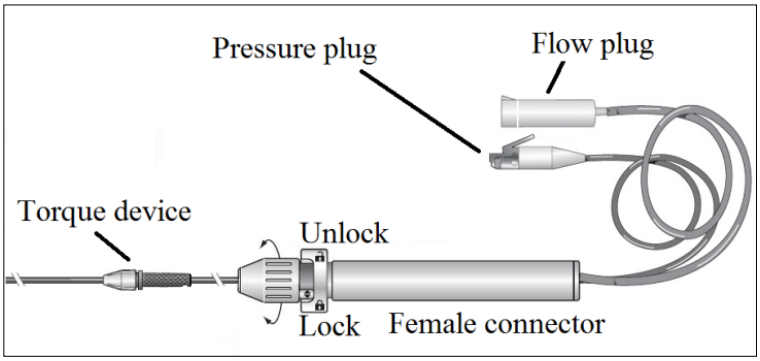

(3.b)

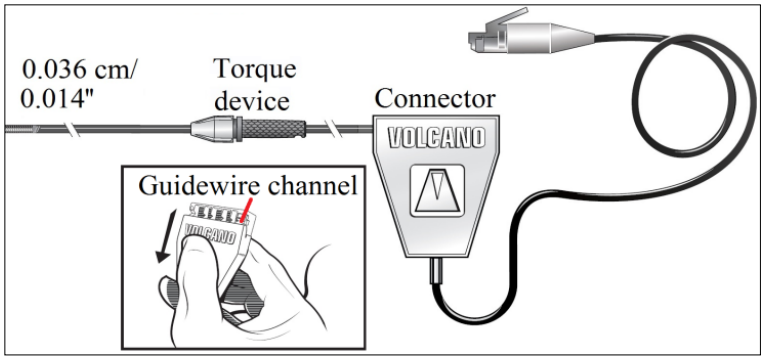

(3.c)

Figure 3: Volcano Corporation: a) Flowire Doppler Guidewire, b) Combowire XT Guidewire, c) Verrata Pressure Guidewire. Adopted from [21].

2.3.3 Type of connection for signal transmission

In this Section we review the state-of-the-art of the signal and power distribution in a sensing guidewire. The focus lies on the connection type on the proximal side, see Fig. 4.

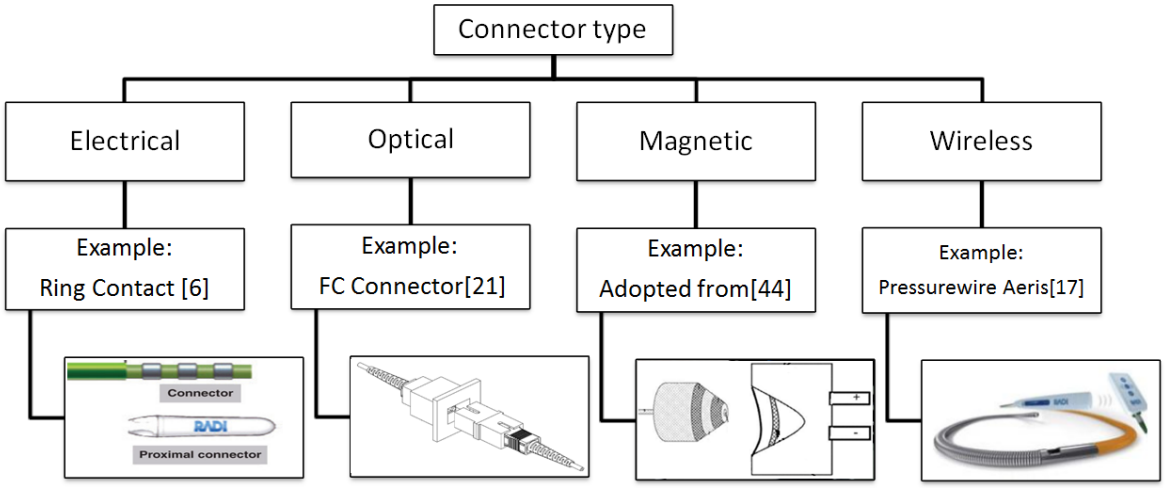

Figure 4: Connector type classification (a combination is also possible)

Electrical Connector

The male connector and its female counterpart are presented in [26–30] and [4, 22, 30–32] respectively. A conventional male connector is made up of a few conductive members which are separated from each other by means of insulating materials (Fig. 2.a and 2.b) and connected to distal side of the guidewire by passing wires through the length. When the male connector is inserted into the female connector, the conductive members transfer the signals to matching conductive members, which are located in the female connector. The other end of the female connector includes a plug, which connects to an appropriate monitoring device [4]. It is important to bear in mind that manufacturing electrical contacts on devices such as guidewires or catheters, which have a very small diameter (in the order

of 400 μm or less for a guidewire), is a challenging issue. In [27–28], using flexible materials (e.g., a polyimide such as KAPTON developed by DuPont in the late 1960s) to form these electrical contacts is proposed (Fig. 2.a). The thickness of the substrate varies from 2.5μm [33] to 25μm [27], thus, it can be re-shaped in order to roll around the proximal tip of the guidewire. However, it is still a time-consuming and thus expensive procedure. Additionally, the risk of manufacturing mistakes is high which can cause disconnection and short circuiting problems either during the manufacturing process or, in the worst case, during usage.

Optical Connector

Optical fibers have a variety of features which made them attractive in medical devices. Such features include the electrical isolation (MRI compatible [35, 36]), small size/weight, flexible, easy to be manufactured, great bandwidth, variable bandwidths, and low cost. Moreover, in guidewire application, where the optical fiber navigates inside the blood vessel and needs to bend, it does not become warm, like an electrical or an ultrasonic conductor [36, 39].

Below, first we review the basics of optical communication and fiber connector, then we present an overview on the state-of-the-art of guidewires employing optical fibers.

- Optical fiber technology: A general optical fiber system is shown in Fig. 5. On on side, an optical transmitter converts the signal into the optical form. The resulting optical signal is sent into the optical fiber via an optical source, typically a semiconductor laser or a light-emitting diode. On the other side, an optical receiver converts the optical signal back to its original form and recovers the data; this is done by a photo detector [34].

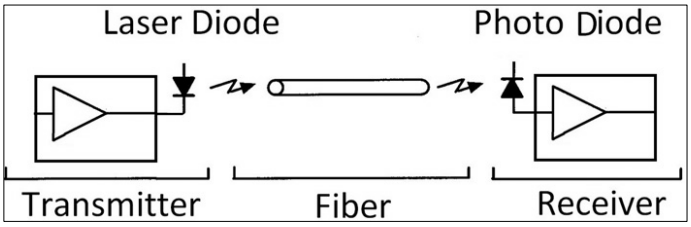

Figure 5: Optical Fiber System.

- Using optical fiber in guidewire: Examples of using optical pressure sensor in the guidewire/ catheter are presented in [11, 20, 37, 38]. Although none of the studies articles focuses on the proximal side connector, it is an essential part for their final prototype. The main idea is to use optical fibers inside the guidewire, extended from the distal side to the proximal side, as a transmitter and on the other side placing optical fiber in the female connector as a receiver. In some cases (e.g., in [37]) the receiver optical fiber has a different core diameter from the transmitter one to ensure minimal loss (note: when a large core fiber is connected to a small core fiber, this will result in high losses, whereas it is possible to couple a small core fiber to a large core fiber with minimal loss).

In [18, 39-41], the use of optical fiber is presented to not only readout the sensor but also replace all the wires and other electrical and mechanical devices currently used to power

and/or to communicate.

To generate a useful image with the help of an ultrasound array (IVUS) at the tip of the guidewire, which is a relatively new development, high speed data communication is needed [42-44, 47]. Moreover, the limited space available in a guidewire eliminates the existing options used in catheter (like the coaxial cable). Therefore, due to the previously mentioned properties of the optical fiber, it seems to be a promising solution. In [45, 46], the ultrasound energy is first sensed by a Fiber Bragg Grating (FBG) sensor, then the responsive signal is optically transmitted to the proximal end of the guidewire, so that it can be processed to develop a 2D or 3D image. In [47], one optical fiber, Ø80µm multi-mode, and several insulated wires run through the guidewire to transfer the signal and to power the system. The idea is to convert the signal into an optical signal by a Vertical-Cavity Surface-Emitting Laser (VCSEL) at the distal part of the guidewire; the optical signal is coupled to the optical fiber which is transferred through the guidewire to the proximal side.

Magnetic Connector

Keeping the interchangeable parts of a connector in place with magnetic attraction and repulsion principles has become popular in recent years. In [12] an electrical and mechanical micro-connector which works with the help of magnetic force is presented. However, the diameter of this micro- connector (2.5 mm) is still much bigger than the guidewire. In [48], an electrical and optical fiber connector that relies on magnetic contact is presented (Fig. 6). This magnetic force can be generated by permanent magnets or electromagnets. By using ferromagnetic materials, which have both electrical and magnetic properties, the magnetic elements can also function as electrical contacts. However, creating enough magnetic force to achieve a safe connection in such a small diameter of the guidewire is still a challenge. In [49], an inductive coupling arrangement for connecting an ultrasound probe to a measuring device is presented. The coupling is comprised of a first coil connected to a transducer and a second coil connected to a measuring circuit. Both coils are enclosed in separate housings. Therefore, the electrical energy is transferred without the use of electrical connectors. This method is more useful in situations where exposed electrical connections are undesirable.

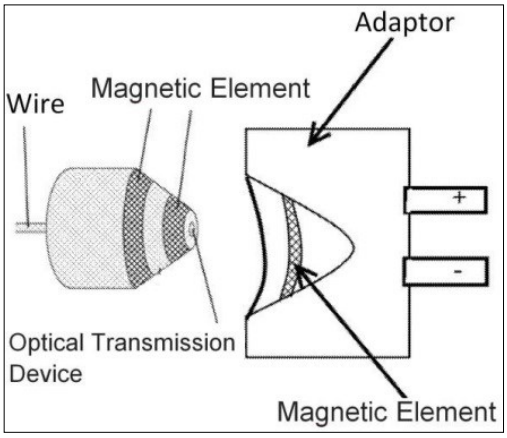

Figure 6: An electrical and optical fiber connector. Adopted from [48].

Wireless Connection

During an intravascular procedure, a guidewire or a catheter is inserted inside patient's body. Using a wireless arrangement on the proximal side to transfer measured data to the external device not only has the advantage of electrical insulation, but reducing also the number of cables [9]. In [9, 44], the transceiver unit is placed in the female connector and communicates wirelessly with a communication unit. The communication unit is in connection with an external device, though the male/female connection is still physical.

2.4 Discussion

In this review, we focused on guidewires that have different types of sensors at the distal tip and therefore require different types of proximal connectors. Connectors are classified according to the types of connections found including physical (e.g., electrical, optical, magnetic.), wireless and combinations of them (Fig. 4). A summary of the available guidewires and their characteristics, listing the relevant up-to-date patents for each connector type category is presented in Table I.

The electrical connection often employs ring-contact is used. However, soldering the corresponding rings on such a small guidewire diameter is a difficult task. Moreover, manufacturing the wire with several conductors to be passed through the length of the guidewire is very time-consuming and expensive to integrate. Additionally, the risk of manufacturing mistakes is high which can cause disconnection/short circuiting problems either during the manufacturing process or, in the worst case, during usage.

Employing an optical fiber as a data link in a guidewire is a challenging concept. The very first pressure wires (RAdi Medical) were fiber optic. The problem was that these pressure wires were stiffer and thicker than wires with electrical conductors. Although new developments have improved on that issue (e.g., ACIST Medical Systems, in the Navvus Micro Catheter of ∅0.667 μm, which diameter about 1.5 times thicker than a guidewire), a full solution has not yet been proposed. Therefore, providing safe and robust proximal connection for the guidewire remains a challenge. Wireless connection is also an interesting solution due to the need of less cables and freedom to place the receiver where it is most convenient. However, the connection between the male connector and the wireless female connector still has its difficulties.

Consequently, there remains a strong need for a proper connector on the proximal side of a sensing guidewire; the male part requires a less expensive, easy and straightforward to manufacture connector, and the female part requires to provide an easy to use, robust and secure connection.

This review provides essential input for the development of novel solutions to have proper communication from the proximal side of a guidewire to the external device.

Table 1:Listing the relevant up-to-date patents for the connector at proximal side of a guidewire.

Assignee	Patent Number	Type of connection	Merit
Volcano Corporation	US20140275950 A1 US20140005573 A1 US20140180139 A1 US20140005561 A1 US20130030303 A1 US20130190633 A1 US20050091833 A1 US20030163052 A1	Electrical	- Removable - Lock mechanism - Disposable - Protective Seal or wiper - Indicator (ready for use)
St. Jude Medical (& Radi Medical Systems before 2008)	US20130045640 A1 US20120289808 A1 US20100262040 A1 US20070106165 A1 US20060009817 A1 US20090124880 A1 US 6428336 B1	Electrical, Wireless	
Boston Scientific Corporation	US5575694 A US 9429713 B2	Electrical, Optical	

References

1. Erglis A, Narbute I, Sondore D, Grave A, Jegere S. Tools and Techniques: coronary guidewires. EuroIntervention, 2010.

2. Colombo A, Staknkivic G. Problem Oriented Approaches in Interventional Cardiology. ISBN- 13 978 1 84184 631 6, pp 9-21, 2007.

3. Schafer S, Hoffmann KR, Noel PB, Ionita CN, Dmochowski J. Evaluation of guidewire path reproducibility. Medical physics 2008; 35(5), 1884-1892.

4. Ahmed M, Oliver E, Puleo J, Ingman C, Walker BD. Combination Sensor Guidewire and Methods of Use. Patent US20130030303 A1, 2013, Volcano Corporation.

5. Tian Y, Wu N, Zou X, Zhang Y, Barringhaus K, Wang X. A Study on Packaging of Miniature Fiber Optic Sensors for In-Vivo Blood Pressure Measurements in a Swine Model, IEEE Sensors Journal 2014, 14(3), 629-635.

6. Tulkki S. Sensor wire assembly. Patent US 8187195 B2, 2012, Radi Medical Systems Ab.

7. Martin, R.W. and Johnson, C.C., 1989. Design characteristics for intravascular ultrasonic catheters. In Intravascular ultrasound (pp. 201-216). Springer Netherlands.

8. Wu N, Tian Y, Zou X, Zhai Y, Barringhaus K, Wang X. A miniature fiber optic blood pressure sensor and its application in in vivo blood pressure measurements of a swine model. Sensors and Actuators B: Chemical 181, 2013, 172-178.

9. Smith L. Removable energy source for sensor guidewire. Patent US20090124880 A1, 2009, Radi Medical Systems Ab.

10. Hubmette U. Sensor guidewire device and system including a sensor guide wire device, Patent US20120289808 A1, 2012, St Jude Medical Systems Ab.

11. Tohyama O, Kohashi M, Fukui M, Itoh H. A fiber-optic pressure microsensor for biomedical applications. International Conference on Solid State Sensors and Actuators, 1997, 1489-1492.

12. Okuyama H, Haga T, Emura K, Takada H. Development of microconnector with automatic connecting/ disconnection mechanism, Twelfth IEEE International Conference on Micro Electro Mechanical Systems, 1999, 257-262.

13. Schurr MO, Schostek S, Ho CN, Rieber F, Menciassi A. Microtechnologies in medicine: An overview. Minimally Invasive Therapy & Allied Technologies, 2007, 16(2), 76-86.

14. Gleason KR, Miller KE, Mcgiboney KA, Daane LA, Fazla D. Image guide wire connection, Patent US 8342887 B2, 2013, Tyco Electronics Corporation.

15. Lee C, Mc Namara C, Viohl I. Guidewire and connector therefor, Patent US20040181177 A1, 2004, Surgivision Inc.

16. St. Jude Medical Corporation, http://professional.sjm.com, [cited 1 Nov 2015].

17. Dorando D, Wong D, Alpert H. Interface Devices, Systems, and Methods for Use With Intravascular Pressure Monitoring Devices. Patent US20130190633 A1, 2013, Volcano Corporation.

18. Carlin DB, Alphonse GA, Ajgaonkar M, Paunescu A. Connectors for multi-fiber optical probes. Patent US7717624 B2, 2010, Medeikon Corporation.

19. Miraki M, Passafaro J, Walker B, Allen T, Pecor R, Janacek J, Diaz C, Sirimanne L. Catheters having a reusable proximal body. Patent US6248092 B1, 2001, Advanced Cardiovascular Systems.

20. Thornton Jr P. Self-cleaning optical connector, Patent US 9429713 B2, 2015, Boston Scientific Corporation

21. Volcano Corporation, http://eu.volcanocorp.com, [cited 1 Nov 2015].

22. Burkett DH. Side-Loading Connectors for Use With Intravascular Devices and Associated Systems and Methods, Patent US20140005536 A1, 2014, Volcano Corporation.

23. Boston Scientific Corporation, http://www.bostonscientific.com, [cited 1 Nov 2015].

24. Banerjee S, Sarode K, Das T, Hadidi O, Thomas R, Vinas A, Garg P, Mohammad A, Baig MS, Shammas NW, Brilakis ES. Endovascular Treatment of Infrainguinal Chronic Total Occlusions Using the TruePath Device: Features, Handling, and 6-Month Outcomes. Journal of Endovascular Therapy, 2014, 21(2), 281-288.

25. Park JB. Techniques for Successful Crossing With the TruePath CTO Device. Endovascular Today, 2014.

26. Kiepen HF, Eberle MJ, Rizzuti GP, Brunicardi DA. Flexible elongate member having one or more electrical contacts, Patent US 6210339 B1, 2001, Endosonics Corporation.

27. Akerfeldt D, Egneloev P. Guidewire having a male connector, Patent US6090052 A, 2000, Radi Medical Systems Ab.

28. Malmborg PV. Male connector, Patent US 20100262040 A1,2010, St.Jude Medical Systems Ab.

29. Mahlin F. Male connector and a method of producing the male connector, Patent US 20130045640 A1, 2013, St.Jude Medical Systems Ab.

30. Ortiz JE. Rotary connector for use with small diameter flexible elongate member having electrical capabilities, Patent US 5348481 A, 1994, Cardiometrics.

31. Akerfeldt D. Female connector, Patent US 6428336 B1, 2002, Radi Medical Systems Ab.

32. Millett BC, Huynh K, Milton L. Connectors for Use With Intravascular Devices and Associated Systems and Methods, Patent US20140180139 A1, 2014, Volcano Corporation.

33. Mimoun, Benjamin, Vincent Henneken, Arjen van der Horst, and Ronald Dekker.

"Flex-to-rigid (F2R): A generic platform for the fabrication and assembly of flexible sensors for minimally invasive instruments." IEEE Sensors Journal 13, no. 10 (2013): 3873-3882.

34. Agrawal, Govind P. Fiber-Optic Communication Systems, Third Edition, ISBNs: 0-471-21571-6, Wiley, New York, 2002.

35. Fandrey, Stephan, Steffen Weiss, and Jörg Müller. "A novel active MR probe using a miniaturized optical link for a 1.5T MRI scanner." Magnetic resonance in medicine 67, no. 1 (2012): 148-155.

36. Sonmez, Merdim, Christina E. Saikus, Jamie A. Bell, Dominique N. Franson, Majdi Halabi, Anthony Z. Faranesh, Cengizhan Ozturk, Robert J. Lederman, and Ozgur Kocaturk. "MRI active guidewire with an embedded temperature probe and providing a distinct tip signal to enhance clinical safety." Journal of Cardiovascular Magnetic Resonance 14, no. 1 (2012): 1.

37. Belleville C, Lalancette S, Proulx A. Method for disposable guidewire optical connection, Patent US 20130051731 A1, 2013, Opsens Inc.

38. Haga Y, Matsunaga T, Makishi W, Totsu K, Mineta T, Esashi M. Minimally invasive diagnostics and treatment using micro/nano machining. Minimally Invasive Therapy & Allied Technologies, 2006, 15(4), 218-225.

39. Fitch JP, Matthews DL, Hagans KG, Lee AP, Krulevitch P, Benett WJ, Clough RE, Da Silva LB, Celliers PM. Medical devices utilizing optical fibers for simultaneous power, communications and control, Patent US 6575965 B1, 2003, The Regents Of The University Of California.

40. Pekar M, Van Dusschoten A, Van der Mark M. Integrated Pressure Sensor Powered and Read- out via a Single Optical Fiber. Design of Medical Devices Conference- Europe, 2014.

41. Van der Mark M, Van Dusschoten A. An optical probe system. Patent WO2014072891 A1, 2012, Koninklijke Philips N.V.

42. Donnell M, McVeigh ER, Strauss HW, Tanaka A, Bouma BE, Tearney GJ, Guttman MA, Garcia EV. Multimodality Cardiovascular Molecular Imaging Technology. Journal of Nuclear Medicine, 2010, 38S-50S.

43. Bourantas CV, Garcia HM, Naka K, Sakellarios A, Athanasiou L, Fotiadis DI, Michalis LK, Serruys PW. Hybrid Intravascular Imaging: Current Applications and Prospective Potential in the Study of Coronary Atherosclerosis. Journal of the American College of Cardiology, 61(13), 2013, 1369-1378.

44. Lim, Jaemyung, Coskun Tekes, F. Levent Degertekin, and Maysam Ghovanloo. "Towards a Reduced-Wire Interface for CMUT-Based Intravascular Ultrasound Imaging Systems." IEEE Transactions on Biomedical Circuits and Systems (2016).

45. Eberle MJ, Tasker MD, Rourke HN, Optical ultrasound receiver. Patent US 8560048 B2, 2013, Vascular Imaging Corporation.

46. Vardi GM, Spivak V. Optical-acoustic imaging device. Patent US 7527594 B2, 2009, Vascular Imaging Corporation.

47. Stoute R, Louwerse MC, Van Rens J, Henneken VA, Dekker R. Optical Data Link Assembly for 360 m Diameter IVUS on Guidewire Imaging Devices. IEEE Sensors conference, 2014, 217-220.

48. Persion R, Tirelli J. Electrical and fiber optic connector with magnetic electrical contacts. Patent US20140120746 A1, 2014.

49. Baily G, Leyson CT. Connector with inductive coupling, Patent US 7210940 B2, 2007, Huntleigh Technology Plc

3. Navigation of Guidewires and Catheters- A Review

Hoda Sharei, Tanja Alderliesten, John J. van den Dobbelsteen, Jenny Dankelman

Published in the Journal of Medical Imaging, SPIE (2018)

Background: Guidewires and catheters are used during minimally-invasive interventional procedures to traverse in vascular system and access the desired position. Computer models are increasingly being used to predict the behavior of these instruments. This information can be used to choose the right instrument for each case and increase the success rate of the procedure. Moreover, a designer can test the performance of new instruments before the manufacturing phase. A precise model of the instrument is also useful for a training simulator. Therefore, to identify the strengths and weaknesses of different approaches used to model guidewires and catheters, a literature review of the existing techniques has been performed.

Method: The literature search was carried out in Google Scholar and Web of Science and limited to English for the period 1960 to 2017. For a computer model to be used in practice, it should be sufficiently realistic and, for some applications, real-time. Therefore, we compared different modelling techniques with regard to these requirements and, the purposes of these models are reviewed. Important factors that influence the interaction between the instruments and the vascular wall are discussed. Finally, different ways used to evaluate and validate the models are described.

Results: We classified the developed models based on their formulation into Finite Element Method (FEM), Mass-Spring Model (MSM), and Rigid Multibody Links. Despite its numerical stability, FEM requires a very high computational effort. MSM, on the other hand, is faster but there is a risk of numerical instability. The Rigid Multibody Links method has a simple structure and is easy to implement. However, as the length of the instrument is increased, the model becomes slower. For the level of realism of the simulation, friction and collision were incorporated as the most influential forces applied to the instrument during the propagation within a vascular system. To evaluate the accuracy, most of the studies compared the simulation results with the outcome of physical experiments on a variety of phantom models and only a limited studies have done face validity. Although a subset of the validated models is considered to be sufficiently accurate for the specific task for which they were developed and therefore are already being used in practice, these models are still under an ongoing development for improvement

Conclusion: Realism and computation time are two important requirements in catheter and guidewire modelling; however, the reviewed studies made a trade-off depending on the purpose of their model. Moreover, due to the complexity of the interaction with vascular system, some assumptions have been made regarding the properties of both instruments and vascular system. Some validation studies have been reported but without a consistent experimental methodology.

3.1 Introduction

Endovascular interventions include a variety of techniques that give access to the vascular system through small incisions. The access is mainly via guidewires and catheters. Despite the advantages of these procedures, such as decreased surgical trauma and accelerated recovery [1-3], new challenges are imposed on specialists. For example, they lose the direct access and the visual feedback and instead they have to manipulate the instrument (i.e., the guidewire and the catheter) from outside the body by applying a translation and/ or rotation motion at its proximal side.

Traditionally, the way to learn these skills is by iterative learning on a patient. However, this incorporates a high risk for the patient and is also time consuming. Another way is using cadavers or live animals. These methods are expensive and neither of them completely resemble an actual human vascular system. Employing phantoms is another emerging way to practice the new skills; however, the trainee is restricted to limited possible geometries. An additional drawback of the mentioned training methods is the exposure to X-ray during the training since the visual feedback is provided by X-ray imaging. Consequently, there is no single method which satisfies all the requirements [4-5].

Another complicating factor is that each instrument has different mechanical properties, and a high degree of expertise is required to select the best one for a particular case. Until now, selecting the instrument has been often based on specialist's experience, which does not always result in a successful procedure [6].

Recently, the use of computer models to predict the behavior of guidewire and catheter has become increasingly popular [5, 7]. The purposes of these models include training simulator, pre-intervention planning (specifically evaluating the performance of an instrument for a specific procedure), and designing new instruments.

Despite the growing trend towards computer models, a comprehensive review of different modelling approaches has not yet been performed. Therefore, this article has four goals: to introduce the purposes of guidewire and catheter modelling, to survey different approaches used for instrument modelling and identify their strengths and weaknesses, to study the important factors that affect the interaction between the instrument and the vascular wall, and finally, to review the different strategies used to validate the simulation. We will outline the key areas where future research can improve.

3.2 Review method

To obtain a comprehensive overview of guidewire and catheter models developed in different studies, we first used Google Scholar as the main search engine and then Web of Science for supplementary information. The keywords were "Guidewire", "Catheter", "Modelling", "Simulation", "Training", "Virtual Reality", and "Vascular Phantom". Boolean operators (AND, OR, NOT) were used to combine search terms, and wildcards

were applied to deal with spelling variations. Next, criteria for exclusion/inclusion of publications were set; articles were selected based on their title. Then, the abstract of each selected article was fully read, and the article was either included or excluded based on the relevance and applicability of the content. Finally, to complete the literature search, extra resources from citations and references of the included articles were screened and added when appropriate. In case of duplicate publications, the most recent was included.

3.3 Results

3.3.1 Purposes of computer models

In guidewire/ catheter modelling, researchers have focused on purposes such as training, pre-intervention planning and, designing new instruments. Although achieving these might overlap (Figure 1), we will review each one separately.

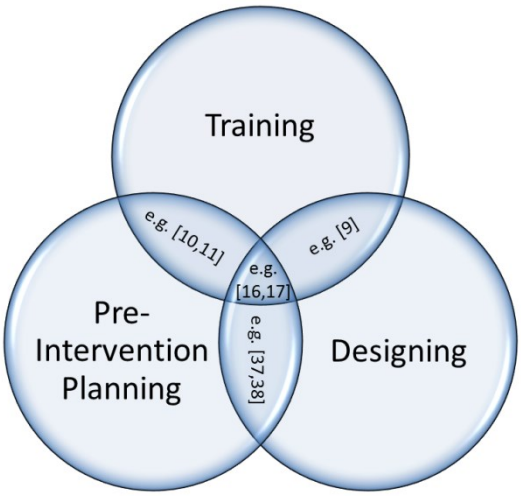

Figure 1:Purposes of a guidewire/ catheter model

Training: Simulation-based training is a virtual environment which helps the specialists to learn complex skills and new catheterization techniques by trial and error without risking patient safety [7-8]. In this way, the training becomes more efficient and cost-effective compared to traditional training methods (e.g., using human cadavers and animals). Researchers follow two main approaches: developing a model while focusing on the modelling techniques [9-32] and, investigating the effectivity and the necessity of using these simulations for training purposes [7-8, 33-36].

Pre-intervention planning: A simulation can also be used to evaluate the performance of an instrument for a specific anatomy prior to the procedure. This information assists the specialist to select an instrument with the proper mechanical properties and, as a result, increases the success rate of a procedure in accessing the target location. The research done in this field either focuses on catheter [10-11, 16-17, 20, 37-38] or on guidewire selection [39-41]. However, in practice, the instrument selection procedure is still based on the specialist's experience, which is subjective rather than objective.

Designing new instruments: Design optimization of new instruments by predicting their behavior inside the body is another purpose of the computer models [9-10, 16-17, 37-38, 42-43]; they are used to test different materials and structures for such instruments and to assess their performance in order to achieve optimal design. Both numerical (e.g., [38]) and analytical (e.g., [9]) methods have been used to model instrument behavior.

3.3.2 Instrument modelling

A variety of methods and different techniques have been used to govern the behavior of the instrument in a certain environment [44-47, 78]. The following provides an overview of techniques and applied equations, and discusses the strengths and weaknesses of each.

Finite Element Method (FEM): FEM is a common numerical technique to model a deformable object [47–49] including the behavior of the guidewire and catheter inside the body [5, 15-16, 20-22, 24-28, 31-32, 34, 37, 39, 41, 50-51, 68-81, 85, 96, 102]. In this method, the instrument is first divided into a set of basic elements connected by nodes. A function that solves the equilibrium equations is found for each element. The equations incorporate the geometry and material information of the instrument. There are different ways to solve these equations. In [5, 15, 22, 24-28, 37, 64-81, 102], the instrument is considered as a rod-like structure, a long and thin circular structure with the length being much larger than the diameter. For rod modelling, there are different choices such as Euler-Bernoulli beam theory (deformation due to bending), Kirchhoff rod [15, 22, 24, 26, 69] which is the geometrically nonlinear generalization of the Euler-Bernoulli beam theory [100], Timoshenko beam theory (deformation due to bending and shear), and Cosserat rod [25, 27-28, 72, 75, 79-81, 102] which is the geometrically nonlinear generalization of the Timoshenko beam theory [100]. In [15, 22, 37, 41, 75], the position of the instrument is expressed based on the principles of energy minimization. Thus, the energy function is expressed as:

$$E(de) = \min\left(E_{int}(de) + E_{ext}(de)\right) \quad (1),$$

in which *de* is the deformation, E_{int} is the internal energy, associated with the flexibility of the instrument and E_{ext} is the external energy, associated with the applied forces. To solve equation (1), the instrument is discretized into multiple segments (see Figure 2), and the equation is applied to each segment.

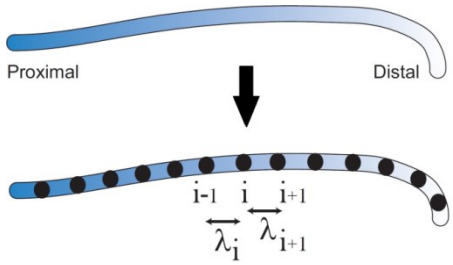

Figure 2: Discretization of the instrument into small segments; λ_i and λ_{i+1} are not necessarily of the same length

FEM is widely used in simulation in different fields because of its numerical stability. Applying this method to model the guidewire and catheter requires a very high computational effort due to the non-linear underlying effects of FEM [85, 96]. However, the computational time is highly important and specially in some cases like training, being real-time is necessary.

Mass-Spring Model (MSM): In this method, the instrument is considered as a network of masses connected to each other by springs/dampers (Figure 3) [12, 23, 44-45, 53–56]. The springs not only give flexibility to the model but also constrain the distance between masses. Thus, the number of springs influences the behavior of the model [56].

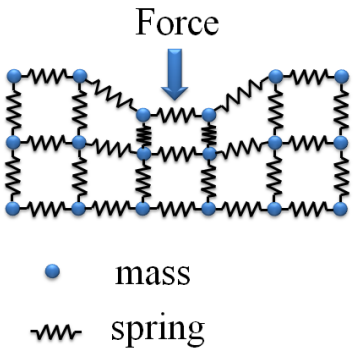

Figure 3: Mass-Spring model

The deformable properties of the instrument depend on the parameters of the masses, springs, and dampers as follows:

$$m\ddot{x} = k(x_0 - x) - d\dot{x} \quad (2),$$

in which m is the mass of the particle, k is the spring constant related to the stiffness of the instrument, d is the damping coefficient related to the viscous behavior of the instrument, x_0 is the rest position of the mass, and x is the current position. Thus, concatenating equation (2) of all individual masses (N) into a single 3N-dimensional vector and solving them, results in the solution for the entire system.

The main advantage of this method is its relative simplicity compared to FEM. However, it is more suited for modelling soft tissue behavior (e.g., the abdominal skin or muscles). In case of a more rigid object, such as the guidewire and catheter, it requires a high computational power, which is against the real-time requirements. Moreover, it is not necessarily accurate, and there is also a risk of numerical instability [45, 48].

Rigid Multibody Links: In this method, the instrument is discretized into a set of rigid bodies connected by massless springs and dampers (Figure 4). The stiffness and damping coefficients are selected based on the material properties of the segments [97].

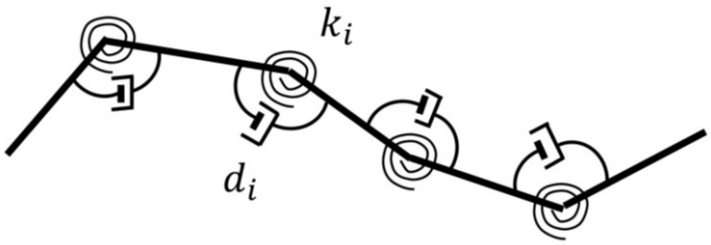

Figure 4: Multiple rigid bodies connected by joints: k_i is the spring constant related to the stiffness and, d_i is the damping coefficient related to the viscous behavior of joint *i*.

In [13, 18, 29, 38, 40, 57,59-62, 87, 98], the instrument is modelled as rigid bodies connected to their neighbors by joints, and the Newton–Euler equations are used to describe the translational and rotational dynamics [38, 57-59, 62]. Since the speed of propagating the instrument is slow, the Newton-Euler equations are typically simplified by neglecting inertia and centrifugal force.

In contrast to MSM, in this method the length of each segment might be different. Particularly in guidewire or catheter modelling, it is possible to have shorter segments in the distal side because of more flexibility, and longer ones in the proximal side due to more stiffness. This will result in less computational time compared to MSM. Another advantage of this method is that because of its simple structure, it is easy to understand and interpret the results. Moreover, it is relatively easy to incorporate other phenomena such as friction and/or material properties to each individual segment [43]. On the other hand, the disadvantage of this method is that even though differently sized segment lengths are possible, the simulation is limited to a maximum number of segments and, otherwise it will run into problems.

Hybrid models: The mechanical properties of a guidewire/catheter change along the length: more flexibility at the distal side and more stiffness at the proximal side. Due to this property, some studies came with the idea of applying hybrid models, which means using either a combination of different techniques to model different parts of the instrument [10-11, 28, 56, 82-85] or a new approach in which inspired by different models [9, 64-67, 88, 101, 103]. In this way, they endeavored to make the simulation computationally more efficient.

In [28] the Cosserat rod model is used for the main body and a rigid multibody approach for the flexible tip. Then, the Lagrangian equations of motion are used to solve the dynamics of both parts (body and tip). In [82, 84], the flexible tip and the stiff body are modeled by MSM, separately, after which the connection between them is modeled with an additional rigid link (rigid multibody system). In [10-11, 83], the instrument is discretized into a finite number of flexible multi-bodies. The deformations of bodies are assumed to be relatively small compared to the displacements. Thus, the segments of the instrument are treated as rigid bodies, and displacements are handled by the multi-body dynamics approach. Finally, the deformations at their equilibrium position are found by applying FEM.

In [9, 30, 64-67, 88, 101, 103], the principles of energy minimization are used to predict the path of the instrument. In contrast to FEM, analytical approximation is applied to solve the optimization problem. In [9, 64-67], Hooke's law [86] is used as the basis for the modelling. In [88, 103], a graph-based modelling is described to find the optimal path for the guidewire in different vascular geometries. Table 1 includes a summary of reviewed models.

Table 2: Summary of the reviewed studies

Modelling technique \ Purpose of the model		Training	Pre-intervention planning	Designing
FEM	Kirchhoff rod theory	[15], [22], [24], [26], [69]		
	Cosserat rod theory	[25], [27], [72], [75], [80], [102]	[75]	[75]
	Energy minimization	[15], [22], [68], [75]	[41], [37]	[37]
	Others	[16], [21], [32], [34]	[16], [39]	[16], [43]
MSM		[12], [23], [45], [53-55]		
Rigid Multibody links		[13], [18-19], [29], [59], [61], [87]	[38], [40], [60], [62], [98]	[38], [43]
Hybrid		[9-11], [17], [20], [28], [30], [64-67], [82], [84], [101]	[10-11], [17], [20], [83], [88], [103]	[9-11], [17], [20], [83]

3.3.3 Vessel-instrument interaction

The orientation of the instrument is the result of interaction with the vascular wall and is mainly dominated by the forces experienced during propagation. These forces include the manipulation forces, contact forces with the vascular wall and, frictional forces. In this section, our focus is on the contact forces and frictional forces.

Collision: During the propagation, if the normal distance between the instrument and the vessel is smaller than zero, collision has occurred. Detecting this intersection is referred to as collision detection.
To detect the collision, some studies [10, 15, 37, 41, 55, 58, 68] considered a circular cross section for the vessel in which the radii might vary. Therefore, the shape of the vessel is

defined by its centerline and its radius, and the distance between the instrument and the centerline of the vessel is calculated as follows:

$$D = \boldsymbol{d_i} - (\boldsymbol{R_V} - \boldsymbol{R_G}) \quad (1),$$

in which d_i is the nearest point to the centerline of the vessel, and R_V and R_G the radii of the vessel and the instrument, respectively (Figure 5). If $D \geq 0$, a contact has been occurred.

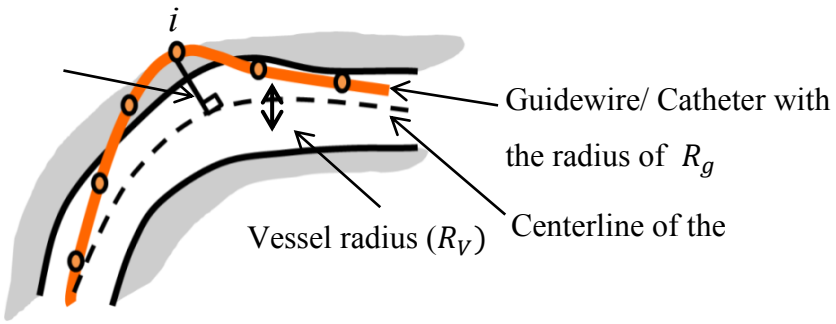

Figure 5: Collision detection

In [10, 16-17, 37, 69], the vessel is assumed to be rigid and no deformation occurs due to the contact. Thus, D is used to calculate the normal force based on Hooke's law [86]. In [58, 101], vessel deformation is not neglected, and an extra term regarding the reaction force from deformation of the wall in radial direction is considered.

In another collision detection approach, an object is approximated by bounding volumes, and instead of the original object, the intersections of bounding volumes are detected. This method is widely used in simulations [45]. In [28, 37, 68, 79, 81, 83, 87, 101], the Axis-Aligned Bounding Boxes (AABB) method is used, calculating 3D boxes that bound the object and using them to test for collision instead of the original object. In [23, 69], the object is bounded by spheres instead of boxes. The advantage of this method is less complexity of collision detection and thus, less computation time. On the other hand, the accuracy depends on the bounding volumes' size [45].

Friction: During the propagation of an instrument, friction with the vascular wall influences its orientation [95] and provides force feedback to the user. For the sake of realism of the simulation, modelling the friction is important. However, the coefficient of the friction is not known from the manufacturers and it is determined empirically. There are two forms of friction: kinetic (or sliding) and static. In [28, 64-67, 69, 98, 101], the simulation is based on a quasi-static approach. Therefore, the velocities and accelerations of the instrument in the vessel are small and the velocity dependent friction forces are neglected. Although in [13, 59, 95, 104] both types of the friction are considered, they didn't discussed if a higher accuracy achieved. Some studies [9, 16, 27, 33, 38, 41] ignored the friction to trade off the realism against computation time. However, in reality, friction is not zero and the instrument that encounters friction results in a different path in the vascular system [66, 95].

Blood flow: Modelling blood flow can be useful to distinguish between a normal and a narrowed vessel [34]. However, in most of the studies on guidewire and catheter modelling the effect of blood flow is neglected in order to reduce the complexity, and only a few studies considered it [11, 13, 20, 61, 87]. Considering the blood flow when designing catheters with a side hole for the drug delivery might be interesting as the flow condition can affect the injection procedure [105]. Moreover, in the presence of vascular malformations, modelling the blood flow might provide a better understanding of the pathological conditions [13, 20].

3.3.4 Validation and evaluation

The accuracy of any developed model needs to be evaluated. One way to validate a model is by letting a specialist try it out and judge the outcome based on his or her real experiences (face validity) [99]. Most of the reviewed studies validated the simulation results by comparing them with experimental results in phantoms. Phantoms are used both for training and experimental validation. For validation purposes, most of the studies use custom-made phantoms. To fabricate such a phantom, first, they need to extract the vascular geometry in the area of the interest. Thus, DICOM data (Digital Imaging and Communications in Medicine) are obtained via different medical imaging techniques, such as Magnetic Resonance Angiography (MRA) [15, 89] and Computed Tomography (CT) [28, 30, 37, 68, 83]. Then, a variety of segmentation techniques are used to extract the required information. Next, a cast is constructed based on the extracted data. Recently, 3D-printing has been used to manufacture phantoms [106]. Different materials can be used to fabricate the phantom model. For example, to test a guidewire or a catheter behavior, phantom's materials used in the literature include Poly Vinyl Alcohol (PVA) [91], PVA-Hydrogel (PVA-H) [38, 62, 92], PVA-H and silicone (high transparency) [93] and, PVA-Cryogel (PVA-C) [94]. Table 2 includes a summary of some commercially available systems with their applications.

3.4 Discussion and conclusion

This paper has reviewed the existing computer models for both guidewire and catheter navigation in the body. The purposes of these models are categorized in three main groups: training, pre-intervention planning, and designing new instruments. The main techniques used in the modelling are FEM, MSM, and Rigid Multibody Links. In addition, some studies applied different techniques in different parts of the instrument and introduced hybrid methods. FEM is widely used in simulation in different fields because of its numerical stability. However, due to the non-linear underlying effects, applying FEM to model the guidewire and catheter requires a very high computational effort. Though MSM is easier than FEM to implement, it is more suited for modelling soft tissue behavior (e.g., the abdominal skin or muscles); modelling a more rigid object, such as the guidewire and catheter, requires high computational power. Therefore, these two methods are not suitable for real time purposes such as training. The Rigid Multibody Links technique has a simple structure, which makes it easy to understand and interpret the results. Moreover, adding other phenomena such as friction and/or material properties to each individual segment is

relatively easy. Additionally, this method is relatively faster than the first two methods and can be used for real time applications.

Table 3: Example of commercially available systems

Device/ manufacture	**Modelling technique**	**Purpose**	**Application**	**Vessel-Instrument interaction**	**Validation method**
CathSim; HT Medical Systems [18, 19, 78]	Rigid Multibody links	Training	Interventional radiology, Peripheral intravenous	No available information	No available information
da Vinci[16]	FEM	Training, Pre-intervention planning, Designing	Interventional radiology	-Rigid vessel wall -No friction	Face validity (clinical validation)
ICTS/VIST[13]	Rigid Multibody links	Training	Cardiology	-Blood flow -Friction	No validation based on [13]
ICard [10, 17]	Hybrid*	Training, Pre-intervention planning, Designing	Cardiology	-Rigid vessel wall	Face validity (clinical validation)
Neuro Cath [11, 20]	Hybrid*	Training, Pre-intervention planning, Designing	Neuro-radiological procedures	-Blood flow	Face validity (clinical validation)
CathI [21]	FEM	Training	Endovascular intervention	-Rigid vessel wall	Face validity (clinical validation)

*Refer to section 3.2

Capturing all details in one model is a hard task. Thus, each study has made the choice to model only the relevant details for their purpose. One advantage of this selection is that it reduces the computational complexity. However, the results might be biased towards the selected details. Moreover, due to the complexity of the interaction with vessels, different studies have made different assumptions and, therefore, they had to make compromises. For example, in most of the research, the modelling is based on quasi-static mechanics, which is acceptable as the loading of these instruments is slow and inertial effects can be ignored. Some studies assumed a perfect torque control (the torsion coefficient is considered to be infinite). This feature is taken into account in the design of these instruments, and the

assumption is close enough to reality. Furthermore, as the manufacturers do not provide information about the mechanical properties of the instruments, this information is determined empirically. Likewise, vessel properties such as diameter, wall thickness, and stiffness, are determined empirically. In many studies, the vessel wall is assumed to be rigid with a circular cross section; thus, deformation of the vessel is not considered. However, a stiff instrument might cause deformation in the vessel. Additionally, the cross section of the vessels might change due to vascular diseases. Therefore, more studies are required to consider different cross sections and, to investigate the deformations especially around the tip of the instrument. Validation is the final step in evaluating the accuracy and effectiveness of a model. Face validity, which is done by letting a specialist try it out and judge the outcome based on his or her real experiences, is a reliable method to test a model. However, in practice, most of the reviewed studies have validated their model by comparing the results with phantom experiment results and some of them didn't perform any validation.

The knowledge provided in this review helps to determine a modelling technique for the instrument which satisfies the necessary requirements for a particular application.

References

1. Dankelman, Jenny, Cornelis A. Grimbergen, and Henk G. Stassen, eds. Engineering for patient safety: issues in minimally invasive procedures. CRC Press, 2004.

2. Kaufman, John A., and Michael J. Lee. Vascular and interventional radiology. Elsevier Health Sciences, 2013.

3. Aklog, Lishan, David H. Adams, Gregory S. Couper, Reuben Gobezie, Samuel Sears, and Lawrence H. Cohn. "Techniques and results of direct-access minimally invasive mitral valve surgery: a paradigm for the future." The Journal of thoracic and cardiovascular surgery 116, no. 5 (1998): 705-715.

4. Lasala, John M., and Jason H. Rogers. Interventional Procedures for Adult Structural Heart Disease: Expert Consult-Online. Elsevier Health Sciences, 2013.

5. Badash, Ido, Karen Burtt, Carlos A. Solorzano, and Joseph N. Carey. "Innovations in surgery simulation: a review of past, current and future techniques." Annals of Translational Medicine 4, no. 23 (2016).

6. M Al-Moghairi, Abdulrahman, and Hussein S Al-Amri. "Management of retained intervention guide-wire: a literature review." Current cardiology reviews 9, no. 3 (2013): 260-266.

7. Kunkler, Kevin. "The role of medical simulation: an overview." The International Journal of Medical Robotics and Computer Assisted Surgery 2, no. 3 (2006): 203-210.

8. Aggarwal, R., S. A. Black, J. R. Hance, A. Darzi, and N. J. W. Cheshire. "Virtual reality simulation training can improve inexperienced surgeons' endovascular skills." European Journal of Vascular and Endovascular Surgery 31, no. 6 (2006): 588-593.

9. M. K. Konings, E. B. van de Kraats, T. Alderliesten, W. J. Niessen, “Analytical guide wire motion algorithm for simulation of endovascular interventions”, Medical and Biological Engineering and Computing 2003, Volume 41, Issue 6, pp 689-700.

10. Wang, Yaoping, Cheekong Chui, Honglip Lim, Yiyu Cai, and Koonhou Mak. "Real-time interactive simulator for percutaneous coronary revascularization procedures." Computer Aided Surgery 3, no. 5 (1998): 211-227.

11. Zirui Li, Chee-Kong Chui, James H. Anderson, Xuesong Chen, Xin Ma, Wei Hua, Qunsheng Peng, Yiyu Cai, Yaoping Wang, Wieslaw L. Nowinski, “Computer environment for interventional neuroradiology procedures”, SIMULATION and GAMING, Vol. 32 No. 3, September 2001.

12. Basdogan, Cagatay, C-H. Ho, and Mandayam A. Srinivasan. "Virtual environments for medical training: graphical and haptic simulation of laparoscopic common bile duct exploration." IEEE/Asme Transactions On Mechatronics 6, no. 3 (2001): 269-285.

13. Cotin, Stephane, S. Dawson, Dwight Meglan, D. Shaffer, M. Ferrell, R. Bardsley, F. Morgan et al. "ICTS, an interventional cardiology training system." Studies in health technology and informatics (2000): 59-65.

14. W. Shaffer, D., S. L. Dawson, D. Meglan, S. Cotin, M. Ferrell, A. Norbash, and J. Muller. "Design principles for the use of simulation as an aid in interventional cardiology training." Minimally Invasive Therapy & Allied Technologies 10, no. 2 (2001): 75-82.

15. Li, Shun, Jixiang Guo, Qiong Wang, Qiang Meng, Yim-Pan Chui, Jing Qin, and Pheng-Ann Heng. "A catheterization-training simulator based on a fast multigrid solver." IEEE computer graphics and applications 32, no. 6 (2012): 56-70.

16. Anderson, J. H., R. Raghavan, Y. P. Wang, R. Mullick, and C. C. Kong. "daVinci—A vascular catheterization simulator." Journal of Vascular and Interventional Radiology 8, no. 1 (1997): 261.

17. Chui, C., Y. Wang, Y. Cai, H. Lim, Y. Ooi, and K. Mak. "Icard: An interventional cardiology simulator for percutaneous coronary revascularisation." Computer Assisted Radiology and Surgery (CAR'98), Tokyo (1998).

18. Meglan, Dwight. "Making surgical simulation real" ACM SIGGRAPH Computer Graphics 30, no. 4 (1996): 37-39.

19. Ursino, Michele, Joseph L. Tasto, Binh H. Nguyen, Richard Cunningham, and Gregory L. Merril. "CathSim: an intravascular catheterization simulator on a PC." Studies in health technology and informatics 62 (1998): 360-366.

20. Nowinski, Wieslaw Lucjan, and Chee-Kong Chui. "Simulation of interventional neuroradiology procedures." In Medical Imaging and Augmented Reality, 2001. Proceedings. International Workshop on, pp. 87-94. IEEE, 2001.

21. Rebholz, Philipp, Carsten Bienek, Dzmitry Stsepankou, and Jürgen Hesser. "CathI–training system for PTCA. A step closer to reality." In Medical Simulation, pp. 249-255. Springer Berlin Heidelberg, 2004.

22. Li, Shun, Jing Qin, Jixiang Gao, Yim-Pan Chui, and Pheng-Ann Heng. "A novel FEM-based numerical solver for interactive catheter simulation in virtual catheterization." Journal of Biomedical Imaging (2011): 3.

23. Wang, Fei, Lindo Duratti, Evren Samur, Ulrich Spaelter, and Hannes Bleuler. "A computer-based real-time simulation of interventional radiology." In 2007 29th Annual International Conference of the IEEE Engineering in Medicine and Biology Society, pp. 1742-1745. IEEE, 2007.

24. Luo, Maisheng, Hongzhi Xie, Le Xie, Ping Cai, and Lixu Gu. "A robust and real-time vascular intervention simulation based on Kirchhoff elastic rod." Computerized Medical Imaging and Graphics 38, no. 8 (2014): 735-743.

25. Duratti, Lindo, Fei Wang, Evren Samur, and Hannes Bleuler. "A real-time simulator for interventional radiology." In Proceedings of the 2008 ACM symposium on Virtual reality software and technology, pp. 105-108. ACM, 2008.

26. Zhou, Chaozheng, Le Xie, Xianglong Shen, Maisheng Luo, Zhaoli Wu, and Lixu Gu. "Cardiovascular-interventional-surgery virtual training platform and its preliminary evaluation." The International Journal of Medical Robotics and Computer Assisted Surgery

11, no. 3 (2015): 375-387.

27. Korzeniowski, Przemyslaw, Francisco Martinez-Martinez, Niels Hald, and Fernando Bello. "Simulation of Catheters and Guidewires for Cardiovascular Interventions Using an Inextensible Cosserat Rod." In International Symposium on Biomedical Simulation, pp. 112-121. Springer International Publishing, 2014.

28. Tang, Wen, Tao Ruan Wan, Derek A. Gould, Thien How, and Nigel W. John. "A stable and real-time nonlinear elastic approach to simulating guidewire and catheter insertions based on cosserat rod." IEEE Transactions on Biomedical Engineering 59, no. 8 (2012): 2211-2218.

29. Wang, Yu, Shuxiang Guo, Takashi Tamiya, Hideyuki Hirata, Hidenori Ishihara, and Xuanchun Yin. "A virtual-reality simulator and force sensation combined catheter operation training system and its preliminary evaluation." The International Journal of Medical Robotics and Computer Assisted Surgery (2016).

30. Zhang, Dapeng, Tianmiao Wang, Da Liu, and Guo Lin. "Vascular deformation for vascular interventional surgery simulation." The International Journal of Medical Robotics and Computer Assisted Surgery 6, no. 2 (2010): 171-177.

31. Guo, Jin, Shuxiang Guo, Nan Xiao, and Baofeng Gao. "Virtual reality simulators based on a novel robotic catheter operating system for training in minimally invasive surgery." Journal of Robotics and Mechatronics 24, no. 4 (2012): 649.

32. Wu, Xunlei, Vincent Pegoraro, Vincent Luboz, Paul F. Neumann, Ryan Bardsley, Steven Dawson, and Stéphane Cotin. "New approaches to computer-based interventional neuroradiology training." Studies in health technology and informatics 111 (2005): 602-607.

33. Alaraj, Ali, Michael G. Lemole, Joshua H. Finkle, Rachel Yudkowsky, Adam Wallace, Cristian Luciano, P. Pat Banerjee, Silvio Rizzi, and Fady T. Charbel. "Virtual reality training in neurosurgery: review of current status and future applications." (2011).

34. Anderson, James, Chee-Kong Chui, Yiyu Cai, Yaoping Wang, Zirui Li, Xin Ma, Wieslaw Nowinski et al. "Virtual reality training in interventional radiology: the Johns Hopkins and Kent Ridge Digital Laboratory experience." In Seminars in Interventional Radiology, vol. 19, no. 02, pp. 179-186. Copyright© 2002 by Thieme Medical Publishers, Inc., 333 Seventh Avenue, New York, NY 10001, USA. Tel.:+ 1 (212) 584-4662, 2002.

35. Gosai, Jivendra, Makani Purva, and Julian Gunn. "Simulation in cardiology: state of the art." European heart journal 36, no. 13 (2015): 777-783.

36. Voelker, Wolfram, Nils Petri, Christoph Tönissen, Stefan Störk, Ralf Birkemeyer, Erhard Kaiser, and Martin Oberhoff. "Does Simulation-Based Training Improve Procedural Skills of Beginners in Interventional Cardiology?—A Stratified Randomized Study." Journal of interventional cardiology 29, no. 1 (2016): 75-82.

37. Lawton, W., R. Raghavan, S. R. Ranjan, and R. R. Viswanathan. "Tubes in tubes: catheter navigation in blood vessel s and its applications." International journal of solids and structures 37, no. 22 (2000): 3031-3054.

38. Takashima, Kazuto, Shotaro Tsuzuki, Atomu Ooike, Kiyoshi Yoshinaka, Kaihong Yu, Makoto Ohta, and Koji Mori. "Numerical analysis and experimental observation of guidewire motion in a blood vessel model." Medical engineering & physics 36, no. 12 (2014): 1672-1683.

39. Suraj Bhat, Thenkurussi Kesavadas, Kenneth R. Hoffmann, ”A physically-based model for guidewire simulation on patient-specific data”, Computer Assisted Radiology and Surgery, Volume 1281, May 2005, Pages 479-484.

40. Vincent Guilloux, Pascal Haigron, Cemil Goksu, Carine Kulik, Antoine Lucas, ”Simulation of guidewire navigation in complex vascular structures”, Proc. SPIE 6141, Medical Imaging 2006.

41. Cardoso, Fernando M., and Sergio S. Furuie. "Guidewire path determination for intravascular applications." Computer methods in biomechanics and biomedical engineering 19, no. 6 (2016): 628-638.

42. Martin, Roy W., and Christopher C. Johnson. "Design characteristics for intravascular ultrasonic catheters." In Intravascular ultrasound, pp. 201-216. Springer Netherlands, 1989.

43. Cai, Y. Y., C. K. Chui, X. Ye, J. H. Anderson, K. M. Liew, and I. Sakuma. "Simulation-based virtual prototyping of customized catheterization devices." Journal of Computing and Information Science in Engineering 4, no. 2 (2004): 132-139.

44. Burgner-Kahrs, Jessica, D. Caleb Rucker, and Howie Choset. "Continuum robots for medical applications: A survey." IEEE Transactions on Robotics 31, no. 6 (2015): 1261-1280.

45. Torpey, Luke. "A Virtual Environment Simulation for Guidewire/catheter and Blood Vessel Interaction." PhD diss., University of Leeds, School of Computing Studies, 2010.

46. Zorcolo, Antonio, Enrico Gobbetti, Gianluigi Zanetti, and Massimiliano Tuveri. "A volumetric virtual environment for catheter insertion simulation." In Virtual Environments, pp. 125-134. Springer Vienna, 2000.

47. Sarah F. F. Gibson, Brian Mirtich,” A Survey of Deformable Modelling in Computer Graphics”, Mitsubishi Electric Information Technology Center America, 1997.

48. Liu, Alan, Frank Tendick, Kevin Cleary, and Christoph Kaufmann. "A survey of surgical simulation: applications, technology, and education." Presence: Teleoperators and Virtual Environments 12, no. 6 (2003): 599-614.

49. T. Halic, “Virtual environments and their applications in surgical training”, PhD thesis, University of Arkansas, 2008. ProQuest, 2008.

50. Cotin, S., Duriez, C., Lenoir, J., Neumann, P. and Dawson, S., “New Approaches to Catheter Navigation for Interventional Radiology Simulation”, 2006, Computer Aided Surgery 11 (6), pp. 300-308.

51. Peng Wei, Zhen-Qiu Feng, Xiao-Liang Xie, Gui-Bin Bian, Zeng-Guang Hou, ”FEM-based Guide Wire Simulation and Interaction for a Minimally Invasive Vascular Surgery Training System”, Proceedings of the 11th World Congress on Intelligent.

52. Qiukui, Zhang, and Pascal Haigron. "A FEM Model for Interactive Simulation of Guide Wire Navigation in Moving Vascular Structures." In Intelligent Systems Design and Engineering Applications (ISDEA), 2015 Sixth International Conference on, pp. 13-16. IEEE, 2015.

53. Vincent Luboza, Jianhua Zhai, Tolu Odetoyinbo, Peter Littler, Derek Gould, Thien How, Fernando Bello, “Simulation of endovascular guidewire behavior and experimental validation”, Computer Methods in Biomechanics and Biomedical Engineering Vol. 14, No. 6, June 2011, 515520.

54. Vincent Luboz, Rafal Blazewski, Derek Gould, Fernando Bello, “Real-time guidewire simulation in complex vascular models”, Visual Computer, 2009,25(9), 827-834.

55. V. Luboz, , Y. Zhang, S. Johnson, Y. Song, C. Kilkenny, C. Hunt, H. Woolnough, S. Guediri, J. Zhai, T. Odetoyinbo, P. Littler, A. Fisher, C. Hughes, N. Chalmers, D. Kessel, P.J. Clough, J.Ward, R. Phillips, T. How, A. Bulpitt, N.W. John, F. Bello, D. Gould, “ImaGiNe Seldinger: First simulator for Seldinger technique and angiography training”, Computer Methods and Programs in Biomedicine, Volume 111, Issue 2, August 2013, Pages 419434.

56. Cotin, Stéphane. “Computer Based Interactive Medical Simulation.” PhD diss., Université des Sciences et Technologie de Lille-Lille I, 2008.

57. David E. Stewart, “Rigid-Body Dynamics with Friction and Impact”, Society for Industrial and Applied Mathematics (SIAM), Vol. 42, No. 1, pp. 339, 2000.

58. Farid Amirouche, ”Fundamentals of Multibody Dynamics: Theory and Applications”, ISBN 0-8176-4236-6.

59. K. Ikuta, K. Iritani, J. Fukuyama, and M. Takeichi, “Portable virtual endoscope system with force and visual display for insertion training”, In Proc. of the IEEE/RSJ International Conference on Intelligent Robots and Systems (IROS), volume 1, pages 720726, 2000.

60. Markus Kukuk, “A Model-Based Approach to Intra operative Guidance of Flexible Endoscopy”, PhD thesis, Princeton, 2002.

61. Dawson, Steven L., Stephane Cotin, Dwight Meglan, David W. Shaffer, and Margaret A. Ferrell. "EQUIPMENT AND TECHNOLOGY-Designing a Computer-Based Simulator for Interventional Cardiology Training." Catheterization and Cardiovascular Interventions 51, no. 4 (2000): 522-527.

62. Takashima, Kazuto, Atomu OIKE, Kiyoshi YOSHINAKA, Kaihong YU, Makoto OHTA, Koji MORI, and Naoki TOMA. "Evaluation of the effect of catheter on the guidewire motion in a blood vessel model by physical and numerical simulations." Journal of Biomechanical Science and Engineering 12, no. 4 (2017): 17-00181.

63. Timoshenko, Stephen, S. Timoshenko, and J. N. Goodier. “Theory of Elasticity”. McGraw-Hill book Company, 1951.

64. Alderliesten T, Konings MK, Niessen WJ. Simulation of minimally invasive vascular interventions for training purposes. Comput Aided Surg. 2004;9(1-2):3-15. PMID: 15792932

65. Alderliesten T, Bosman PA, Niessen WJ.Towards a real-time minimally-invasive vascular intervention simulation system. IEEE Trans Med Imaging. 2007 Jan;26(1):128-32. PMID: 17243591

66. Alderliesten T, Konings MK, Niessen WJ. Modelling friction, intrinsic curvature, and rotation of guide wires for simulation of minimally invasive vascular interventions. IEEE Trans Biomed Eng. 2007 Jan;54(1):29-38. PMID: 17260853

67. Alderliesten T, Konings MK, Niessen WJ. Robustness and complexity of a minimally invasive vascular intervention simulation system. Med Phys. 2006 Dec;33(12):4758-69. PMID: 17278829.

68. Becherer, Nico, Jürgen Hesser, Ulrike Kornmesser, Dietmar Schranz, and Reinhard Männer. "Interactive physical simulation of catheter motion within mayor vessel structures and cavities for ASD/VSD treatment." In Medical Imaging, pp. 65090U-65090U. International Society for Optics and Photonics, 2007.

69. Tang, Wen, Pierre Lagadec, Derek Gould, Tao Ruan Wan, Jianhua Zhai, and Thien How. "A realistic elastic rod model for real-time simulation of minimally invasive vascular interventions." The Visual Computer 26, no. 9 (2010): 1157-1165.

70. [70] Huang, Dongjin, Yin Wang, Pengbin Tang, Zhifeng Xie, Wen Tang, and Youdong Ding. "Modelling and Simulation of Multi-frictional Interaction Between Guidewire and Vessel." In International Conference on Image and Graphics, pp. 524-537. Springer International Publishing, 2015.

71. Chembrammel, Pramod, Habib Mohd Younus, and Thenkurussi Kesavadas. "Modelling and Simulation of Guide-Wire Interaction With Vessel Using Constrained Multibody Dynamics." In ASME 2013 International Mechanical Engineering Congress and Exposition, pp. V04AT04A083-V04AT04A083. American Society of Mechanical Engineers, 2013.

72. Nuti, Sravani, Annie Ruimi, and J. N. Reddy. "Modelling the dynamics of filaments for medical applications." International Journal of Non-Linear Mechanics 66 (2014): 139-148.

73. Liu, Taoming, Nate Lombard Poirot, Dominique Franson, Nicole Seiberlich, Mark A. Griswold, and M. Cenk Cavusoglu. "Modelling and Validation of the Three-Dimensional Deflection of an MRI-Compatible Magnetically Actuated Steerable Catheter." IEEE Transactions on Biomedical Engineering 63, no. 10 (2016): 2142-2154.

74. Khoshnam, Mahta, Mahdi Azizian, and Rajni V. Patel. "Modelling of a steerable catheter based on beam theory." In Robotics and Automation (ICRA), 2012 IEEE

International Conference on, pp. 4681-4686. IEEE, 2012.

75. Lawton, Wayne, Raghu Raghavan, S. R. Ranjan, and Raju Viswanathan. "Ribbons and groups: a thin rod theory for catheters and filaments." Journal of Physics A: Mathematical and General 32, no. 9 (1999): 1709.

76. Zhao, Helen, Robert J. Stango, Yuanming Chen, and Rick Albano. "Aspects of contact force and path configuration generated during catheter navigation." In Proceedings of the 2009 Spring Simulation Multiconference, p. 174. Society for Computer Simulation International, 2009.

77. Wang, Yanzhen, Ferdinand Serracino-Inglott, Xiaodong Yi, Xue-Feng Yuan, and Xue-Jun Yang. "Real-time Simulation of Catheterization in Endovascular Surgeries." Computer Animation and Virtual Worlds 27, no. 3-4 (2016): 185-194.

78. Bro-Nielsen, M. "Simulation techniques for minimally invasive surgery." Minimally Invasive Therapy & Allied Technologies 6, no. 2 (1997): 106-110.

79. Back, Junghwan, Thomas Manwell, Rashed Karim, Kawal Rhode, Kaspar Althoefer, and Hongbin Liu. “Catheter contact force estimation from shape detection using a real-time Cosserat rod model”, In Intelligent Robots and Systems (IROS), 2015 IEEE/RSJ International Conference on, pp. 2037-2042. IEEE, 2015.

80. Gao, Zhan-Jie, Xiao-Liang Xie, Gui-Bin Bian, Jian-Long Hao, Zhen-Qiu Feng, and Zeng-Guang Hou. "Fast and stable guidewire simulator for minimally invasive vascular surgery." In 2015 37th Annual International Conference of the IEEE Engineering in Medicine and Biology Society (EMBC), pp. 5809-5812. IEEE, 2015.

81. Pai, Dinesh K. "Strands: Interactive simulation of thin solids using cosserat models." In Computer Graphics Forum, vol. 21, no. 3, pp. 347-352. Blackwell Publishing, Inc, 2002.

82. Shao-Hua Mi, Zeng-Guang Hou, Fan Yang, Xiao-Liang Xie, and Gui-Bin Bian, “A Multi-body Mass-spring Model for Virtual Reality Training Simulators Based on a Robotic Guide Wire Operating System”, Proceeding of the IEEE International Conference on Robotics and Biomimetics (ROBIO) Shenzhen, China, December 2013.

83. YP Wang, CK Chui, YY Cai, KH Mak, “Topology Supported Finite Element Method Analysis of Catheter/ Guidewire Navigation in Reconstructed Coronary Arteries”, IEEE, Computers in Cardiology 1997 Vol 24.

84. Mi, Shao-Hua, Zeng-Guang Hou, Fan Yang, Xiao-Liang Xie, and Gui-Bin Bian. “A collision response algorithm for 3D virtual reality minimally invasive surgery simulator”, In The 26th Chinese Control and Decision Conference (2014 CCDC), pp. 4594-4599. IEEE, 2014.

85. Meier, Ullrich, Oscar López, Carlos Monserrat, Mari C. Juan, and M. Alcaniz. “Real-time deformable models for surgery simulation: a survey”, Computer methods and programs in biomedicine 77, no. 3 (2005): 183-197.

86. G. Arfken, Mathematical methods for physicists. San Diego, California: Academic Press, Inc., 1985.

87. Wang, Weiwei, Shuai Li, Hong Qin, and Aimin Hao. "Novel, Robust, and Efficient Guidewire Modelling for PCI Surgery Simulator Based on Heterogeneous and Integrated Chain-Mails." In Computer-Aided Design and Computer Graphics (CAD/Graphics), 2015 14th International Conference on, pp. 105-112. IEEE, 2015.

88. Schafer, Sebastian, Vikas Singh, Kenneth R. Hoffmann, Peter B. Noël, and Jinhui Xu. "Planning image-guided endovascular interventions: guidewire simulation using shortest path algorithms." In Medical imaging, pp. 65092C-65092C. International Society for Optics and Photonics, 2007.

89. O'Flynn, Padraig M., Ellen T. Roche, and Abhay S. Pandit. "Generating an ex vivo vascular model." Asaio Journal 51, no. 4 (2005): 426-433.

90. Schaap, Michiel, Coert T. Metz, Theo van Walsum, Alina G. van der Giessen, Annick C. Weustink, Nico R. Mollet, Christian Bauer et al. "Standardized evaluation methodology and reference database for evaluating coronary artery centerline extraction algorithms." Medical image analysis 13, no. 5 (2009): 701-714.

91. Funamoto, Kenichi, Osamu Yamashita, and Toshiyuki Hayase. "Poly (vinyl alcohol) gel ultrasound phantom with durability and visibility of internal flow." Journal of Medical Ultrasonics 42, no. 1 (2015): 17-23.

92. ChangHo, Y. U., Hiroyuki KOSUKEGAWA, Keisuke MAMADA, Kanju KUROKI, Kazuto TAKASHIMA, and Kiyoshi YOSHINAKA. "Development of an in vitro tracking system with poly (vinyl alcohol) hydrogel for catheter motion." Journal of Biomechanical Science and Engineering 5, no. 1 (2010): 11-17.

93. Yu, Chang-Ho, Tae-Kyu Kwon, Chan Hee Park, Makoto Ohta, and Sung Hoon Kim. "Comparative analysis for evaluating the traceability of interventional devices using blood vessel phantom models made of PVA-H or silicone." Technology and Health Care 23, no. s2 (2015): S301-S310.

94. Surry, K. J. M., H. J. B. Austin, A. Fenster, and T. M. Peters. "Poly (vinyl alcohol) cryogel phantoms for use in ultrasound and MR imaging." Physics in medicine and biology 49, no. 24 (2004): 5529.

95. Takashima, Kazuto, Rei Shimomura, Takayuki Kitou, Hiroki Terada, Kiyoshi Yoshinaka, and Ken Ikeuchi. "Contact and friction between catheter and blood vessel" Tribology International 40, no. 2 (2007): 319-328.

96. Preim, Bernhard, and Charl P. Botha. Visual Computing for Medicine: Theory, Algorithms, and Applications. Newnes, 2013, chapter 21, pp 154-156.

97. Ding, Wenjing. Self-Excited Vibration: Theory, Paradigms, and Research Methods. Springer Science & Business Media, 2013, pp 374-375.

98. Jung, Jinwoo, R. Penning, Nicola J. Ferrier, and Michael R. Zinn. “Model validation and simulation studies: Effects of nonlinear internal device friction on continuum robotic manipulators”, In IEEE Int. Conf. Robotics and Automation. 2012.

99. Carter, F. J., M. P. Schijven, R. Aggarwal, T. Grantcharov, N. K. Francis, G. B.

Hanna, and J. J. Jakimowicz. "Consensus guidelines for validation of virtual reality surgical simulators." Surgical Endoscopy and Other Interventional Techniques 19, no. 12 (2005): 1523-1532.

100. Lang, Holger, Joachim Linn, and Martin Arnold. "Multi-body dynamics simulation of geometrically exact Cosserat rods." Multibody System Dynamics 25, no. 3 (2011): 285-312.

101. Tran, Phuong Toan, Gabrijel Smoljkic, Caspar Gruijthuijsen, Dominiek Reynaerts, Jos Vander Sloten, and Emmanuel Vander Poorten. "Position control of robotic catheters inside the vessel based on a predictive minimum energy model." In Systems, Man, and Cybernetics (SMC), 2016 IEEE International Conference on, pp. 004687-004693. IEEE, 2016.

102. Cheng, Xiao-Ran, Qing-Kun Song, Xiao-Liang Xie, Long Cheng, Li Wang, Gui-Bin Bian, Zeng-Guang Hou, Tingwen Huang, and Pusit Prasong. "A fast and stable guidewire model for minimally invasive vascular surgery based on Lagrange multipliers." In Information Science and Technology (ICIST), 2017 Seventh International Conference on, pp. 109-114. IEEE, 2017.

103. Xu, Lei, Yong Tian, Xuhui Jin, Jie Chen, Sebastian Schafer, Kenneth Hoffmann, and Jinhui Xu. "An improved endovascular guidewire position simulation algorithm." In Biomedical Imaging (ISBI), 2012 9th IEEE International Symposium on, pp. 1196-1199. IEEE, 2012.

104. Ahn, Woojin, Hyun Soo Woo, Jun Yong Kwon, Jae Kyung Joo, Doo Yong Lee, and Sun Young Yi. "Model of frictional contact with soft tissue for colonoscopy simulator." In Systems, Man and Cybernetics, 2005 IEEE International Conference on, vol. 3, pp. 2714-2719. IEEE, 2005.

105. Mongrain, R., K. Kandarpa, A. Garon, O. F. Bertrand, and M. Bertrand. "Study of catheter designs and drug mixing processes using 2D steady numerical simulations." Medical and Biological Engineering and Computing 37, no. 1 (1999): 64-70.

106. Ionita, Ciprian N., Maxim Mokin, Nicole Varble, Daniel R. Bednarek, Jianping Xiang, Kenneth V. Snyder, Adnan H. Siddiqui, Elad I. Levy, Hui Meng, and Stephen Rudin. "Challenges and limitations of patient-specific vascular phantom fabrication using 3D Polyjet printing." In Proceedings of SPIE--the International Society for Optical Engineering, vol. 9038, p. 90380M. NIH Public Access, 2014.

4. A Multi-Body Dynamic Model of Guidewires

Hoda Sharei, Jeroen Kieft, Kazuto Takashima, Norihiro Hayashida, John J. van den Dobbelsteen, Jenny Dankelman

Submitted

Background: During Percutaneous Coronary Interventions, a guidewire is used as an initial way of accessing a specific vasculature. There are varieties of guidewires on the market and choosing an appropriate one for each case is critical for a safe and successful intervention. The main objective of this study is to predict the behavior of the guidewire and its performance in a vasculature prior to the procedure. Therefore, we evaluate the effectiveness of different mechanical properties of the guidewire on the translational behavior.

Method: A 2D model has been developed in which a guidewire is considered as a set of small rigid segments connected to each other by revolute joints. These joints have two degrees of freedom to allow rotation. Linear torsional springs and dampers are applied in each joint to account for the elastic properties of the guidewire; the elastic properties have been measured for two commercially available guidewires (Hi-Torque Balance Middleweight Universal II-Abbot and Amplatz Super Stiff -Boston Scientific) and these are used in the model. The effect of bending stiffness of the guidewire and also friction between guidewire and vasculature on its behavior are investigated. The results are validated with actual movement of the guidewires in a simple phantom model.

Results: Behavior of a guidewire in a vasculature was predicted using the developed model. The results of both simulation and experiment show that the translational behavior of a guidewire is influenced by its mechanical properties and by the friction between the guidewire and vasculature.

Conclusion: The present study is the first step to develop a complete model which can predict the behavior of a guidewire inside the vasculature. We compared the tip trajectory for two commercial guidewires in one vasculature geometry. In future, this kind of knowledge might support not only the interventionist in choosing the best suitable guidewire for a procedure but also the designer to optimize new instrument to have the desired behavior.

4.1 Introduction

Over the past decade, more than 7.4 million people have died as a result of Coronary Artery Disease (CAD), which is the narrowing or blockage of coronary arteries [1]. Percutaneous Coronary Intervention (PCI) is a minimally invasive procedure for diagnosis and treatment of CAD [2]. During PCI, initially a guidewire is used to access a specific vasculature. The choice of guidewire plays an important role in the success of an intervention. Although there are different types of guidewires, a systematic classification of the characteristics of guidewires has not yet been defined and there is no metric to select an appropriate guidewire for a specific vasculature. Hence, interventionists tend to perform the procedure on the basis of their experience. The main objective of this study is therefore to predict the behavior of the guidewire in a vasculature and its performance prior to the procedure. To achieve this, we have developed a computationally efficient computer-based model and have endeavored to investigate a relation between different mechanical properties, focusing on the stiffness of the guidewire and friction, and its behavior. We start this paper by reviewing the essential preliminaries of components and performance characteristics of guidewires. Moreover, the geometrical properties of the selected vasculature is presented. Then, the developed model, a short introduction on the rigid multibody dynamics technique, the simulation environment and experimental set-up are explained. Finally, we discuss the results on the basis of the properties of two commercial guidewires and evaluate the accuracy of the model by a validation experiment.

4.2 Method

4.2.1 Preliminaries

Guidewire: A guidewire is a long, thin, and flexible wire commonly used in combination with a catheter to facilitate the navigation through the vasculature's branches. Each guidewire consists of three main components: *Core*, *Distal Tip* and *Covering*. The core (or central part) of the guidewire is commonly made of stainless steel, nitinol or combination of them. The material, diameter, and tapering of the core influence the performance of the guidewire. The distal tip, which is situated inside the vasculature during the procedure, has either a one piece (core-to-tip) or a two-piece (shaping ribbon) tip design and its length and diameter are influential in specifying the function of the guidewire. The covering varies along the length of the guidewire; at the distal tip, coils or a polymer are mostly used to provide more flexibility. Moreover, the distal part often has either a hydrophilic or hydrophobic coating to reduce the friction between the guidewire and the vasculature, and between the guidewire and the interventional devices over the guidewire (e.g., catheter or stent).

The wide range of guidewires available in the market is the result of a change in these components. In other words, the construction of a guidewire and its performance are inextricably interwoven and the smallest variation in each of the components changes the overall properties of the guidewire and its performance [3-12].

To describe performance of a guidewire, several terms are used in literature such as pushability, trackability, bending stiffness/ flexibility, torqueability, etc [5,11-17]. Based on these characteristics one classification for guidewires is presented as: starting (e.g., Balance Middleweight), selective (e.g., Universal II, Glidwire) and exchange guidewires (e.g., Amplatz Super Stiff). This classification is mainly based on the requirements during different phase of a procedure [11] and although it gives a general grouping, the choice of a guidewire within each group is still subjective. We will focus on the influence of the flexibility/ stiffness of the guidewire on its translational motion. Flexibility/ stiffness is the resistance of a guidewire against bending deformation (also known as bending stiffness, bending rigidity, and flexural rigidity). To measure this property, the guidewire must be intact and unused, since cutting the guidewire into segments would have disrupted the structural integrity of the wire and produced inaccurate results. We have measured the bending stiffness of two guidewires with a 3-point bending test method at different places along the length of new guidewires. In this method, the guidewire is set between two supports (Figure 1). A semicircular loading nose, placed at a point midway between the supports, is displaced at a test speed of *1 mm/sec*. To limit the influence of the gravity, the force is applied horizontally. By means of an attached 10-*N* load cell (Kyowa Electronic Instruments Co., Ltd.), the reaction force experienced by the loading nose is continuously measured. For consistency in the results, the measurements were done in the middle of every 30mm, for a length of 150 mm from the distal side (in total 5 points). The test was performed three times for each segment and the average is presented. Finally, *EI* is a measure for the bending stiffness and is calculated by [18]:

$$EI = \frac{Fl^3}{48d} \quad (\mathbf{Nm^2}) , \qquad (2)$$

in which *F* is the applied force, *l* is the length of the guidewire, *d* is the maximum displacement of the segment. As *EI* consists of two terms: *E* is the Young's Modulus, and *I* is the cross sectional inertia. Therefore, material and diameter of the core of the guidewire influence the bending stiffness.

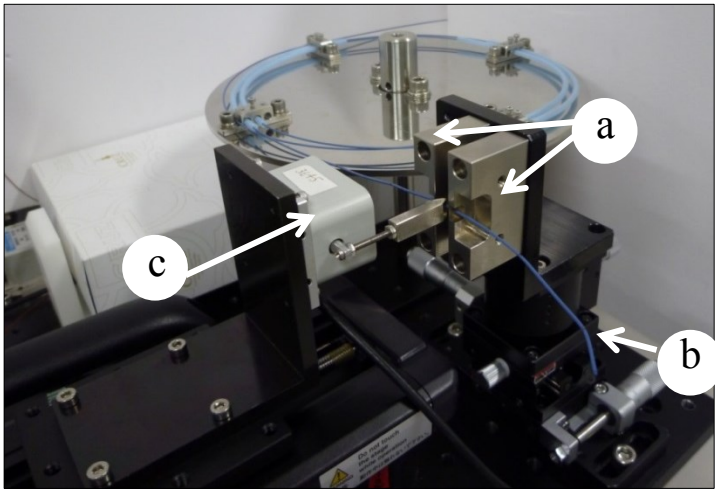

Figure 1: Experimental setup: 3-point bending test: a) supports, b) guidewire, c) load cell.

Vasculature: During interventional procedures, it is not only the properties of the guidewire but also the properties of the vasculature that influence the choice of guidewire. Depending on the properties of a vasculature such as its diameter, angle in bifurcation, stiffness of the wall, etc., a different guidewire has to be chosen. Recent research on extracting the geometry of the vasculatures has yielded some interesting results [19-23] which inspired us with our phantom model (Figure 2). Our vasculature model includes branches with diameters between 2 mm and 8 mm, and bifurcation angels between 60 degree and 120 degree. The ProJet 3500 HD 3D printer is used to print the phantom model. Data regarding wall stiffness is extracted from the catalogue of the printer (material: VisiJet M3 Crystal, flexural strength: 49 MPa) [24]. The guidewire can't deform the vasculature phantom due to high stiffness of the material. Although we can take into account the deformation of the vascular wall in the simulation model, due to high value of the wall stiffness in the phantom model deformation will be neglected.

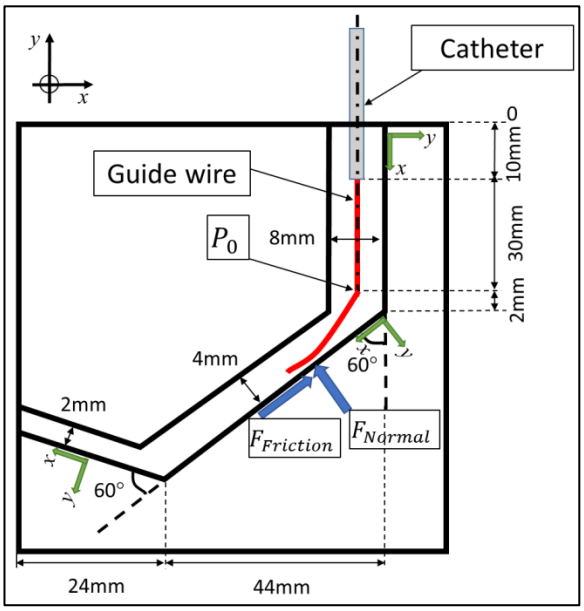

Figure 2: Schematic of guidewire and vasculature interaction forces: $\mathbf{P_0}$ is the initial position of the guidewire tip.

4.2.2 Model

Modelling guidewires and catheters and their behavior within the vasculature, for different purposes, is an emerging research area and a variety of techniques have been used [3, 22, 25-38]. We have developed a multibody dynamic model to simulate the translational motion of a guidewire. An advantage of this method is that because of its simple structure, it is easy to understand and in comparison with FEM modelling, it is very fast. Moreover, adding other phenomena such as friction and/or material properties to different parts of the body is easier to incorporate [39]. In the following, we will first discuss the applied forces to the guidewire while navigating inside the vasculature. These forces play an important role in the orientation of the guidewire. Then, the multibody dynamics method will be explained to pave the way to formulate the equations of motion for the guidewire model.

Forces on the guidewire inside the vasculature: Orientation of a guidewire inside the vasculature is determined by the applied forces (Figure 2.a). Due to the contact with the vascular wall, collision and friction are considered as the most influential forces [40-41]. In case of a collision, detecting and responding to it are two important parts of the simulation. In our model, we have implemented a simple collision detection algorithm in which a collision occurs when the distance between the guidewire and the vasculature wall is smaller than the guidewire diameter. With x and y being the position in x- and y-direction, we apply Eq. 2 and Eq. 3 to add constraints to the contact force:

$$|\mathbf{x}| \leq \frac{\mathbf{1}}{\mathbf{2}}\mathbf{l_v}\,, \tag{3}$$

$$|\mathbf{y}| \leq \frac{\mathbf{1}}{\mathbf{2}}\mathbf{t_v} + \mathbf{r_{wire}}\,, \tag{4}$$

in which l_v and t_v are the length and the thickness of the vasculature, respectively and r_{wire} is the radius of the guidewire. If the contact constraints are met, regarding the collision response, a normal force is exerted onto the wire. Since the vasculature is modeled as a spring-damper-system, the normal force consists of a spring-component, calculated using the penetration depth (u) and a damping component calculated with the penetration velocity. This force prevents the guidewire from penetrating inside the vasculature wall and Hooke's law is used to account for it (the wall stiffness is based on material properties used in the phantom model):

$$\mathbf{u} = (\frac{\mathbf{1}}{\mathbf{2}}\mathbf{t_v} + \mathbf{r_{wire}} - |\mathbf{y}|)\,, \tag{5}$$

$$\mathbf{F_n} = -\mathbf{k_w}\cdot\mathbf{u} - \mathbf{c_w}\cdot\mathbf{v_y}\,, \tag{6}$$

in which k_w and c_w are the spring stiffness and the damping coefficient and v_y is the speed of guidewire in y- direction. For the friction between the guidewire and the vasculature wall, the Coulomb friction model is used; the friction force is calculated from the normal force (F_n) by multiplying it with a friction coefficient (μ):

$$F_f = F_n \cdot \mu \cdot \left(-\frac{v_x}{|v_x|}\right), \tag{7}$$

in which v_x is the speed of guidewire in x-direction. When $|v_x| = 0$ (namely, static condition), F_f is zero. Therefore, only dynamic friction is considered in this equation. The value for the friction coefficient is based on information provided in [48].

Multibody dynamics model: The multibody dynamics approach follows a discrete representation of a continuum body. The body is discretized to smaller segments interconnected with each other by joints [42-44]. The dynamic behavior of the total system is investigated by deriving and solving the equations of motion of the whole body [27-28, 45-47]. The segments are considered as rigid bodies, i.e. each segment can translate and rotate but its shape is fixed.

Based on the above-explained theory of multibody dynamics, we consider the guidewire as a set of rigid segments. As the guidewire is under planar motion, revolute joints are used between each two segments to allow for rotation. The length of the segments are variable: the segments at the distal end have shorter length than at the proximal end (Figure 3). This is due to the variation in mechanical properties of the guidewire along the length: more flexible at the distal side and more stiff at the proximal side. In the modelling, the proximal side of the guidewire is inserted into a catheter which is fixed and is considered as the initial position of the guidewire and the distal side of guidewire, which is outside the catheter, navigates inside the vasculature.

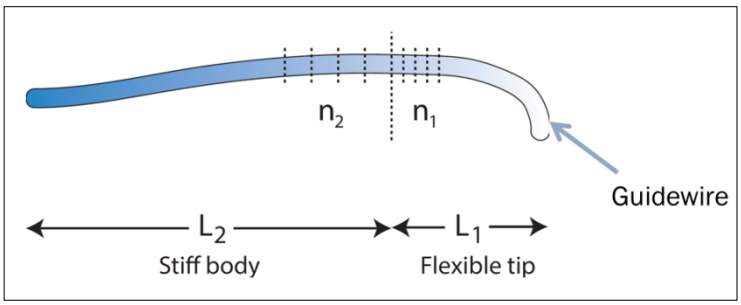

Figure 3: Visual representation of guidewire model: the guidewire is considered as a chain of small rigid segments connected to each other by joints.

Mathematical formulation of equations of motion: We defined the relative position of each two segments by means of the relative angle between them (θ_i). Thus, the motion is described by the generalized coordinates $[\theta_1, \theta_2, \dots, \theta_n]$ and the coordinates of each joint α_i is expressed as:

$$\alpha_i = T_i(\theta_i) \,, \tag{8}$$

in which T_i is the transformation matrix. The corresponding velocity and acceleration of joint α_i in the new coordinate system are then

$$\dot{\alpha}_i = \frac{\partial T_i}{\partial \theta_i}\dot{\theta}_i \,, \tag{9}$$

$$\ddot{\alpha}_i = \frac{\partial T_i}{\partial \theta_i}\ddot{\theta}_i + \frac{\partial^2 T_i}{\partial \theta_i \partial \theta_j}\dot{\theta}_i\dot{\theta}_j \,. \tag{10}$$

To account for the bending stiffness of the guidewire, linear torsional springs and dampers are applied in the joints. From the mechanics of materials ([18]), the relation between the torque T_s and the angle of twist in a torsional spring is:

$$T_s = k(\theta - \theta_0) \,, \tag{11}$$

where k is the torsional spring stiffness, θ_0 is the neutral angle where restoring torque is zero and θ is the joint angle. In the same way, for the torsional viscous damper, we have:

$$T_d = C\dot{\theta} \,, \tag{12}$$

in which C is the torsional coefficient of viscous damping and $\dot{\theta}$ is the joint angular velocity. From [18] and based on Eqs. 10 and 11 , the differential equation of motion for a n-degree-of freedom system is written in the matrix form as:

$$M\ddot{\alpha} + D\dot{\alpha} + K(\alpha - \alpha_0) = Q\,, \qquad (13)$$

where M is the mass matrix, D and K are damping and stiffness matrices, α_0 is the angular position in equilibrium and Q is the vector of generalized non-conservative forces. As the mass of each segment of the guidewire is very small compared to its length, it can be neglected (i.e. $M \approx 0$). Substituting Eqs. 8 and 9 into Eq. 12, and conducting a number of simplifications, we have:

$$-D\dot{\theta} = -T^{T}(F + M_t) + K(\theta - \theta_0)\,, \qquad (14)$$

where T is the transformation matrix that transfers the global coordinates to local coordinates, F and M_t contain the applied forces and the applied moments, respectively. The derived equation (Eq.13) consists of a set of equations where all of them are needed to be solved at the same time (simultaneous or coupled equations [27]).

The developed model is based on the forward dynamic method, i.e. given initial conditions and applied forces and/or applied moments, over a given time interval to predict the motion. By applying a defined force to the proximal side of the guidewire, the tip moves by a speed of 2 mm/s.

4.2.3 Simulation

We simulated the translational motion of the guidewire inside the vasculature and assessed the effect of different parameters: bending stiffness of the guidewire, friction between guidewire and vasculature wall, and the transition of applied force on the guidewire. Moreover, as we discretized the guidewire to smaller segments, the influence of number of segments (*n*) on the computation time and the accuracy of simulation is investigated. The measured data of Hi-Torque Balance Middleweight Universal II-Abbot and Amplatz Super Stiff -Boston Scientific guidewires (Figure 5) are used regarding the bending stiffness. We will refer to these two guidewires as Universal and Amplatz. The model is developed in a MATLAB/Simulink (The MathWorks, Inc) environment. In Table 1 and Figure 5, the guidewires' parameters used in the simulation are listed.

Table 4: Guidewires data

Name & Trade	Diameter (mm)	Core Material	Flexible Tip (mm)	Length used in simulation (mm)
Amplatz Super Stiff (Boston Scientific)	0.89	Stainless steal	70	150
Universal II (Abbot Vascular)	0.36	Nitinol	45	150

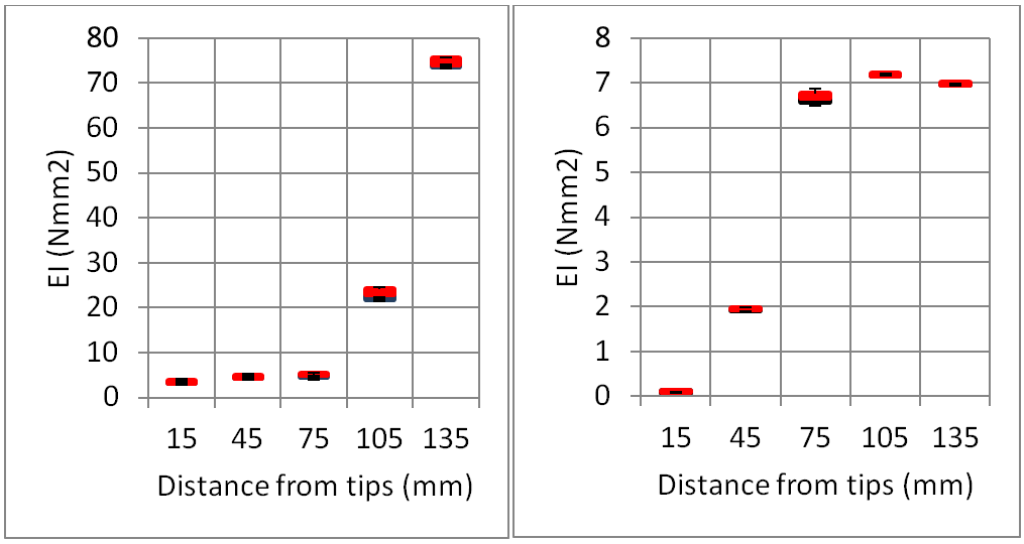

(a) (b)

Figure 4: Bending stiffness measurement: a) Amplatz, b) Universal.

4.2.4 Experiment

The experimental setup for the validation is shown in Figure 4. Details about the set-up are explained in [44]. We inserted the two guidewires, which were also used in the simulation (Universal and Amplatz), into the phantom model using a two-axis automatic stage (Sigma Koki Co., Ltd.,SGSP20-85(X), SGSP-40YAW). The guidewire is manipulated by pushing and pulling at the proximal side. One camera (15 frames per second, 1920 × 1080 screen resolution (Logicool)), positioned in front of the model, is used to record the trajectory during the experiment. Furthermore, 10 N load cells are placed under the phantom model to measure the applied forces in y-direction. Since the applied forces for Universal guidewire were very small, we have changed the load cells to 1N to be able to measure small forces. Finally, to evaluate the accuracy of the simulation, the trajectory results are compared and the root-mean-square (RMS) is calculated to measure error as follow:

$$\text{Error} = \sqrt{\frac{1}{\text{i}}\sum_i \sum_j (\text{P}_{tip}^{V}(\text{i}) - \text{P}_{\text{tip}}^{S}(\text{j}))^2}\,, \qquad (15)$$

in which P_{tip}^{V} and P_{tip}^{S} are the position of the distal tip in the experiment and in the simulation, respectively.

4.3 Results

4.3.1 Bending stiffness

Figure 5 shows the results of bending stiffness measurement for the two guidewires: Amplatz and Universal. It can be seen that, although the bending stiffness is non-homogeneous along the length of the guidewire(s), it follows almost the same pattern for

both guidewires: first a considerable flexibility at the distal side, then an abrupt increase in the transition part toward the proximal side. In Figure 6 the propagation of the two guidewires with different bending stiffness is shown. These results show that the flexibility of a guidewire impacts its behavior during advancement: a higher flexibility results in a different trajectory and more contact with the vasculature wall.

4.3.2 Number of segments and error measurement

The total number of segments (n) to define the length of the guidewire in the simulation model has a significant effect on the behavior and the computation time. Figure 7 shows that lower number of segments results into bigger error. On the other hand, increasing the number above a certain threshold does not change the behavior anymore, but the computation time increases (Table. 2). Moreover, comparing the results for two guidewires show that the stiffer guidewire (Amplatz) is more sensitive to the number of segments.

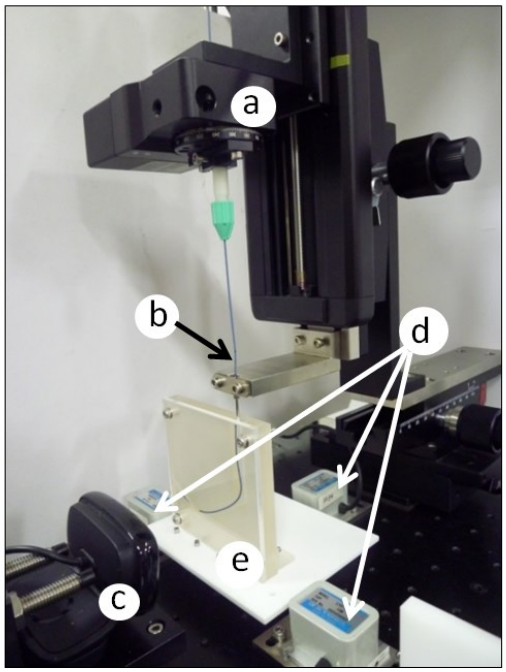

Figure 5: Experimental set-up: a) automatic stage, b) guidewire, c) camera, d) load cell, e) phantom model.

4.3.3 Friction coefficient and applied forces

Figure 8 shows the transition of applied force between the guidewire and vasculature wall along the y-axis for both Amplatz and Universal guidewires in the experiments. These results show that the contact force is much higher for the stiffer guidewire. Furthermore, the contact force is influenced by the geometry of vasculature, i.e., there are peaks in the applied force in the corners. At t=22 s in Figure 9, a small peak is seen which is due to the contact with the wall in the second corner. In Figure 9, the effect of friction for Amplatz guidewire is assessed and is shown that with a higher friction coefficient the contact force increases.

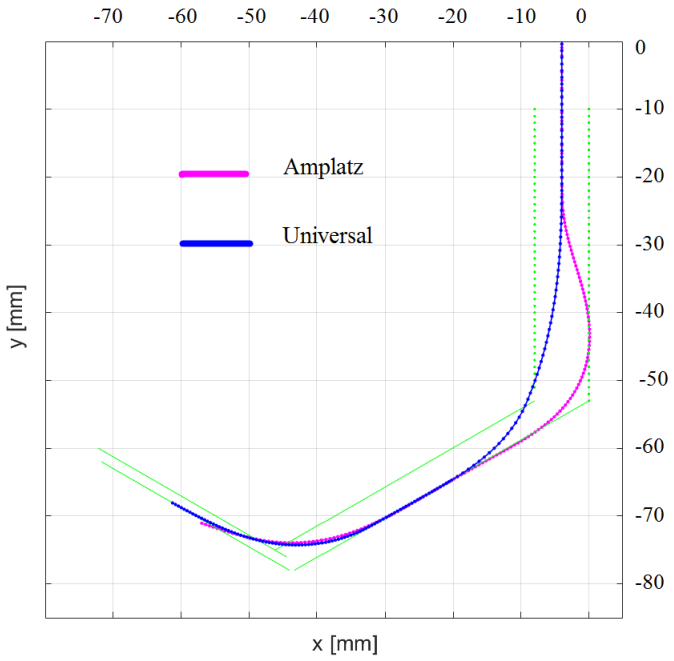

Figure 6: Comparing the trajectory of Amplatz and Universal guidewires in simulation for n=200.

Table 5: Simulation computation time for different number of segmentas and error measurment, friction coefficient= 0.4.

Guidewire	Number of segments	Computation time (s)	Error (mm)
Amplatz Super Stiff - Boston Scientific	20	4	4.91
	40	15	3.12
	100	96	1.68
	200	469	0.87
	400	3534	0.38
Universal II- Abbot Vascular	20	4	0.76
	40	14	0.70
	100	91	0.69
	200	455	0.56
	400	2857	0.56

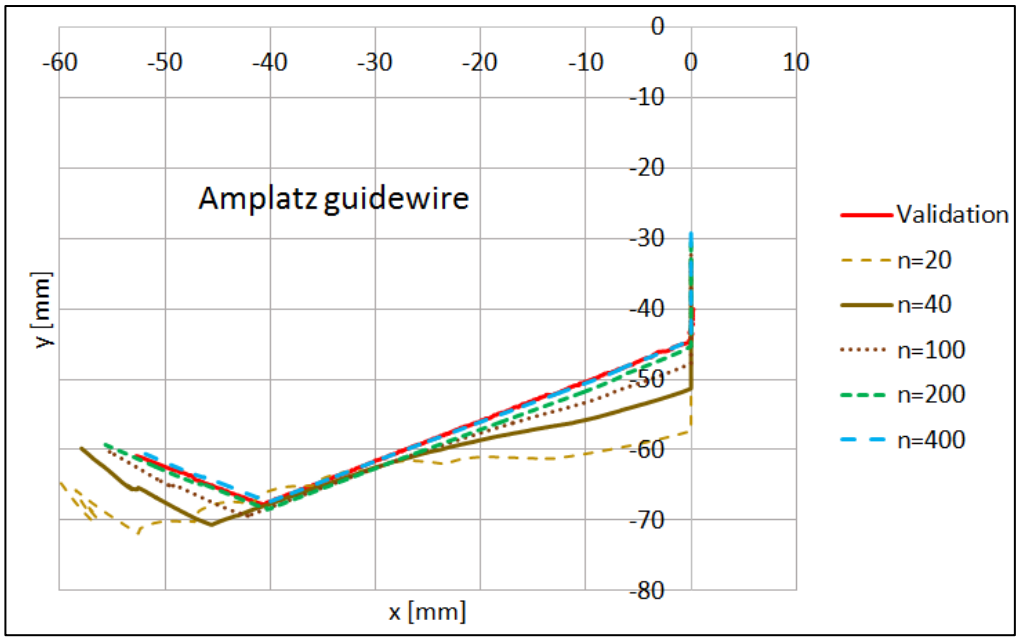

(a)

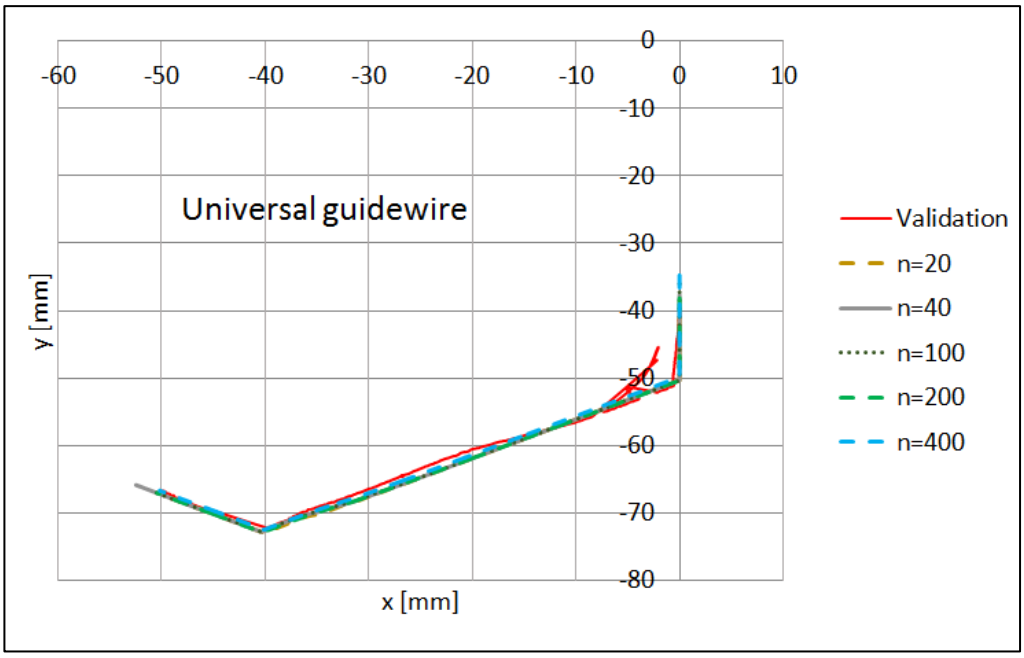

(b)

Figure 7: Trajectory of the tip of the guidewires in the simulation and the validation experiment: a) Amplatz, b) Universal.

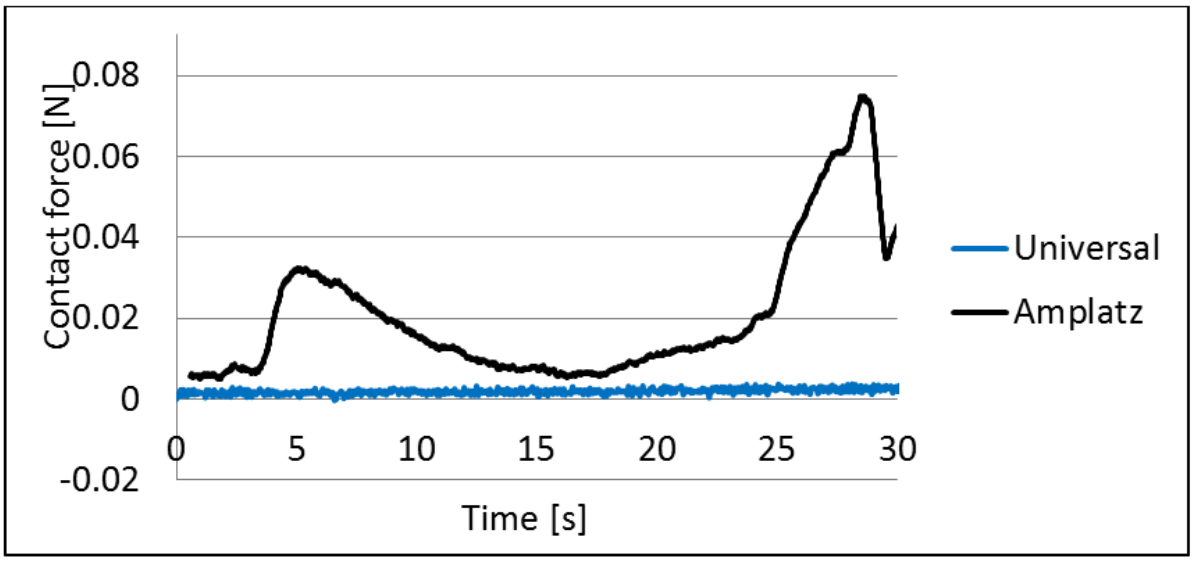

Figure 8: Comparing the transition of applied forces for two guidewires: Amplatz and Universal.

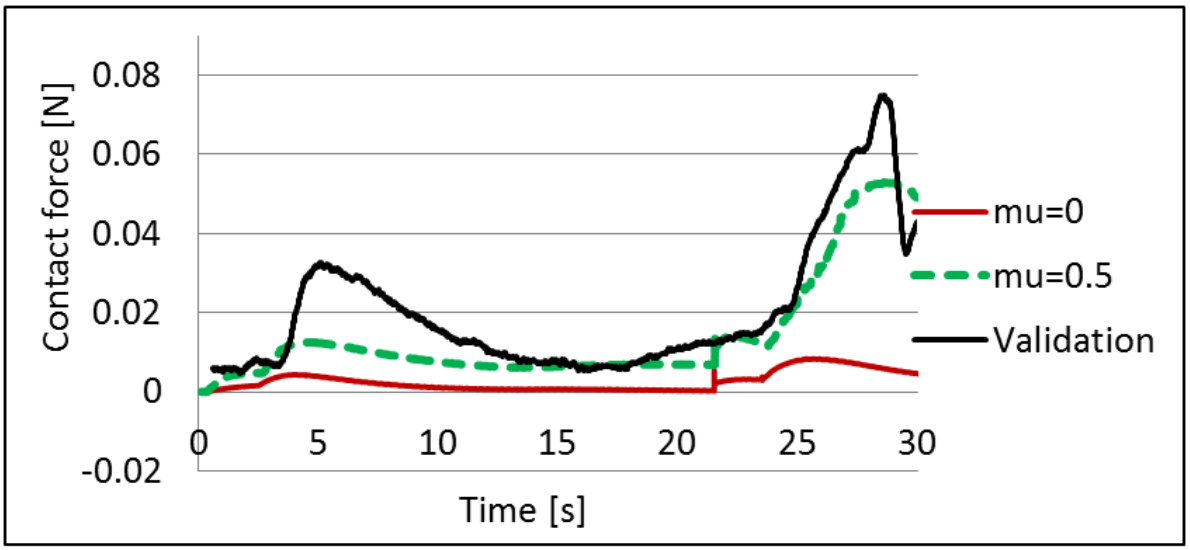

Figure 9: Comparing the transition of applied forces between guidewire and vasculature wall along y-axis in simulation (n=200) with different friction coefficient and the validation experiment: Amplatz guidewire.

4.4 Discussion

The goal of this study was to develop a guidewire simulation model and predict the behavior of the guidewire and its performance inside a vasculature. We have investigated the effect of bending stiffness and friction on the behavior of a guidewire and validated the results.

4.4.1 Bending stiffness

The results of bending stiffness measurement conform with the expected properties from a

guidewire: sufficient flexibility at the tip to pass through the vasculatures and high rigidity in the body to transfer the force from the proximal side. Moreover, the results confirm that the guidewire with nitinol have more flexibility than ones with stainless steel. The developed model has shown how these differences influence the behavior of the guidewire inside the vasculature: e.g., a guidewire with higher flexibility results in less contact force with the vasculature wall. This can be explained by the fact that the flexible tip deflects easier than the stiff one and thus, it needs less force to navigate. This property also affects the simulation time; in the simulation, the flexible one takes slightly longer than the stiff one to be computed (Table. 2).

4.4.2 Friction

We have changed the friction coefficient in the simulation to see the effect of this parameter on the behavior. It has been shown that more friction causes the guidewire to navigate with more bending and the tip applies more force to the vasculature wall.

4.4.3 Limitation

A 3D printed model has been used for the experiments. The material of this model has a flexural strength of 49 MPa which is very stiff relative to a guidewire, i.e., a guidewire cannot deform the vasculature. In the simulation, although it is possible to consider the deformation of the vascular wall, due to high value of the wall stiffness in the phantom model, deformation was neglected.

The differences between simulation and experiments may be due to the following reasons:

- Only the translational motion in 2D has been investigated. Thus, a perfect torque control is assumed.
- Estimated data regarding friction and high stiffness for vasculature wall are used.
- Plastic deformation of the guidewire during the experiments is ignored.

4.5 Conclusion

The present study is the first step to develop a complete model which can predict the behavior of a guidewire inside the vasculature. We have investigated the trajectory of two guidewires with different mechanical properties. We conclude that knowledge of the behavior of the guidewire might help the interventionist to choose an appropriate one. Furthermore, this information makes the design requirements clear and might help to optimize new instruments to follow the desired behavior.
For future research, we will extend the model to 3D with a deformable wall and the combination of a guidewire and a catheter will be modeled. Moreover, we will modify the simulation parameters to minimize the differences of the guidewire behavior in the experimental and simulation results.

Nomenclature

Symbol	Description	Symbol	Description
L	Guidewire length	T_s	Torque
λ_i	Segment length	k_w	Vasculature wall stiffness
n	Number of segments	k	Torsional spring stiffness
F_P	Applied force at the proximal side	θ_0	Neutral angle where restoring torque is zero
F_D	Received force at the distal side	T_d	Torsional viscous damper
m	Number of force measurements	C	Torsional coefficient of viscous damping,
F	Applied force	$\dot{\theta}$	Joint angular velocity
d	Maximum displacement	$\dot{\theta}_0$	Joint angular velocity where T_d is zero
E	Young's Modulus	M	Mass matrix
I	Cross sectional inertia	α_0	Angular position in equilibrium
M_t	Applied moment	Q	Generalized non-conservative forces
θ	Rotation angle	D	Damping matrix
K_t	Rotational stiffness	K	Stiffness matrix
α_i	Coordinates of joint i	t	Wall thickness
T	Transformation matrix that transfers the global coordinates to local coordinates		

References

1. World Health Organization — Who | The top 10 causes of death, http://www.who.int/mediacentre/factsheets/fs310/en/ [Accessed:15-April-2015].

2. Smith, SC. Jr., Dove, J. T., Jacobs, A. K., Kennedy, J. W., Kereiakes, D., Kern, M. J., Kuntz, R. E., Popma, J. J., Schaff, H. V., Williams, D.O., 2001, ACC/AHA guidelines of percutaneous coronary interventions (revision of the 1993 PTCA guidelines)executive summary, Journal of the American College of Cardiology Vol. 37, No. 8.

3. El-Khalili, Nuha H. ”Surgical Training on the World Wide Web.” PhD diss., The University of Leeds, 1999.

4. Lanzer, Peter, ed. Catheter-based Cardiovascular Interventions: A Knowledge-based Approach. Springer Science and Business Media, 2012, pp. 469-471.

5. Erglis, I. Narbute, D. Sondore, A. Grave, S. Jegere, Tools and Techniques: coronary guidewires, EuroIntervention, 2010.

6. Gabor G Toth, Masahisa Yamane, Guy R Heyndrickx, ”How to select a guidewire: technical features and key characteristics”, Heart heartjnl-2013-304243, Published Online First: 17 June 2014.

7. Craig Walker, ”Guidewire Selection for Peripheral Vascular Interventions”, Endovascular Today May 2013.

8. Antonio Colombo, Rade Babic, and Simon Corbett, “Coronary guidewires”, Problem Oriented Approaches in Interventional Cardiology, Chap 2, p. 9-19, ISBN-10 1 84184 631 7, 2007.

9. Vijay S. Ramanath and Craig A. Thompson, “Guidewires and Angioplasty Balloons: The Primer”, Textbook of Cardiovascular Intervention, 2014, p. 91-98.

10. Ellis SG, Holmes DR, “Strategic approaches in coronary intervention”, 3rd edition, 2005, p.91-100.

11. Peter A. Schneider, ”Endovascular Skills: Guidewire and Catheter Skills for Endovascular Surgery”, Third Edition, Ch. 5, ISBN: 1-4200-6937-3 (Hardcover), 2008.

12. von Schmilowski, E., and R. H. Swanton. ”Fundamentals.” Essential Angioplasty (2012): Ch.2.

13. Topaz, On, ed. Lasers in Cardiovascular Interventions. Springer, 2015, pp 8-9.

14. Schmidt W, Lanzer P, Behrens P, Topoleski LD and Schmitz KP, A, ”Comparison of the mechanical performance characteristics of seven drug-eluting stent systems”, Catheter Cardiovasc Interv 73:350360, 2009.

15. Brandt, W. Schmidt, P. Behrens, K.-P. Schmitz,”The effect of different guide wires on the trackability of coronary stent delivery systems”, Biomedical Engineering, Volume 57, Issue SI-1 Track-S, Pages 880881, September 2012

16. Sundeep Mishra, Vinay K Bahl, ”Curriculum in Cath Lab: Coronary Hardware-Part

II: Guidewire Selection for Coronary Angioplasty", Indian Heart J. 2009; 61:178-185.

17. Sutou, Y., K. Yamauchi, M. Suzuki, A. Furukawa, T. Omori, T. Takagi, R. Kainuma, M. Nishida, and K. Ishida. "High maneuverability guidewire with functionally graded properties using new superelastic alloys." Minimally Invasive Therapy and Allied Technologies 15, no. 4 (2006): 204-208.

18. Leonard Meirovitch, "Fundamentals of Vibrations",pp.23-39, ISBN 0071181741, 2000.

19. Pflederer, Tobias; Ludwig, Josef; Ropers, Dieter; Daniel, Werner G.; Achenbach, Stephan; "Measurement of Coronary Artery Bifurcation Angles by Multidetector Computed Tomography", Investigative Radiology: November 2006 - Volume 41 - Issue 11 - pp 793-798, doi: 10.1097/01.rli.0000239318.88270.9f

20. J T Dodge Jr; B G Brown; E L Bolson; H T Dodge, "Lumen diameter of normal human coronary arteries. Influence of age, sex, anatomic variation, and left ventricular hypertrophy or dilation", Circulation, 1992; 86: 232-246, doi: 10.1161/01.CIR.86.1.232

21. Helene clogenson, "MRI-Compatible Endovascular Instruments: Improved Maneuverability during Navigation", PhD Thesis, 2014.

22. M. K. Konings, E. B. van de Kraats, T. Alderliesten, W. J. Niessen, "Analytical guide wire motion algorithm for simulation of endovascular interventions", Medical and Biological Engineering and Computing 2003, Volume 41, Issue 6, pp 689-700.

23. Tobias Pflederer, Josef Ludwig, Dieter Ropers, Wernr G Daniel, Stephan Achenbach, "Measurement of coronary artery bifurcation angles by multidetector computed tomography", Investigative Radiology, Vol 41: 793798, 2006.

24. http://ja.3dsystems.com/sites/www.3dsystems.com/files/projet_3500_plastic_0115_usen_web.pdf (accessed on 25/1/2017).

25. Vincent Guilloux, Pascal Haigron, Cemil Goksu, Carine Kulik, Antoine Lucas, "Simulation of guidewire navigation in complex vascular structures", Proc. SPIE 6141, Medical Imaging 2006.

26. Rosen, Joseph M., Hooman Soltanian, Richard J. Redett, and Donald R. Laub. "Evolution of virtual reality [Medicine]." Engineering in Medicine and Biology Magazine, IEEE 15, no. 2 (1996): 16-22.

27. K. Ikuta, K. Iritani, J. Fukuyama, and M. Takeichi, "Portable virtual endoscope system with force and visual display for insertion training", In Proc. of the IEEE/RSJ International Conference on Intelligent Robots and Systems (IROS), volume 1, pages 720726, 2000.

28. Markus Kukuk, "A Model-Based Approach to Intra operative Guidance of Flexible Endoscopy", PhD theisi, Princeton, 2002.

29. Seo, Jong-Hwi, Il-Ho Jung, Tae-Won Park, and Jang-Bom Chai. "Dynamic analysis of a multibody system including a very flexible beam element", JSME International Journal

Series C Mechanical Systems, Machine Elements and Manufacturing 48, no. 2 (2005): 224-233.

30. T. Alderliesten, ”Simulation of minimally-invasive vascular interventions for training purposes”, PhD thesis, Utrecht University, The Netherlands, 2004.

31. Wen Tang, Tao Ruan Wan, Derek A. Gould, Thien How, and Nigel W. John, ”A Stable and Real-Time Nonlinear Elastic Approach to Simulating Guidewire and Catheter Insertions Based on Cosserat Rod”, IEEE TRANSACTIONS ON BIOMEDICAL ENGINEERING, VOL. 59, NO. 8, AUGUST 2012.

32. Shao-Hua Mi, Zeng-Guang Hou, Fan Yang, Xiao-Liang Xie, and Gui-Bin Bian, ”A Multi-body Mass-spring Model for Virtual Reality Training Simulators Based on a Robotic Guide Wire Operating System”, Proceeding of the IEEE International Conference on Robotics and Biomimetics (ROBIO) Shenzhen, China, December 2013.

33. YP Wang, CK Chui, YY Cai, KH Mak,”Topology Supported Finite Element Method Analysis of CathetedGuidewire Navigation in Reconstructed Coronary Arteries”, IEEE, Computers in Cardiology 1997 Vol 24.

34. Wang Y, Chui C, Lim H, ”Real-time interactive simulator for percutaneous coronary revascularization procedures”, Computer Aided Surgery 1998;3:21127.

35. Zirui Li, Chee-Kong Chui, James H. Anderson, Xuesong Chen, Xin Ma, Wei Hua, Qunsheng Peng, Yiyu Cai, Yaoping Wang, Wieslaw L. Nowinski, ”Computer environment for interventional neuroradiology procedures Zirui”, SIMULATION and GAMING, Vol. 32 No. 3, September 2001.

36. Sebastian Schafer, Vikas Singh, Peter B. Noel, Alan M.Walczak, Jinhui Xu, Kenneth R. Hoffmann, ”Real-time endovascular guidewire position simulation using shortest path algorithms”, International Journal of Computer Assisted Radiology and Surgery, November 2009, Volume 4, Issue 6, pp 597-608.

37. J T Dodge Jr, B G Brown, E L Bolson, H T Dodge, ”Lumen diameter of normal human coronary arteries. Influence of age, sex, anatomic variation, and left ventricular hypertrophy or dilation”, Circulation, Vol 86:232246, 1992.

38. Jitendra Khatait, “Motion and force transmission of a flexible instrument inside a curved endoscope”, PhD thesis, University of Twente, (2013).

39. Burgner-Kahrs, Jessica, D. Caleb Rucker, and Howie Choset. "Continuum robots for medical applications: A survey." IEEE Transactions on Robotics 31, no. 6 (2015): 1261-1280.

40. Olaf Korner, Reinhard Manner, ”Implementation of a Haptic Interface for a Virtual Reality Simulator for Flexible Endoscopy”, 11th Symposium on Haptic Interfaces for Virtual Environment and Teleoperator Systems, 2003.

41. Wei, Peng, Zhen-Qiu Feng, Xiao-Liang Xie, Gui-Bin Bian, and Zeng-Guang Hou. ”FEM-based guide wire simulation and interaction for a minimally invasive vascular surgery training system.” In Intelligent Control and Automation (WCICA), 2014 11th World

Congress on, pp. 964-969. IEEE, 2014.

42. Valembois, R. E., Paul Fisette, and Jean-Claude Samin. ”Comparison of various techniques for modelling flexible beams in multibody dynamics.” Nonlinear Dynamics 12, no. 4 (1997): 367-397.

43. Javier Garcia de Jalon, Eduardo Bayo, ”Kinematic and Dynamic Simulation of Multibody Systems: The Real-Time challenge”, ISBN 0-387-94096-0, 440 pp. Springer-Verlag, New-York, 1994.

44. Takashima, K., Tsuzuki, S., Ooike, A., Yoshinaka, K., Yu, K., Ohta, M. and Mori, K., 2014. Numerical analysis and experimental observation of guidewire motion in a blood vasculature model. Medical engineering and physics, 36(12), pp.1672-1683.

45. David E. Stewart, ”Rigid-Body Dynamics with Friction and Impact”, Society for Industrial and Applied Mathematics (SIAM), Vol. 42, No. 1, pp. 339, 2000.

46. Farid Amirouche, ”Fundamentals of Multibody Dynamics: Theory and Applications”, ISBN 0-8176-4236-6.

47. Fritzkowski, Pawel, and Henryk Kaminski. ”A discrete model of a rope with bending stiffness or viscous damping.” Acta Mechanica Sinica 27, no. 1 (2011): 108-113.

48. Schröder, J., 1993. The mechanical properties of guidewires-Part III: Sliding friction. Cardiovascular and interventional radiology, 16, pp.93-97.

5. Interactive Manipulation of Guidewires and Catheters

Hoda Sharei, John J. van den Dobbelsteen, Kazuto Takashima, Jenny Dankelman

Submitted

Background: In every endovascular intervention, guidewires and catheters are the basic tools, used together to gain access to the desired place in the vascular system. Therefore, knowledge of their behavior and also the interaction between them, prior to the procedure might be of a great help in order to choose proper instruments. Therefore, the goal of this study is to develop an interactive guidewire-catheter model, and investigate the effect of bending stiffness of the instruments and friction on their behavior

Method:. A simulation model was developed in Matlab, based on the rigid multibody dynamics method and the Newton-Euler method was applied to simulate the dynamics of the instrument. The mechanical properties of two guidewires and one catheter have been measured and implemented in the developed model. The effect of bending stiffness (ranging from 1-10 Nmm^2 for the guidewires and 300-500 Nmm^2 for the catheter) and friction ($\mu \leq 0.5$) on the trajectory of the instrument as well as on the amount of applied forces to the vascular wall and to each other were examined. The sensitivity of the model to the friction coefficient as well as to the stiffness coefficient of the vascular wall were tested by changing these coefficients in the model.

Results: An interactive model of guidewire and catheter was presented to predict the behavior of instruments inside the vascular system. The user can easily rotate or move the angle of view, by mouse operation, in the x, y and z direction to have a better look on the position of the instrument relative to the vascular wall. The results show that the more flexible instrument causes more contact points with the artery's wall because the flexible tip deflects easier than the stiff one. Moreover, a higher friction causes less fluctuation of the instrument's tip.

Conclusion: With the developed model, the specialists can acquire information about the possible trajectories taken by each guidewire and catheter, and the amount of applied forces by them to the vascular walls. This information gives insight into the performance of different instruments prior to the procedure, and can be helpful in selecting a proper instrument in each specific case.

5.1 Introduction

Guidewires and catheters are the basic instruments used in endovascular interventions. A common procedure starts by placing a guidewire into the major arterial segment of interest. Then a catheter is inserted over the guidewire, and the procedure is continued by further manipulation of these instruments [1].

Due to various vascular geometries in the body, variety of guidewires and catheters, with different shapes and mechanical properties, are available in the market [2]. The specialist has to choose a guidewire and a catheter which interact well with each other, and fits with the vascular geometry. This selection is mainly based on experience. Therefore, it is common to repeat the procedure with different instruments until gaining access to the desired vasculature. This repetition leads to a number of drawbacks such as a longer procedure time as well as more cost due to frequent exchange of the instruments, and more importantly, less comfort for the patient. Thus, evaluating the performance of the instruments prior to a procedure can help the specialist with a better decision and increase the success rate of the procedure in a shorter time.

Recently, using computer models to simulate the behavior of guidewires and catheters has emerged as an important research area [3]. For such simulation systems to be used in practice, two requirements should be met: the system should be sufficiently realistic, and they must be (near) real-time. Therefore, researchers have applied different kinds of modelling techniques to achieve these requirements, including the Finite Element Method (FEM) [4-12], the Mass-Spring Model (MSM) [13-19], and the rigid multibody dynamics method [20-31]. Because of the numerical stability of FEM, it is widely used in the simulations, with a broad variety of applications. However, due to the non-linear underlying effects of FEM, applying this method to model guidewires and catheters involves to a very high computational effort. Moreover, due to the complex mathematical background of FEM, it is difficult to interpret the results. Despite the simplicity of MSM compared to FEM, MSM is more suited for modelling soft tissue behavior (e.g., the abdominal skin or muscles). For more rigid objects such as guidewires and catheters, a high computational power is required. In contrast with FEM and MSM, the rigid multibody dynamics method has a simple structure, which makes it faster, and also easy to understand and interpret the results. Moreover, adding friction or material properties to each individual segment is relatively easy [3]. Therefore, we selected the multibody approach to model the instruments.

Until now, the focus of most studies has been mainly on the modelling of a catheter or (in fewer studies) a guidewire, and researchers have tended to consider only the interaction between the instrument and the vascular wall. However, in reality, guidewires and catheters are used together, and the interaction between them influences their behavior [1, 32]; a catheter is a hollow instrument and its behavior changes while a guidewire is traversing inside it [33]. Thus, to have a high degree of realism in the modelling, it is important to consider not only the individual behavior of each instrument but also their interaction with each other [34-35]. There is only limited research done with considering this interaction [36-

37] on which they considered the combination of guidewire and catheter as a single composite model and the collision between the two instruments was ignored. Therefore, the novelty of our model is that not only the behavior of each instrument inside a vasculature, but also the interaction between the instruments are considered while they are moving together. Moreover, the presented model is interactive, i.e., the user can easily rotate or move the angle of view, by mouse operation, in the x, y and z direction to explore the position of the instrument more precisely relative to the vascular wall. This feature is very useful in comparing the exact location of the instruments with different mechanical properties.

We start this chapter by describing the developed model which is based on the rigid multibody dynamics method, along with the simulation environment. Then we explain the method governing the interactions of the instruments with the vascular wall and also with each other. Finally, we present the navigation results of a few instrument in the left coronary artery as an example of vascular geometry and discuss the results.

5.2 Method

To model guidewires and catheters the multibody approach has been used. In this approach, the long instruments were discretized to a set of small rigid segments connected to each other by joints. In the current model, a non-uniform segmentation was chosen due to different mechanical properties of an instrument at the tip and the body. Then, gimbal joints were used between the segments to model the deformations in the 3-dimensional space. As a gimbal joint is represented by three revolute primitives, the elastic properties of the instrument were implemented in the spring stiffness and damping coefficient of each revolute primitive. The displacement was determined by three translations and three rotations.

While modelling a guidewire and catheter together, the catheter was discretized with a lower resolution than the guidewire (see Figure 1). The reason is that the guidewire is more flexible than the catheter, and tends to deflect easier. Therefore, smaller segments are required to be able to track the guidewire inside the catheter [refer to chapter 4].

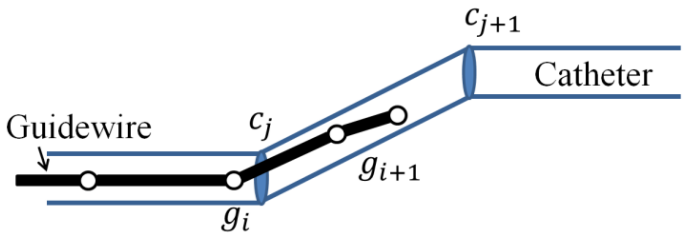

Figure 4: Discretized model of a guidewire moving inside a catheter: the segments are connected to each other by joints (g_i, c_j,…) to account for the bending and torsional deformations of the instruments.

5.2.1 Mathematical formulation of motion for each instrument

We used the Newton-Euler method to simulate the dynamics of the instrument. The Newton-Euler equations are determined by considering the system as a connected system of free bodies. Therefore, three equations for the linear accelerations (Newton), and three equations for the rotational accelerations of each element (Euler) were created [38].

Figure 2 shows a configuration of two segments in the space; joint *i* connects segment ① to segment ② and allows the segments to rotate with three DOF's with respect to each other. The relative position of each two joints is defined in spherical coordinate system by means of two angles (θ and φ), and the segment's length (λ_i). Rotations in plane x and y explains the bending movements whereas a rotation in plane z accounts for the torsional movements of the instrument.

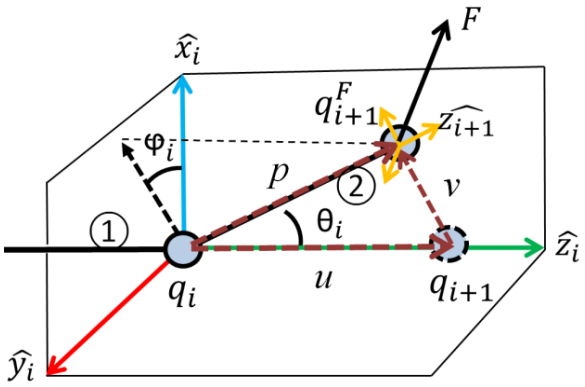

Figure 5: Two segments are connected via joint *i*. The position of segment ② is calculated with respect to segment ① via a spherical coordinate system.

From the 2D model presented in the previous chapter, the equations of motion can be written as follows:

$$-D\dot{\theta} = -T^T F + M_t + K(\theta - \theta_0)\,, \quad \text{(Eq.1)}$$

where θ is the angular position of the segment, θ_0 the angular position in equilibrium, D the damping matrix consist of damping constants, T the transformation matrix which transfers the applied forces in the global coordinate system (F) to applied moments at the segments, M_t the applied moments at the segments, and K the stiffness matrix consisting of stiffness constants.

For a 3D model, in a similar way, a local coordinate is considered at each joint, i.e. $\boldsymbol{q_i}$= (λ_i, θ_i, φ_i). In Figure 2, $\hat{z}_{i+1}$ was considered parallel to segment ②, and then, an arbitrary force F was applied at joint i+1. By projecting F on the ($\hat{x}_{i+1}, \hat{y}_{i+1}$) plane, the normal force to segment ② is as follows:

$$F_n = \frac{\hat{x}_{i+1}.F}{\hat{x}_{i+1}.\hat{x}_{i+1}}\hat{x}_{i+1} + \frac{\hat{y}_{i+1}.F}{\hat{y}_{i+1}.\hat{y}_{i+1}}\hat{y}_{i+1}. \quad \text{(Eq.2)}$$

Therefore, the moment around joint i in the direction of θ_i is:

$$M_a = \lambda_i \|F_n\|. \qquad \text{(Eq.3)}$$

The angular position of joint i (θ_i) in Figure 2 was calculated by replacing term $T^T F$ in Eq.1 with M_a from Eq.3 and then one time integration. Likewise, we projected the force F on the ($\hat{x}_i$, $\hat{y}_i$) plane and calculated variable φ_i which is the angle between the local vector x_i and the projected vector. Thus, we calculated the position vector of joint i+1 (p_{i+1}) with respect to joint i, by knowing these two angles (θ_i, φ_i), and the length of the segment (λ_i) as follows:

$$\begin{bmatrix} x \\ y \\ z \end{bmatrix}_{i+1} = \begin{bmatrix} x \\ y \\ z \end{bmatrix}_i + \lambda_i \begin{bmatrix} \sin\theta_i \cos\varphi_i \\ \sin\theta_i \sin\varphi_i \\ \cos\theta_i \end{bmatrix}_i \qquad \text{(Eq. 4).}$$

5.2.2 Interaction of the instrument with the surrounding area

The instruments encounter resistance while they traverse inside the vascular system because of the contact with the vascular wall or with each other, and due to friction. These contact and friction forces affect the orientation of the instruments inside the vasculature.

In our model, we described each instrument and also the vasculature by the centerline and radius because of their circular cross section. Additionally, each instrument, as explained before, was discretized into segments with known length interconnected with each other by joints (see Figure 1). Likewise, the vascular data is discrete with a resolution of 30μm. Therefore, we investigated the interaction between the guidewire, catheter, and the vasculature by calculating the relative position of joints in each one with respect to the other one. Following, first the contact detection algorithm will be presented, and then, the normal force and friction force will be calculated. It worth to note that although in the following we will explain the interaction between the instrument and vasculature, the same principles has been applied for the interaction between the instruments together.

Contact detection: Detecting the contact between the instrument with the vascular wall is an important part of the simulation. In our algorithm, we detect a contact if the normal distance between the vasculature and the instrument exceed a certain threshold. Following, we will explain the calculation of the normal distance and the threshold.

To find the normal distance between the instrument and the vascular wall, first the algorithm finds the nearest point of the centerline of the vasculature (s_i) to the joint of the instrument (q_i), and then the distance between them ($\boldsymbol{Y}$) is calculated as follows:

$$\boldsymbol{Y} = \boldsymbol{q_i} - \boldsymbol{s_j}, \qquad \text{(Eq. 5)}$$

in which $\boldsymbol{q_i}$,the position vector of each joint of the instrument, was calculated in the previous section. Next, the algorithm finds the second closest node of the vasculature to the instrument by calculating d_1 and d_2 (see Figure 3).

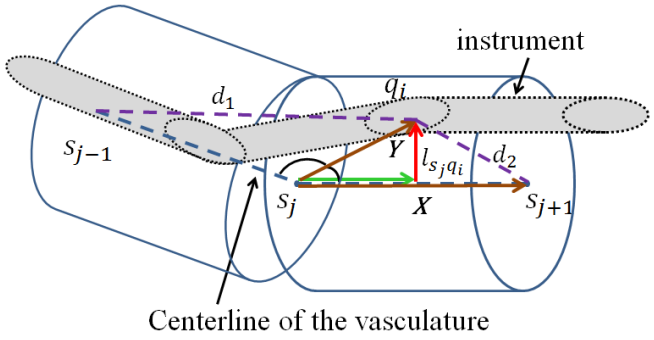

Figure 6: Calculating the relative position of the instrument and the vasculature

Let's assume $d_2 < d_1$ which indicates q_i located inside the $s_j s_{j+1}$ segment of the vasculature. Thus, the normal distance ($l_{s_j q_i}$) between joint q_i and segment $s_j s_{j+1}$ is calculated as follows:

$$l_{s_j q_i} = Y - |Y|\cos(\varphi_{ji})\frac{X}{|X|}, \qquad \text{(Eq. 6)}$$

in which

$$X = s_{j+1} - s_j\ , \qquad \text{(Eq. 7)}$$

$$\cos(\phi_{ji}) = \frac{Y.X}{|Y||X|}. \qquad \text{(Eq. 8)}$$

By considering the normal distance ($l_{s_j q_i}$), the possible configurations of the instrument inside the vasculature are shown in Figure 4. Therefore, after calculating the normal distance, to detect the contact, the threshold is defined as follows:

$$\left|l_{s_j q_i}\right| \geq R_v - R_i\ . \qquad \text{(Eq. 9)}$$

with R_i and R_v being the radii of the instrument and of the vasculature, respectively.

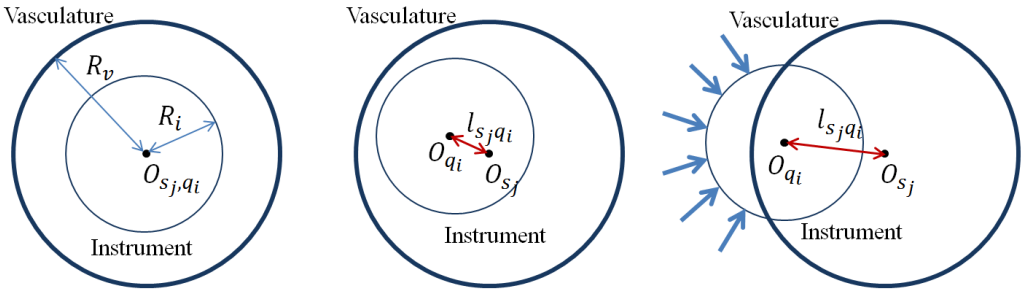

(a) (b) (c)

Figure 7: Position of the instrument and vasculature with respect to each other while the instrument is moving inside the vasculature: a) and b) no contact between the instruments ($\left|\boldsymbol{l_{s_j q_i}}\right| < \boldsymbol{R_v - R_i}$), c)

contact between the instruments occurred ($\left|\boldsymbol{l}_{\mathbf{s_j q_i}}\right| \geq \boldsymbol{R_v} - \boldsymbol{R_i}$); the contact forces are indicated by arrows.

Normal force and friction force: If the contact constraint, explained above, is met, then a normal force is exerted on the instrument as a contact response. To calculate this normal force, the vascular wall was modeled as a spring system; therefore, the normal force consists of a spring-component, is calculated using the penetration depth (u). This force prevents the instrument from penetrating into the vessel wall and Hooke's law is used to account for it as follows:

$$F_{nw} = -k_w . u . \frac{\mathrm{l}_{\mathrm{s_j q_i}}}{\left|\mathrm{l}_{\mathrm{s_j q_i}}\right|}, \qquad \text{(Eq. 10)}$$

in which k_w is the elasticity coefficient of the vascular wall, and u is calculated as:

$$u = \left|\mathrm{l}_{\mathrm{s_j q_i}}\right| - (R_v - R_i) \ , \qquad \text{(Eq. 11)}$$

For the friction between the instrument and the vascular wall, the Coulomb model was used in which the direction of the friction is opposed to the relative velocity of the instrument with respect to the vasculature. Thus, the friction is calculated as follows [39]:

$$F_f = -\mu |F_{nw}| . e_i \ , \qquad \text{(Eq. 12)}$$

in which μ is the friction coefficient (determined based on information provided in [40]), and e_i is the tangential direction and was determined in the direction of the tangential force as follows [26]:

$$e_i = \frac{F_{tw} - F_{nw}}{|F_{tw} - F_{nw}|} \ , \qquad \text{(Eq. 13)}$$

in which F_{tw} is the total force inserted to q_i, and $(F_{tw} - F_{nw})$ is the tangential force. The total force is calculated from the velocity and normal force as follows:

$$F_{tw} = \frac{|F_{nw}|}{\cos \alpha} . \frac{|v|}{v} \ , \qquad \text{(Eq. 14)}$$

in which

$$\cos \alpha = \frac{|F_{nw}| . |v|}{F_{nw} . v} . \qquad \text{(Eq. 15)}$$

A lot of research has been done to reduce the friction between the instrument and the vasculature, and between the instruments (e.g., guidewire and catheter or stent) [41]. Later, we will explore the effect of friction on the applied forces by changing the coefficient of friction in the simulation.

5.2.3 Properties of the instruments and vasculature

The left main coronary artery (LMCA) was chosen as an example of a vascular geometry

due to the high risk of atherosclerotic disease in this artery [42]. The LMCA bifurcates into the left anterior descending (LAD) and the left circumflex (LCX) arteries. Data regarding the centerline and diameter of the RCA were extracted from CT scans of the patients' vascular geometry [43]. The diameter of the LAD and LCX range from less than 1 to 3 mm along the length; consequently, the use of 0.014-inch guidewires (0.36 mm) in combination with 5- or 6-Fr (approximately 2 mm) catheters are recommended to not limit the coronary circulation [1].

Table 1 includes a list of instruments used in our model which were recommended by interventional specialist for the coronary arteries [44]; a multipurpose catheter (MPA1) with a curved tip is used in combination with the guidewires.

Table 6: List of the instruments

Item	**Size**	**Description**	**Core material**	**Poisson's ratio (ν)**
Guidewire	0.014"	Abbott Hi-Torque Pilot 50 Guide Wire: 0.014" x 190cm, J-Tip	Stainless steel	0.3
Guidewire	0.014"	Abbott Hi-Torque Pilot 200 Guide Wire: 0.014" x 190cm, J-Tip	Stainless steel	0.3
Catheter	6 F	Cordis Vista Brite Tip, Guiding Catheter 55cm, MPA1	-	-

Since the manufacturers provide only the basic properties of the instruments (such as diameter and length), and not the exact mechanical properties, we have measured the Young modulus (E) by a 3-point bending test for different guidewires and catheters (for the details of the measurement method refer to [31]). We considered these instruments as isotropic materials and used the data in the mechanical engineering books (e.g., [45]) for the Poisson's ratio (ν). Then, the shear modulus (G) can be calculated as follows:

$$G = \frac{E}{2(1+\nu)}. \qquad (16)$$

Therefore, the bending and torsion stiffness of the instrument are calculated. In addition, the mass properties of the instruments have measured by an electronic balance; to have proper data for the discretized computer model, the real instrument has been cut to segments of 30mm and the weight of each segment was measured separately. Based on these data, the density of the segments were calculated and used in the model.

5.3 Results

5.3.1 Bending stiffness and mass properties measurement

Figure 5 shows the measured data of the bending stiffness for two guidewires, in which Pilot200 is slightly stiffer than Pilot50, and one catheter. It can be seen that, although the bending stiffness is non-homogeneous along the length of the instruments, it follows almost the same pattern: first a considerable flexibility at the distal side, then an increase toward the proximal side.

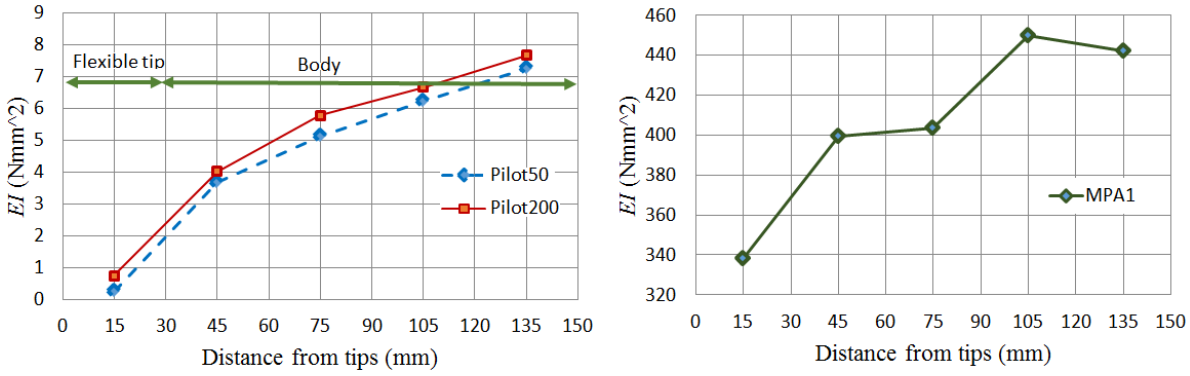

Figure 5: Bending stiffness measurement: a) Pilot50 and Pilot200, b) Catheter MPA1.

Table 2 shows the mass measurement of the instruments along the length. Based on these results, the density of the instruments were calculated and used in the model.

Table 7: Mass measurement for each segment of the instruments

Measurement position [mm]	Mass of each specimen [g]		
	PILOT 50	PILOT200	MPA1
0-30	0.020	0.021	0.065
30-60	0.010	0.011	0.063
60-90	0.010	0.011	0.065
90-120	0.008	0.009	0.065
120-150	0.008	0.009	0.064

5.3.2 The effect of bending stiffness on the tip trajectory and contact forces

In Figure 6, comparison between the tip trajectories of Pilot50 and Pilot200, from different views, are shown. In addition, the tip trajectory of a stiff guidewire (a stiffness of 10^{th} times of Pilot200 stiffness) is shown to highlight the effect of stiffness. In Figure 7 and 8, the configuration of the guidewires in the simulation environment while moving forward are shown. Figure 9 shows the amount of contact forces applied by the these guidewires.

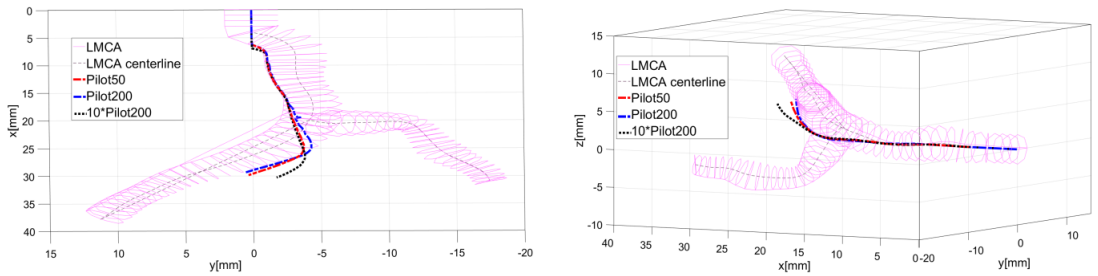

Figure 8: Comparison of tip trajectories of three guidewires

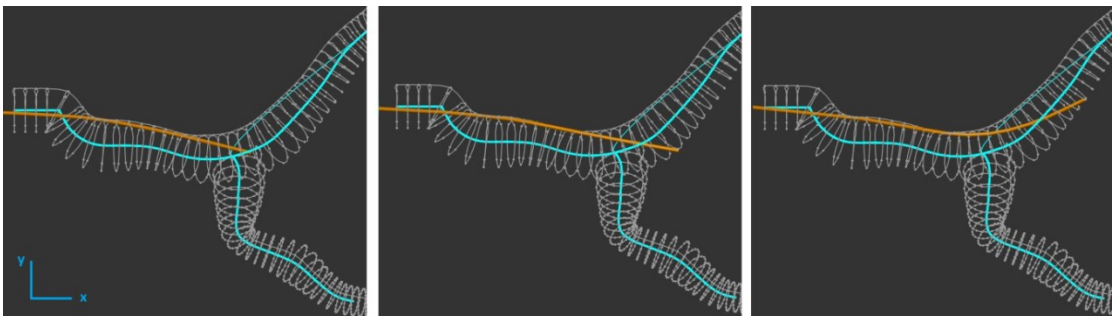

Figure **7**: Trajectory of Pilot50 in the left coronary artery while passing the bifurcation and directing to the left anterior descending (LAD)

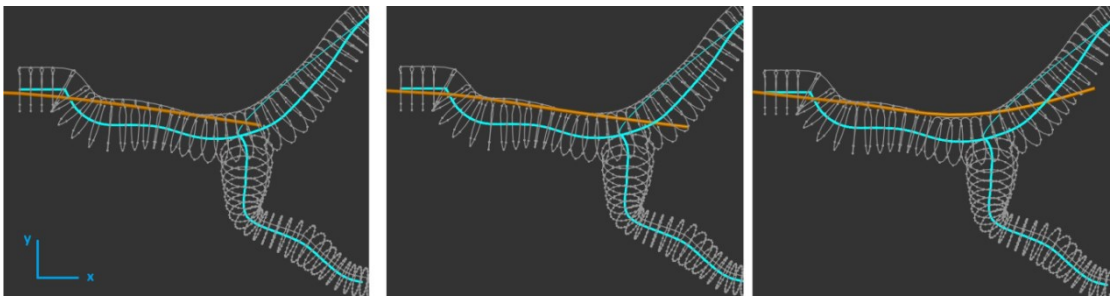

Figure 8: Trajectory of Pilot200 in the left coronary artery while passing the bifurcation and directing to the left anterior descending (LAD)

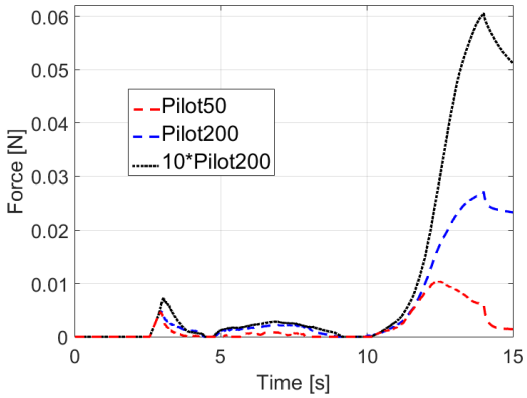

Figure 9: Contact forces caused by guidewires of different bending stiffness

These figures show that as the stiffness of the guidewire increases, the guidewire applies more forces to the vascular wall (Figure 9) and as a result causes deformation in the wall. Although in Figure 6 the deformation caused by the stiffer wire was shown by coming out of the vascular lumen, it is just for demonstration and in reality the wire deforms the wall, and in case of very stiff wire it might puncture the wall.

5.3.3 Sensitivity of the model to the friction coefficient

We have investigated the sensitivity of our model to the friction by changing the coefficient of friction (μ). Figure 10 shows the amount of applied forces to the vascular wall for three different μ while pushing the guidewire into the LAD artery. It is shown that in the absence of friction (i.e., $\mu = 0$), the instrument causes the minimum amount of force, and in the presence of the friction, the higher the μ, the higher the forces applied to the vascular wall.

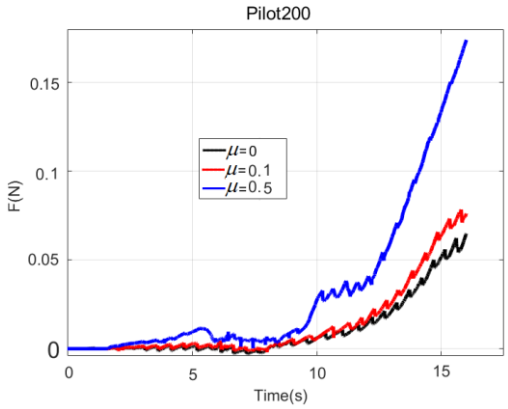

Figure 10: Comparing the transition of applied forces between the guidewire and vascular wall in the simulation with different friction coefficient: Pilot200.

5.3.4 Sensitivity of the model to the vasculature wall stiffness (k_w)

To illustrate the sensitivity and versatility of the model, we changed the stiffness coefficients (k_w) for the vascular wall in our simulation. Figure 11 and 12 show the effect of k_w on the amount of applied forces to the vascular wall and the tip position of the guidewire, respectively, while pushing the wire into the LAD artery.

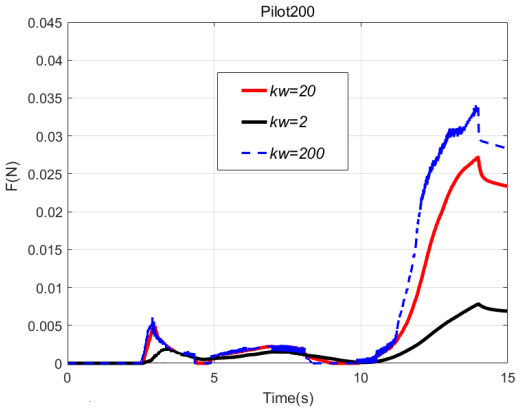

Figure 11: Comparing the transition of applied forces between the guidewire and vascular wall in the simulation with different stiffness coefficient of the vascular wall: Pilot200.

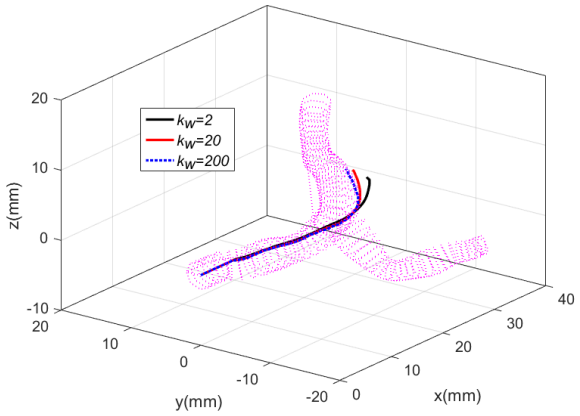

Figure 12: Comparing the trajectory of the guidewire in the simulation with different stiffness coefficient of the vascular wall: Pilot200.

The results show that a higher k_w leads to more forces, and therefore, the guidewire is pushed toward the centerline of the vasculature.

5.3.5 Guidewire and catheter interaction

Figure 13 shows a visualization of the advancement of the guidewire and catheter, together, in the main left coronary artery. The interaction between them was modeled, and the influence of this interaction was investigated by the amount of applied forces between them, during the advancement (Figures 13 and 14).

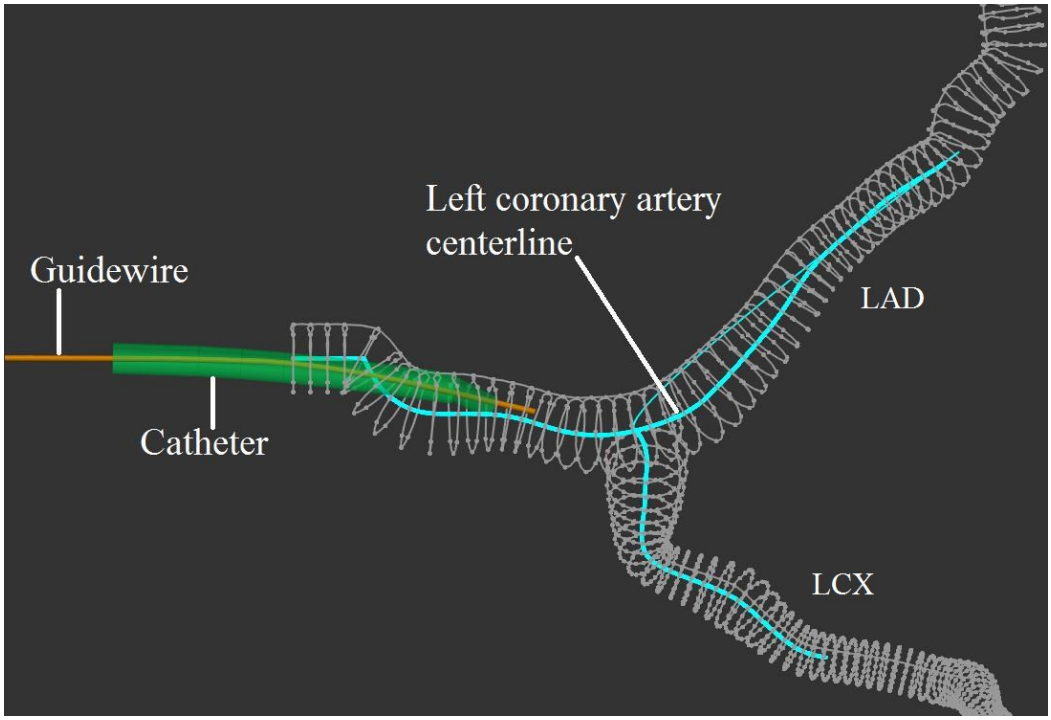

Figure 13: Guidewire and catheter advancement in the main left coronary artery

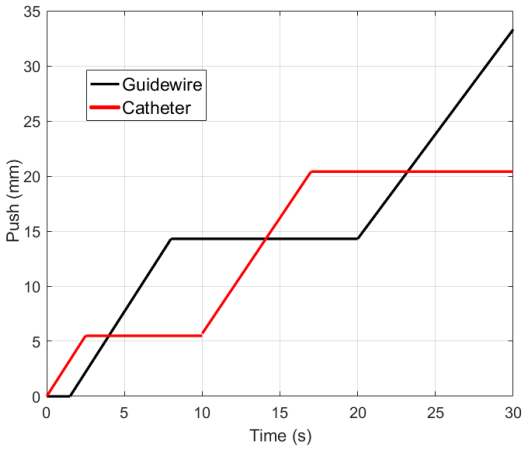

Figure 14: An example of motion pattern in the simulation to push the guidewire and catheter inside the main coronary artery to the LAD direction: first the catheter is pushed forward to give direction and support to the guidewire; next, the guidewire follows the catheter. Then, the catheter is pushed forward and rotated to the direction of the LAD. Last, the guidewire follows the catheter towards the LAD.

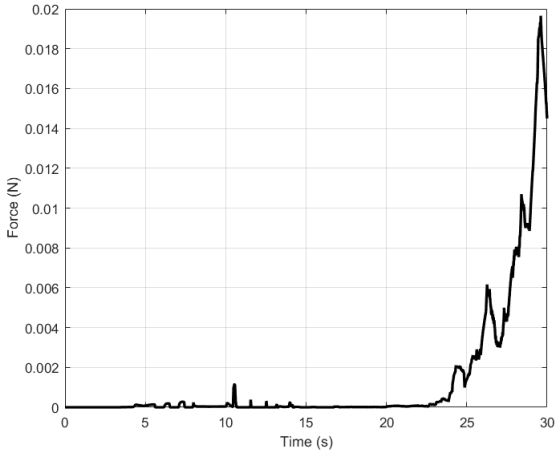

Figure 15: The transition of applied forces between the Pilot50 guidewire and MPA1 catheter in the simulation: first, in the main left coronary artery, the guidewire and catheter move in the same direction and the amount of applied forces from one to another is minimum. Then, when the catheter is rotated and changes the direction towards the LAD, the amount of forces is increasing due to further interaction between them.

5.4 Discussion

The goal of this study was to develop an interactive guidewire-catheter model, and investigate the effect of bending stiffness of the instruments and friction on their behavior. In particular, the effect of these parameters on the trajectory of the instrument as well as on the amount of applied forces to the vascular wall were examined. The sensitivity of the model to the friction coefficient as well as to the stiffness coefficient of the vascular wall were tested by changing these coefficients in the model. Additionally, we considered the interaction between the guidewire and the catheter, and the effects of this interaction.

In the appendix, we endeavored to perform experiments on a developed PVA-H model of the RCA and validate the results of the simulated model. Although these experiments gave us good indications on the accuracy of the model but some improvements are needed in future studies. Some of these improvements are included using a sensor at the tip of the instrument which can measure forces in all direction, and a more precise tracking strategy for tip trajectory.

5.4.1 Bending stiffness

In contrast to the previous studies [e.g., 32], we used a non-uniform bending stiffness for the instrument, i.e., different parts of the instrument may have different bending stiffness to mimic very closely the real instrument. We compared two guidewires with different stiffness: Pilot50 and Pilot200. The results show the higher flexibility of Pilot50 causes more contact points with the artery's wall (Figure 7-8). This can be explained by the fact that the flexible tip deflects easier than the stiff one (Figure 6), and thus, it needs less force to navigate. Figure 9 confirms that the total amount of applied forces to the artery's wall in z-axis for the more flexible wire is less than the stiff one (here, Pilot200).

Here, we should point it out that in the simulation we can measure the amount of forces in all directions, but in Figure 9 we showed the forces only in z direction as an indication of force transition.

5.4.2 Friction

Changing the friction coefficient influences both the trajectory and the amount of applied forces. In Figure 10, we showed that the applied forces increases while the friction increases. An increase in applied forces causes high risk of damaging the vascular wall. A lot of research has been done to reduce the friction between the instrument and the vasculature. However, on the other hand, a higher friction causes less fluctuation of the instrument's tip. Therefore, the friction coefficient needs to be optimized to strike a balance between the increase in the applied forces and the performance of the instrument.

In our simulation, we considered an estimated value of friction coefficient, which was based on the literatures, and later, by comparing Figure 9 and 10, we came to the conclusion that $\mu=0.1$ in the simulation results to similar results as in the phantom experiment (refer to appendix).

5.4.3 Guidewire and Catheter interaction

A catheter is a hollow instrument which together with a guidewire are used in every intervention [1]. While a guidewire is traversing inside a catheter, due to the interaction between them, their behavior change [32-33]. This changing in the behavior is resulting to gain access to a desired location in the vascular system in which was not possible with a guidewire or a catheter alone [1].

The transition of applied forces between the Pilot50 guidewire and MPA1 catheter in the simulation (Figure 15) shows that when the catheter is rotated and changes the direction towards the LAD, the amount of interaction force between the guidewire and the catheter is increasing due to more contact between them. Therefore, the developed model allows to test different combinations of guidewires and catheters, with different mechanical or geometrical properties, in each vascular geometry and investigate which combination gives access without damaging the vascular wall due to too much force.

5.4.4 Vascular data

In this research, we used centre-line and radius data from a human coronary artery, retrieved using computed tomography (CT) angiography data, done in [43]. Although, the CT data of the patients are not always available, a solution would be to determine the severity and complexity of the intervention in a time efficient manner. Subsequently, for those patients for which the procedure is more difficult, a CT scan is made.

5.5 Conclusion

We presented a computer-based model of guidewires and catheters which can predict the behavior of these instruments inside the vascular system on the basis of their mechanical properties. The presented model is interactive, i.e., the user can easily rotate or move the angle of view, by mouse operation, in the x, y and z direction to have a better look on the position of the instrument relative to the vascular wall. This feature is very useful in comparing the exact location of the instruments with different mechanical properties. While we presented the results of a few instruments in the RCA artery, the model is generic and it is applicable in other areas of the body and their specific instruments.

With the developed model, the specialists acquire information about the possible trajectories taken by each guidewire and catheter, and the amount of applied forces by them to the vascular walls. This information gives insight into the performance of different instruments prior to the procedure, and can be helpful in selecting a proper instrument in each specific case.

References

1. Schneider, Peter A. Endovascular skills: guidewire and catheter skills for endovascular surgery. New York, NY, USA: Informa Healthcare, 2009.

2. Patriciu, Alexandru, Dumitru Mazilu, Herman S. Bagga, Doru Petrisor, Louis Kavoussi, and Dan Stoianovici. "An evaluation method for the mechanical performance of guidewires and catheters in accessing the upper urinary tract." Medical engineering & physics 29, no. 8 (2007): 918-922.

3. Hoda Sharei, Tanja Alderliesten, John J. van den Dobbelsteen, Jenny Dankelman, "Navigation of guidewires and catheters in the body during intervention procedures: a review of computer-based models," J. Med. Imag. 5(1), 010902 (2018), doi: 10.1117/1.JMI.5.1.010902.

4. Anderson, J. H., R. Raghavan, Y. P. Wang, R. Mullick, and C. C. Kong. "daVinci—A vascular catheterization simulator." Journal of Vascular and Interventional Radiology 8, no. 1 (1997): 261.

5. Nowinski, Wieslaw Lucjan, and Chee-Kong Chui. "Simulation of interventional neuroradiology procedures." In Medical Imaging and Augmented Reality, 2001. Proceedings. International Workshop on, pp. 87-94. IEEE, 2001.

6. Li, Shun, Jing Qin, Jixiang Gao, Yim-Pan Chui, and Pheng-Ann Heng. "A novel FEM-based numerical solver for interactive catheter simulation in virtual catheterization." Journal of Biomedical Imaging (2011): 3.

7. Guo, Jin, Shuxiang Guo, Nan Xiao, and Baofeng Gao. "Virtual reality simulators based on a novel robotic catheter operating system for training in minimally invasive surgery." Journal of Robotics and Mechatronics 24, no. 4 (2012): 649.

8. Wu, Xunlei, Vincent Pegoraro, Vincent Luboz, Paul F. Neumann, Ryan Bardsley, Steven Dawson, and Stéphane Cotin. "New approaches to computer-based interventional neuroradiology training." Studies in health technology and informatics 111 (2005): 602-607.

9. Anderson, James, Chee-Kong Chui, Yiyu Cai, Yaoping Wang, Zirui Li, Xin Ma, Wieslaw Nowinski et al. "Virtual reality training in interventional radiology: the Johns Hopkins and Kent Ridge Digital Laboratory experience." In Seminars in Interventional Radiology, vol. 19, no. 02, pp. 179-186. Copyright© 2002 by Thieme Medical Publishers, Inc., 333 Seventh Avenue, New York, NY 10001, USA. Tel.:+ 1 (212) 584-4662, 2002.

10. Cotin, S., Duriez, C., Lenoir, J., Neumann, P. and Dawson, S., “New Approaches to Catheter Navigation for Interventional Radiology Simulation”, 2006, Computer Aided Surgery 11 (6), pp. 300-308.

11. Patriciu, Alexandru, Dumitru Mazilu, Herman S. Bagga, Doru Petrisor, Louis Kavoussi, and Dan Stoianovici. "An evaluation method for the mechanical performance of guidewires and catheters in accessing the upper urinary tract." Medical engineering & physics 29, no. 8 (2007): 918-922.

12. Rebholz, Philipp, Carsten Bienek, Dzmitry Stsepankou, and Jürgen Hesser. "CathI-training system for PTCA. A step closer to reality." In Medical Simulation, pp. 249-255. Springer Berlin Heidelberg, 2004.

13. Basdogan, Cagatay, C-H. Ho, and Mandayam A. Srinivasan. "Virtual environments for medical training: graphical and haptic simulation of laparoscopic common bile duct exploration." IEEE/Asme Transactions On Mechatronics 6, no. 3 (2001): 269-285.

14. Wang, Fei, Lindo Duratti, Evren Samur, Ulrich Spaelter, and Hannes Bleuler. "A computer-based real-time simulation of interventional radiology." In 2007 29th Annual International Conference of the IEEE Engineering in Medicine and Biology Society, pp. 1742-1745. IEEE, 2007.

15. Burgner-Kahrs, Jessica, D. Caleb Rucker, and Howie Choset. "Continuum robots for medical applications: A survey." IEEE Transactions on Robotics 31, no. 6 (2015): 1261-1280.

16. Torpey, Luke. "A Virtual Environment Simulation for Guidewire/catheter and Blood Vessel Interaction." PhD diss., University of Leeds, School of Computing Studies, 2010.

17. Vincent Luboza, Jianhua Zhai, Tolu Odetoyinbo, Peter Littler, Derek Gould, Thien How, Fernando Bello, ”Simulation of endovascular guidewire behavior and experimental validation”, Computer Methods in Biomechanics and Biomedical Engineering Vol. 14, No. 6, June 2011, 515520.

18. Vincent Luboz, Rafal Blazewski, Derek Gould, Fernando Bello, ”Real-time guidewire simulation in complex vascular models”, Visual Computer, 2009,25(9), 827-834.

19. V. Luboz, , Y. Zhang, S. Johnson, Y. Song, C. Kilkenny, C. Hunt, H. Woolnough, S. Guediri, J. Zhai, T. Odetoyinbo, P. Littler, A. Fisher, C. Hughes, N. Chalmers, D. Kessel, P.J. Clough, J.Ward, R. Phillips, T. How, A. Bulpitt, N.W. John, F. Bello, D. Gould, ”ImaGiNe Seldinger: First simulator for Seldinger technique and angiography training”, Computer Methods and Programs in Biomedicine, Volume 111, Issue 2, August 2013, Pages 419434.

20. Cotin, Stephane, S. Dawson, Dwight Meglan, D. Shaffer, M. Ferrell, R. Bardsley, F. Morgan et al. "ICTS, an interventional cardiology training system." Studies in health technology and informatics (2000): 59-65.

21. Meglan, Dwight. "Making surgical simulation real" ACM SIGGRAPH Computer Graphics 30, no. 4 (1996): 37-39.

22. Wang, Yu, Shuxiang Guo, Takashi Tamiya, Hideyuki Hirata, Hidenori Ishihara, and Xuanchun Yin. "A virtual reality simulator and force sensation combined catheter operation training system and its preliminary evaluation." The International Journal of Medical Robotics and Computer Assisted Surgery (2016).

23. Takashima, Kazuto, Shotaro Tsuzuki, Atomu Ooike, Kiyoshi Yoshinaka, Kaihong Yu, Makoto Ohta, and Koji Mori. "Numerical analysis and experimental observation of guidewire motion in a blood vessel model." Medical engineering & physics 36, no. 12

(2014): 1672-1683.

24. Takashima, Kazuto, Atomu Oike, Kiyoshi Yoshinaka, Kaihong YU, Makoto Ohta, Koji Mori, and Naoki Toma. "Evaluation of the effect of catheter on the guidewire motion in a blood vessel model by physical and numerical simulations." Journal of Biomechanical Science and Engineering 12, no. 4 (2017): 17-00181.

25. Vincent Guilloux, Pascal Haigron, Cemil Goksu, Carine Kulik, Antoine Lucas, ”Simulation of guidewire navigation in complex vascular structures”, Proc. SPIE 6141, Medical Imaging 2006.

26. K. Ikuta, K. Iritani, J. Fukuyama, and M. Takeichi, “Portable virtual endoscope system with force and visual display for insertion training”, In Proc. of the IEEE/RSJ International Conference on Intelligent Robots and Systems (IROS), volume 1, pages 720726, 2000.

27. Markus Kukuk, ”A Model-Based Approach to Intra operative Guidance of Flexible Endoscopy”, PhD thesis, Princeton, 2002.

28. Dawson, Steven L., Stephane Cotin, Dwight Meglan, David W. Shaffer, and Margaret A. Ferrell. "EQUIPMENT AND TECHNOLOGY-Designing a Computer-Based Simulator for Interventional Cardiology Training." Catheterization and Cardiovascular Interventions 51, no. 4 (2000): 522-527.

29. Wang, Weiwei, Shuai Li, Hong Qin, and Aimin Hao. "Novel, Robust, and Efficient Guidewire Modelling for PCI Surgery Simulator Based on Heterogeneous and Integrated Chain-Mails." In Computer-Aided Design and Computer Graphics (CAD/Graphics), 2015 14th International Conference on, pp. 105-112. IEEE, 2015.

30. Ursino, Michele, Joseph L. Tasto, Binh H. Nguyen, Richard Cunningham, and Gregory L. Merril. "CathSim: an intravascular catheterization simulator on a PC." Studies in health technology and informatics 62 (1998): 360-366.

31. Toma, Naoki, Koji Mori, Kazuto Takashima, Takanori Sano, Yasuyuki Umeda, Hidenori Suzuki, and Takashi Saito. "A Study of the Relationship between the Microcatheter Shape and Stability by Numerical Simulation." Journal of Neuroendovascular Therapy (2017): oa-2016.

32. Estrada, Sean, Cassidy Duran, Daryl Schulz, Jean Bismuth, Michael D. Byrne, and Marcia K. O’Malley. "Smoothness of surgical tool tip motion correlates to skill in endovascular tasks." IEEE Transactions on Human-Machine Systems 46, no. 5 (2016): 647-659.

33. Estrada, Sean, Cassidy Duran, Daryl Schulz, Jean Bismuth, Michael D. Byrne, and Marcia K. O'Malley. "Smoothness of surgical tool tip motion correlates to skill in endovascular tasks." IEEE Transactions on Human-Machine Systems 46, no. 5 (2016): 647-659.

34. Patriciu, Alexandru, Dumitru Mazilu, Herman S. Bagga, Doru Petrisor, Louis Kavoussi, and Dan Stoianovici. "An evaluation method for the mechanical performance of

guidewires and catheters in accessing the upper urinary tract." Medical engineering & physics 29, no. 8 (2007): 918-922.

35. Lenoir, Julien, Stephane Cotin, Christian Duriez, and Paul Neumann. "Interactive physically-based simulation of catheter and guidewire." Computers & Graphics 30, no. 3 (2006): 416-422.

36. Preim, Bernhard, and Charl P. Botha. Visual Computing for Medicine: Theory, Algorithms, and Applications. Newnes, 2013, chapter 21, pp 154-156

37. Becherer, Nico, Jürgen Hesser, Ulrike Kornmesser, Dietmar Schranz, and Reinhard Männer. "Interactive physical simulation of catheter motion within mayor vessel structures and cavities for ASD/VSD treatment." In Medical Imaging, pp. 65090U-65090U. International Society for Optics and Photonics, 2007.

38. E. Otten, "Inverse and forward dynamics: models of multi-body systems." Philosophical Transactions of the Royal Society of London. Series B: Biological Sciences, vol. 358, no. 1437, pp. 1493–1500, 2003.

39. Takashima, Kazuto, Rei Shimomura, Takayuki Kitou, Hiroki Terada, Kiyoshi Yoshinaka, and Ken Ikeuchi. "Contact and friction between catheter and blood vessel." Tribology International 40, no. 2 (2007): 319-328.

40. Schröder, J., 1993. The mechanical properties of guidewires-Part III: Sliding friction. Cardiovascular and interventional radiology, 16, pp.93-97.

41. Lorenzoni, Roberto, Roberto Ferraresi, Marco Manzi, and Marco Roffi. "Guidewires for lower extremity artery angioplasty: a review." EuroIntervention: journal of EuroPCR in collaboration with the Working Group on Interventional Cardiology of the European Society of Cardiology 11, no. 7 (2015): 799-807.

42. Ding, Zhaohua, Tony Biggs, W. Anthony Seed, and Morton H. Friedman. "Influence of the geometry of the left main coronary artery bifurcation on the distribution of sudanophilia in the daughter vessels." Arteriosclerosis, thrombosis, and vascular biology 17, no. 7 (1997): 1356-1360.

43. Schaap, Michiel, Coert T. Metz, Theo van Walsum, Alina G. van der Giessen, Annick C. Weustink, Nico R. Mollet, Christian Bauer et al. "Standardized evaluation methodology and reference database for evaluating coronary artery centerline extraction algorithms." Medical image analysis 13, no. 5 (2009): 701-714.

44. Tóth, Gábor G., Masahisa Yamane, and Guy R. Heyndrickx. "Coronary Guidewires." In Textbook of Catheter-Based Cardiovascular Interventions, pp. 603-622. Springer, Cham, 2018.

45. Rajput, R. K. Engineering Material. S. Chand, 2008, p528.

6. Influence of Guidewire and Vasculature Geometries on Navigation

Hoda Sharei, John J. van den Dobbelsteen, Jenny Dankelman

Partly published in SMIT2018 conference

Background: The geometry of vasculatures varies both intrinsically or due to diseases; on the other hand guidewires with different shapes are available in the market. Therefore, predicting the proper guidewire for each vasculatures is challenging. Goal of this chapter is to use the developed model to investigate the effect of geometry properties of both guidewire and vasculature on the behavior of the guidewire.

Method: The left main coronary artery (LMCA) was chosen as an example of a vascular geometry. Moreover, the model described in Chapter 5 was used for the simulations. In the model, the trajectories of the guidewire with tip angles of 0 to 30 degree were simulated to explore the minimum (threshold) angle for navigation towards the LAD with and without rotation, and the amount of applied forces to the LAD's wall were compared. Moreover, since the diameter of the LAD changes from 3 mm at the proximal side to less than 1 mm at the distal side, we examine the effect of atherosclerosis by increasing the stiffness coefficient of the vasculature wall (k_w) in which the diameter changes along the LAD, and investigate the amount of applied forces to the vascular wall which is an indicator to avoid rupturing the vasculature.

Results & Conclusion: The results show that the performance of a guidewire depends not only on mechanical properties, but also geometrical properties; in other words, both need to be within an appropriate range for a successful procedure.

6.1 Introduction

In the previous chapter, we have developed a computer model to investigate the behavior of guidewires and catheters by considering the mechanical properties of the instrument, and of the vasculature such as bending stiffness and friction. In this chapter, we use the developed model to investigate the effect of geometry properties such as the tip angle of guidewires, and the narrowed cross section of the arteries, due to vascular disease, on the behavior of the guidewire.

6.2 Effects of tip angle of the instrument

The shape of guidewire's tip has an important role in the navigation of the guidewire, in particular in the bifurcations. This is one of the reasons that large variety of guidewires with different tip shapes are available in the market (see Figure 1). Besides, it is common to shape the tip of the guidewire during the procedure to enhance the maneuverability [1]. In addition, using angled-tip guidewires can also decrease the number of catheter changes due to easier access with a guidewire alone [2].

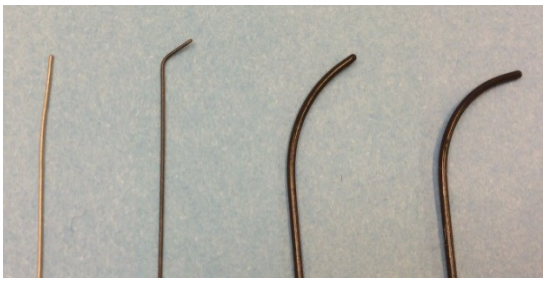

Figure 1: A few example of guidewires with different tip shape

In this section, we focus on variations in angled-tip guidewires and investigate how different angles influence the instrument trajectory. In addition, we apply rotational motion as well as translational motion to investigate how tip-angle can reduce the need for complex steerable instruments.

6.2.1 Method

The left main coronary artery (LMCA) was chosen as an example of a vascular geometry due to the high risk of atherosclerotic disease in this artery [3-4]. The LMCA bifurcates into the left anterior descending (LAD) and the left circumflex (LCX) arteries. The geometry data was extracted from Computed Tomography Angiography (CTA) of a patient [5] and used as input for the modelling of the vasculature.

Considering the diameter of the left main coronary artery (≤3mm), a Pilot50 (0.36mm) was chosen as guidewire to not block the coronary circulation [6]. In the model, the trajectories of the guidewire with tip angles of 0 to 30 degree were simulated to explore the minimum (threshold) angle for navigation towards the LAD with and without rotation, and the amount of applied forces to the LAD's wall were compared.

In the developed model, it is possible to apply different inputs to the proximal side of the instruments including translation and rotation motions. Figure 2 shows an example of input motion in order to go to the LAD artery with a 20 degree tip angle; the guidewire translates and rotates by a constant speed of 2 mm/s and 30 deg/sec, respectively.

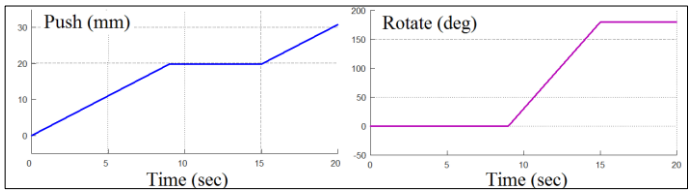

Figure 2: Motion pattern example on the proximal side of the instruments to navigate in the LMCA

6.2.2 Results and Discussion

Based on the simulation results, α=16 is the threshold angle, i.e., the guidewire moves into the LAD artery if the angle is less than 16 degree and it moves into the LCX artery when the angle is more than 16 degree. Figure 3 shows the tip trajectory of the Pilot50 guidewire in the LMCA; the guidewire moves with a tip angle of 15 degree ($<\alpha$) towards the LAD, and with an angle of 20 degree ($>\alpha$) towards the LCX. When a rotation motion is also applied (see Figure 2), the guidewire with 20 degree tip moves into LAD direction; however, as it has been shown in Figure 4, the rotation causes extra forces to the artery's wall.

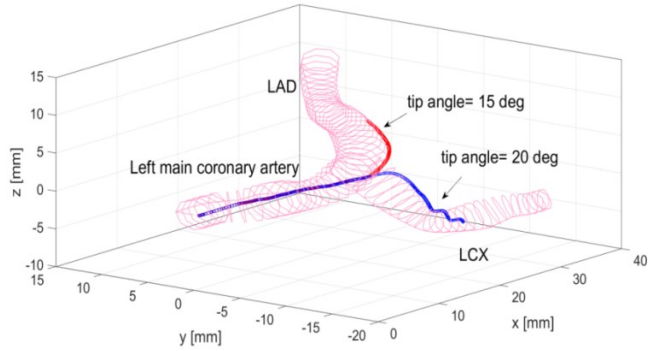

Figure 3: Tip trajectory of the Pilot50 guidewire in the left coronary artery: the guidewire moves with a tip angle of 15 degree towards the LAD, and with an angle of 20 degree towards the LCX

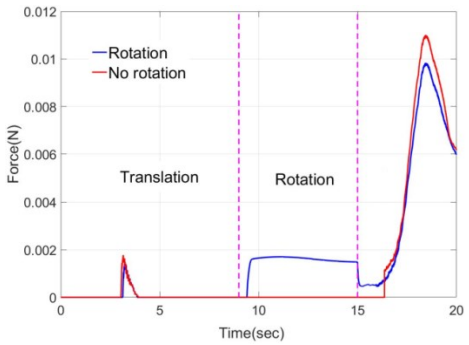

Figure 4: Comparison of the applied forces to the artery's wall with and without applying rotation motion: the rotation applied between 9 to 15 second.

It is noteworthy that in the motion pattern shown in Figure 2, a constant speed of 2 mm/s for the translational motion was chosen based on literature and the rotation pattern was chosen based on the LMCA geometry, and it was applied just as an example in order to compare the influence of the guidewire's tip. Therefore, the overall conclusion is independent of the motion pattern.

6.3 Effects of narrowing of the artery

Atherosclerosis, which is the narrowing of artery due to plaque deposition, is the predominant underlying cause of vascular disease. In response to the atherosclerosis, the arterial walls change to maintain an adequate lumen channel for blood flow, and to retain a regular and round lumen cross section. The first possible change of the artery wall to atherosclerotic plaque deposition is arterial enlargement (Figure 5)[4]. Subsequently, by decreasing the diameter of the artery, the stiffness of the artery wall increases.

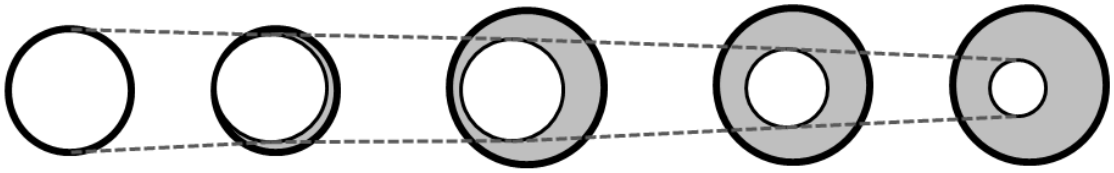

Figure 5: Arterial enlargement to retain a regular and round lumen cross section (Adopted from [3]).

6.3.1 Method

The left anterior descending (LAD) was chosen as an example of a vascular geometry model. The diameter of the LAD changes from 3 mm at the proximal side to less than 1 mm at the distal side, and thus, the guidewire encounters different diameters while inserting to the LAD. Therefore, in the simulation, we examine the effect of atherosclerosis by increasing the stiffness coefficient of the vasculature wall (k_w) in which the diameter changes along the LAD, and investigate the amount of applied forces to the vascular wall which is an indicator to avoid rupturing the vasculature.

6.3.2 Results and Discussion

Figure 6 shows the effect of increasing k_w on the amount of applied forces to the vascular wall by the tip of the guidewire, while pushing the guidewire into the LAD artery. At the proximal side of the LAD, in which the diameter is bigger, lower forces were applied. By inserting the guidewire towards the distal part, in which the diameter decreases, the magnitude of force increased. Fig. 6 shows the influence of k_w on the force between guidewire and vascular wall. Moreover, it shows the increase in force due to narrowing the diameter.

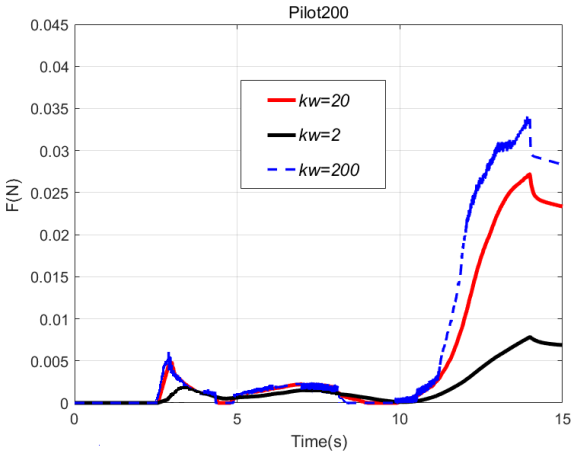

Figure 6: Comparing the transition of applied forces between the guidewire and vascular wall in the simulation with different elastic coefficient of the vascular wall: Pilot200.

6.4 Conclusion

In this chapter, we used the previously developed model of chapter 5 to investigate the effect of geometrical properties such as the tip angle of the guidewire. Moreover, we studied the effect of narrowing of the cross section of the arteries, e.g. due to vascular disease such as atherosclerotic, on the magnitude of applied forces by the guidewire tip to the vascular wall.

The results show that the performance of a guidewire depends on not only mechanical properties (as shown in Chapters 4 and 5), but also geometrical properties; in other words, both need to be within an appropriate range for a successful procedure.

Using a guidewire with angled- tip can enhance the maneuverability. Moreover, choosing a right tip-angle for the guidewire can eliminate the need for using expensive steerable catheters in order to access a specific branch.

The vascular properties such as diameter and elasticity change due to vascular diseases like atherosclerosis. This results in a different reaction against the passage of the guidewires including a higher magnitude of applied forces. The risk of rupture of the artery is thereby increased which further underlines the importance of selecting a guidewire with a proper stiffness to keep the forces as low as possible.

References

1. Tóth, Gábor G., Masahisa Yamane, and Guy R. Heyndrickx. "How to select a guidewire: technical features and key characteristics." Heart 101, no. 8 (2015): 645-652.

2. NEBESAR, ROBERT A., and JAMES J. POLLARD. "A curved-tip guide wire for thoracic and abdominal angiography." American Journal of Roentgenology 97, no. 2 (1966): 508-510.

3. Ding, Zhaohua, Tony Biggs, W. Anthony Seed, and Morton H. Friedman. "Influence of the geometry of the left main coronary artery bifurcation on the distribution of sudanophilia in the daughter vessels." Arteriosclerosis, thrombosis, and vascular biology 17, no. 7 (1997): 1356-1360.

4. Fogarty, Thomas J., and Rodney A. White, eds. Peripheral endovascular interventions. New York: Springer, 2010.

5. Schaap, Michiel, Coert T. Metz, Theo van Walsum, Alina G. van der Giessen, Annick C. Weustink, Nico R. Mollet, Christian Bauer et al. "Standardized evaluation methodology and reference database for evaluating coronary artery centerline extraction algorithms." Medical image analysis 13, no. 5 (2009): 701-714.

6. Schneider, Peter A. Endovascular skills: guidewire and catheter skills for endovascular surgery. New York, NY, USA: Informa Healthcare, 2009.

7. Discussion

In this chapter, we will discuss our accomplishments, and also will give recommendation for future studies.

7.1 Accomplishments

In this thesis, we developed a computer model for supporting pre-intervention planning, in particular, to help objective selection of the guidewires and catheters prior to each procedure. For this aim, we first reviewed the structure of these instruments and their components, with a focus on the proximal connectors in guidewires with a sensor (e.g., flow or pressure) on the distal tip, to learn their working principles. Next, we concentrated on the mechanics of the main body of the guidewires and catheters, along with their performance. A literature study was done in order to investigate guidewire and catheter modelling purposes and applied techniques. We concluded that, in general, guidewire and catheter modelling follows three main purposes including training, pre-intervention planning, and designing new instruments, and, therefore, depending on the purpose, three main techniques have been applied which are FEM, MSM, and Rigid Multibody Links [1-6]. Since the FEM and MSM techniques require a very high computational effort, they have been mainly applied in training purpose. Therefore, we chose the Rigid Multibody Links technique for our pre-interventional planning purpose which has a simple structure and is relatively faster [7-9].

As the first step to develop a simulation model, which is able to predict the behavior of a guidewire inside the vasculature, we focused on two dimensional space. In chapter 4, we introduced a 2D multibody model of a guidewire traversing a simple vascular geometry; the guidewire was considered as a set of small rigid segments connected to each other by revolute joints [7,9-11]. We evaluated the performance of the model by implementing the elastic properties of two commercially available guidewires (Hi-Torque Balance Middleweight Universal II sold by Abbot and Amplatz Super Stiff sold by Boston Scientific) in the model. After evaluating the accuracy of this model, we extended the 2D developed model to a 3D model. Moreover, by adding the catheter to the model, the applicability of the model was increased. The ways in which the instruments interact with each other and with the vascular wall were considered.

Thus, we developed a computer model to evaluate the performance of different instruments for a specific vasculature geometry, prior to the procedure. In particular, the model predicts the behavior of guidewires and catheters by considering the mechanical and geometrical properties of these instruments and of the relevant vasculature. The developed model is generic and we can readily adopt the simulation to a new geometry. Figure 1 shows the simulation environment.

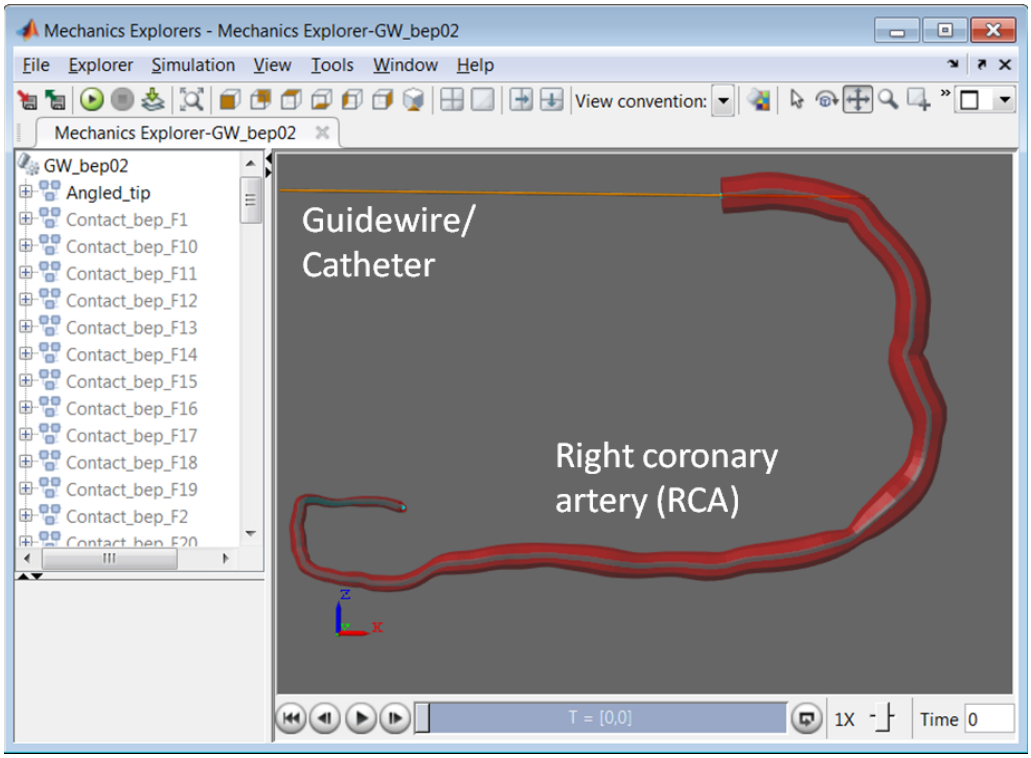

Figure 1: Simulation environment: inserting guidewire to the RAC

7.2 Importance of the findings and clinical relevance

The importance of mechanical properties resulted in a wide variety of guidewires and catheters available in the market. Therefore, one complicating factor of endovascular interventions is that a high degree of expertise is required to select a proper instrument for a particular vascular geometry. Considering the fact that in every intervention, frequent guidewire or catheter exchanges are required to gain access, having additional exchanges due to a wrong choice makes the procedures more expensive, both in cost and time. Adding to that, the comfort of the patient will also decrease. Thus, with our developed model, we are able to predict the performance of the instrument prior to the procedure by evaluating its probable trajectory inside the vasculature, and the amount of force applied to the vasculature's wall. This information gives insight to select a proper instrument and maximizes the success rate of the procedure. It plays an even more decisive role for the newly developed instruments, which are constantly coming to the market and their performance is not fully known even to the experienced specialists.

Guidewire-catheter-vessel wall interaction

Until now, the focus of most studies has been mainly on the modelling of a catheter or (in fewer studies) a guidewire, and researchers have tended to consider only the interaction between the instrument and the vascular wall. However, in reality, guidewires and catheters are used together, and the interaction between them influences their behavior. There is only limited research done that considers this interaction, as often the combination of guidewire and catheter is represented by a single composite model and the collision between the two

instruments is ignored [12-13]. Therefore, the novelty of our model is that not only the behavior of each instrument inside a vasculature, but also the interactions between the instruments are considered while they are moving together. Moreover, the presented model is interactive, i.e., the user can easily rotate or move the angle of view, by mouse operation, in the x, y and z direction to have a better look on the position of the instrument relative to the vascular wall. Thus, a combination of these visual feedbacks and numerical simulation allows clinicians to virtually explore the performance of the instruments with different mechanical properties and to choose objectively.

The data of coronary arteries of a real patient served as an example of vascular geometry. We developed a transparent phantom made of polyvinyl alcohol hydrogen (PVA-H) and dimethyl sulfoxide (DSMO) mixture, and the simulation model was validated by comparing with actual movement of the instruments in the phantom model. The developed models, both simulation and phantom, are generic and allows for the evaluation of a large variety vascular geometries.

7.3 Future research

The developed model is the first step toward a clinically applicable simulation model. During this study, we encountered also some limitations which we highlight here to support and guide future research.

First of all, the mechanical properties of the vascular system, such as elasticity of the walls and friction coefficient, were estimated based on a limited range of data presented in the literature. Because we can easily adopt these properties in our model, it is suggested to measure them more precisely for the intended vasculature. This is especially important in the diseased vasculatures in which their properties greatly change and not much data is available. Therefore, it is recommended to measure these properties more accurately for different vasculatures both in healthy and diseased conditions in order to get realistic results.

The next improvement to our model would be to simulate patient's breathing motion. In the current model, we focused on the modelling of the instrument itself, and the radii and centerline data of the vasculatures were used as geometry information. Therefore, in the future studies, a dynamic centerline instead of a static one has to be considered.

Moreover, to validate the simulation results, we developed a number of phantom models with different materials, and we performed some preliminary experiments. The mechanical properties of the current PVA-H model was estimated based on the literature, and a few measurement has been done. Therefore, as a next step, the mechanical properties of the developed phantoms have to be measured and compared with the real vasculatures. In addition, tracking the movement of the guidewire or catheter inside the phantom was based on a simple image processing of the recorded videos by the cameras. However, using tracking systems which are based on, for example, MRI or acoustic technology may result in more accurate validation[14-17].

The next main step will be to develop a Graphic User Interface (GUI) so that the interventionalist can easily interact with the model. The interventionalist receives information on the patient's anatomy and has to decide which catheter/guidewire is best to use; it is important to have a GUI which is not complicate to use. In Figure 1 an example of such a GUI is shown; in the left, the user can load the images of the patient and intended vascular geometry information. Then, from the instrument library, the user can test different catheters and guidewires, and investigate their behavior based on the position, velocity, amount of applied forces, and finally compare the results of different try-outs and choose the most suitable guidewire and catheter, based on a set of defined criteria. For the purpose of instrument library, it is necessary to measure the mechanical properties of a wide range of guidewires and catheters. Finally, the GUI should be validated with an interventionalist.

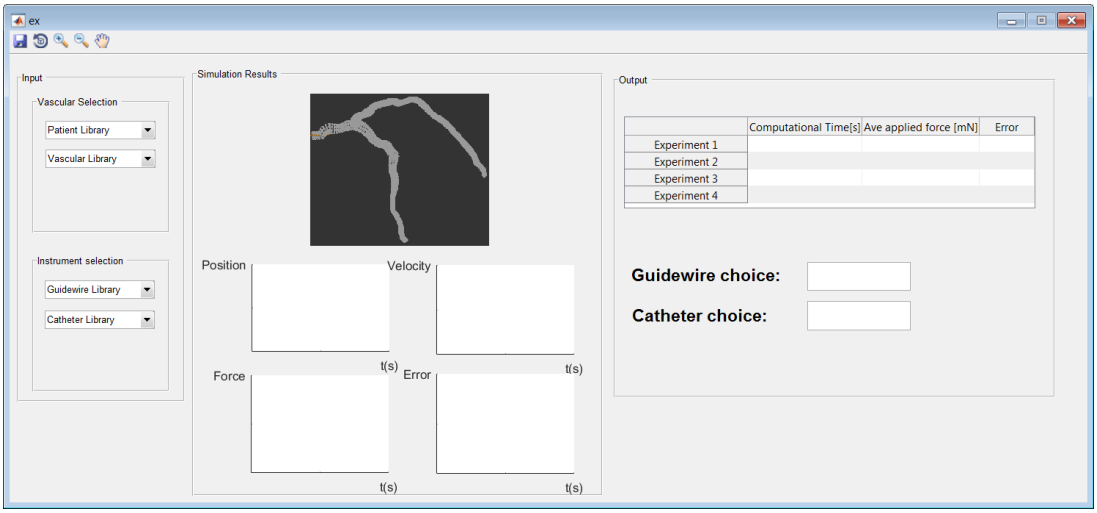

Figure 9: A preliminary GUI. Left side: user can choose the vascular geometry from the library, and test different kind of guidewire (or catheter). Middle: the trajectory of the instrument inside the vascular geometry and other desired output are showed. Right: the results of different choices based on the calculated error are shown and the best instrument is recommended.

7.4 Conclusion

Guidewires and catheters are the basic instruments used together in endovascular interventions. Since the range of vascular geometries are extensive from one organ to another, and from one patient to another, a variety of guidewires and catheters are available. Thus, the interventionalist needs to select a combination of guidewires and catheters in which they perform as desired both individually, and together. Despite the importance of this selection in the success rate of the procedure, it is mainly subjective and based on experience. The developed model in this thesis is the first step towards making this selection more objective by predicting the instrument trajectory and the force transmission between the instrument and the vascular wall; the motion of the guidewires and catheters in the vascular system were simulated, and both the individual performance of each instrument and the effect of the interaction between them were taken into account. These data were determined to assess their performance.

References

1. El-Khalili, Nuha H. “Surgical Training on the World Wide Web.” PhD diss., The University of Leeds, 1999.
2. M. K. Konings, E. B. van de Kraats, T. Alderliesten, W. J. Niessen, “Analytical guide wire motion algorithm for simulation of endovascular interventions”, Medical and Biological Engineering and Computing 2003, Volume 41, Issue 6, pp 689-700.
3. Vincent Guilloux, Pascal Haigron, Cemil Goksu, Carine Kulik, Antoine Lucas, “Simulation of guidewire navigation in complex vascular structures”, Proc. SPIE 6141, Medical Imaging 2006.
4. Rosen, Joseph M., Hooman Soltanian, Richard J. Redett, and Donald R. Laub. “Evolution of virtual reality [Medicine].” Engineering in Medicine and Biology Magazine, IEEE 15, no. 2 (1996): 16-22.
5. K. Ikuta, K. Iritani, J. Fukuyama, and M. Takeichi, “Portable virtual endoscope system with force and visual display for insertion training”, In Proc. of the IEEE/RSJ International Conference on Intelligent Robots and Systems (IROS), volume 1, pages 720726, 2000.
6. W. Shaffer, D., S. L. Dawson, D. Meglan, S. Cotin, M. Ferrell, A. Norbash, and J. Muller. “Design principles for the use of simulation as an aid in interventional cardiology training.”, Minimally Invasive Therapy & Allied Technologies 10, no. 2 (2001): 75-82.
7. Takashima, Kazuto, Shotaro Tsuzuki, Atomu Ooike, Kiyoshi Yoshinaka, Kaihong Yu, Makoto Ohta, and Koji Mori. "Numerical analysis and experimental observation of guidewire motion in a blood vessel model." Medical engineering & physics 36, no. 12 (2014): 1672-1683.
8. Markus Kukuk, “A Model-Based Approach to Intra operative Guidance of Flexible Endoscopy”, PhD thesis, Princeton, 2002.
9. Takashima, Kazuto, Atomu OIKE, Kiyoshi YOSHINAKA, Kaihong YU, Makoto OHTA, Koji MORI, and Naoki TOMA. "Evaluation of the effect of catheter on the guidewire motion in a blood vessel model by physical and numerical simulations." Journal of Biomechanical Science and Engineering 12, no. 4 (2017): 17-00181.
10. Valembois, R. E., Paul Fisette, and Jean-Claude Samin. “Comparison of various techniques for modelling flexible beams in multibody dynamics.” Nonlinear Dynamics 12, no. 4 (1997): 367-397.
11. Javier Garcia de Jalon, Eduardo Bayo, “Kinematic and Dynamic Simulation of Multibody Systems: The Real-Time challenge”, ISBN 0-387-94096-0, 440 pp. Springer-Verlag, New-York, 1994.
12. Preim, Bernhard, and Charl P. Botha. Visual Computing for Medicine: Theory, Algorithms, and Applications. Newnes, 2013, chapter 21, pp 154-156

13. Becherer, Nico, Jürgen Hesser, Ulrike Kornmesser, Dietmar Schranz, and Reinhard Männer. "Interactive physical simulation of catheter motion within mayor vessel structures and cavities for ASD/VSD treatment." In Medical Imaging, pp. 65090U-65090U. International Society for Optics and Photonics, 2007.
14. M. K. Chmarra, C. A. Grimbergen, and J. Dankelman, “Systems for tracking minimally invasive surgical instruments,” Minimally Invasive Therapy and Allied Technologies, vol. 16, no. 6, p. 328340, 2007.
15. J. Honye, D. J. Mahon, and J. M. Tobis, “Intravascular ultrasound imaging,” Trends in Cardiovascular Medicine, vol. 1, no. 7, pp. 305– 311, 1991.
16. C. M. Hillenbrand, D. R. Elgort, E. Y. Wong, A. Reykowski, F. K. Wacker, J. S. Lewin, and J. L. Duerk, “Active device tracking and highresolution intravascular mri using a novel catheter-based, opposedsolenoid phased array coil,” Magnetic resonance in medicine, vol. 51, no. 4, pp. 668–675, 2004.
17. O. Unal, F. R. Korosec, R. Frayne, C. M. Strother, and C. A. Mistretta, “A rapid 2d time-resolved variable-rate k-space sampling mr technique for passive catheter tracking during endovascular procedures,” Magnetic resonance in medicine, vol. 40, no. 3, pp. 356–362, 1998.

Appendix A: Phantom development

Introduction

Phantom models play an essential role in the medical field, both in research and in training. An accurate phantom model can provide better insight into instrument performance and help medical professionals to develop their skills in instrument handling. Moreover, phantoms can be used to evaluate the accuracy of the simulation models. In this thesis, the trajectory of guidewires and catheters were simulated and the amount of applied forces to the vascular walls were estimated. During our research, we endeavored to evaluate the simulation results by comparing them with experimental data, obtained from phantom models. Therefore, the objective of this appendix is to develop phantoms which can be used in our validation experiments, and the main criteria include accurate geometry, comparable material properties to that of coronary arteries walls, easy to use, cost-effective, and robust. Moreover, we prefer a transparent phantom which allows visual feedback for the tracking of the guidewire's tip.

In addition to the phantom development process, we will suggest an experimental set-up and tracking method which can be used to analyze the trajectory, and the amount of applied forces of the instruments inside the phantom models. The results of these experiments can be used to validate the accuracy of our developed model.

Method

Phantom development process

As explained in the introduction, our goal is to develop an accurate phantom which is easily reproducible. Therefore, we started with a simple 2D geometry using data extracted from [1], which includes branches with diameter between 2 and 8 mm, and bifurcations angels between 60 and 120 degree (Figure 1). VisiJet M3 Crystal was used to print the 2D model (P1).

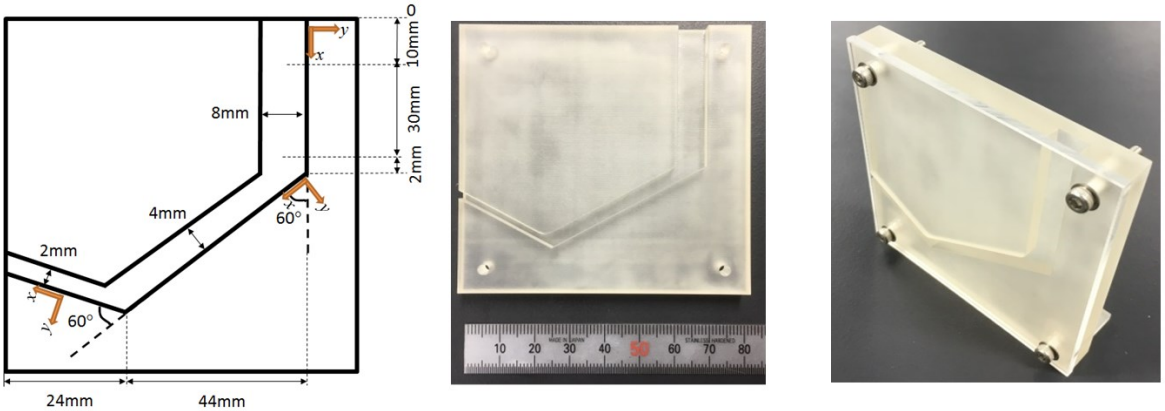

Figure 1: First phantom prototype (P1): a simple 2D geometry printed with VisiJet M3 Crystal

After a few preliminary tests in the P1 ohantom, the same material was used to print a more realistic 3D model of the right coronary artey (RCA) (Figure 2). For this phantom (P2), data

regarding the centerline and diameter of the RCA were extracted from CT scans of the patients' vascular geometry [2]. The merit of using this model is that it is relatively simple, cheap, and accessible. Therefore, it is possible to have a geometrically accurate model for any vascular geometry used in the simulation. The disadvantage of this model is that the friction coefficient and modulus of elasticity differ greatly from a real coronary artery.

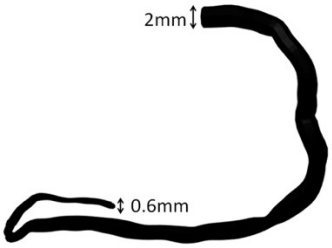

(a)

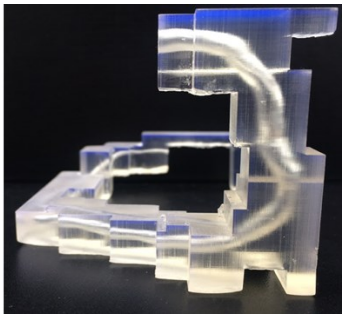

(b)

Figure 2: a) RCA geometry, and b) the 3D printed phantom prototype with actual size (P2)

There are several materials currently used in literature in order to produce a phantom with properties comparable with vascular walls; most notably gelatin, silicon, and polyvinyl alcohol hydrogel (PVA-H). Relevant mechanical properties of each of the three proposed materials and of the coronary artery were obtained from literature and are summarized in Table.1.

Table 1: Material properties

Material	Friction coefficient (μ)		Mechanical loss coefficient tan(δ)	
Coronary artery	0.2<	[3]	~0.081-0.15	[4]
Silicon	0.4 -1.5	[5]	<~0.2	[6]
Gelatin 5%Wt	0.015 -0.035	[7]	~0.14	[8]
PVA-H 5%Wt	0.1-0.2	[5]	~0.050	[5]
PVA-H 10%Wt	0.1-0.2	[5]	~0.052	[5]
PVA-H 15%Wt	0.1-0.2	[5]	~0.083	[5]
PVA-H 18%Wt	0.1-0.2	[5]	~0.097	[5]

Gelatin is the least complex material to work with, however, its properties do not match the coronary arteries (Table 1). Silicon has a comparatively large range of friction coefficients (see Table 1), caused by the large performance difference between old or new and wet or dry silicon. Although silicon is not as flexible as arteries, it is more flexible than our previous developed models. Therefore, we developed a phantom (P3) to examin the possibility of having a more complex geometry (being tortuous) with more flexible material.

A two-piece 3D printed geometry was used as mold (Figure 3a) in which each part was filled seperatly with silicon and hardener (10:1) (Shin-Etsu Chemical Co.Ltd, Japan). The filled molds were placed in a vaccum chamber with a negative pressure in order to make the casts bubble-free. Then, the castings were cured in an oven (Figure 3b). Finally, the molds

were removed, and the two pieces were glued together to release the completed casting (Figure 3c). Although the geometry of the phantom can be precise, silicon forms relatively stiff walls which do not resemble the properties of the coronary arteries.

(a) (b) (c)

Figure 3: a) 3D printed mold, b) castings in the oven, and c) the silicon phantom prototype (P3)

The next material suggusted in Table 1 is PVA-H in which offers both favorable friction condition and desired flexibility compared to other materials; these properties of PVA-H are controlable by changing the weight percent (wt%) of PVA grains and a number of freezing-thaw cycles. Consequently, we used PVA-H, as a final model, to mimic the right coronary artery wall.

As we explained in the introduction, our intention in creating a phantom model was to validate the simulated trajectory of the guidewire and catheter. In order to get visual feedback during the movement of the instrument inside the phantom, the transparency of the phantom is important. Based on the literature (e.g., [9]), we found out that PVA-H becomes transparent by making a mixture of 80 % dimethyl sulfoxide (DMSO) and 20 % deionized water, instead of using 100 wt% deionized water as a solute.

Figure 4 shows two different phantoms of the RCA, which have been made in the colaboration with Takashima lab in Japan. The first model (Figure 4a, P4) has an identical geometry as the RCA, but there are some disadvanteges such as difficulty in fixating the phantom in the exact orientation. Therefore, the idea of box-model, i.e., extruding the same geometry inside a cuboid shape, was emerged to be a convenient option (Figure 4b, P5).

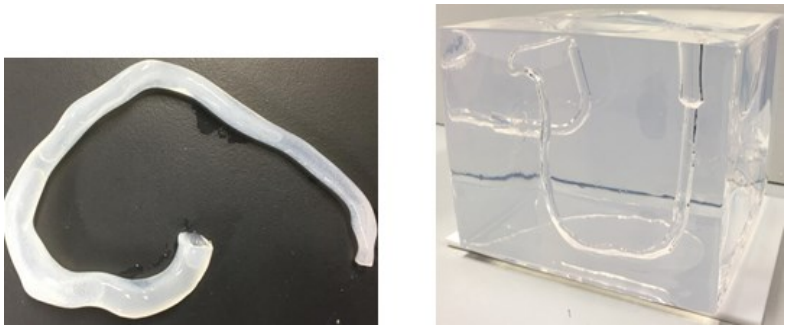

(a) (b)

Figure 4: The RCA phantom with a) 17 wt% PVA concentration without DSMO, b) 12 wt% PVA concentration with DSMO

Figure 5 shows a PVA-H box-model which was made based on the method explained in [9] but with 12 wt% PVA concentration with DSMO in order to test the sensitivity of the flexibility. For this phantom, first a 3D printed PVA coronary artery was created and suspended in a box (Figure 5a); PVA is commonly used as a water solvable support structure for 3D-printing. The 3D print artery was protected by a boundary layer of silicone coating to limit the dissolving in the PVA-H. Then, the box was filled with the PVA-H and DSMO mixture. A single 24-hour freeze-thaw cycle was applied, and then the PVA artery had dissolved completely, resulting in an accurate vessel geometry (Figure 5b).

(a) (b)

Figure 5: The right coronary artery (RCA) a) the 3D printed PVA (printer: Ultimaker 3, Ultimaker inc., Geldermalsen, The Netherlands), b) box model of 6 wt% PVA concentration with DSMO

Tracking set-up

As explained previously, the main objective of developing phantoms was to evaluate the simulation results by comparing them with experimental data, performed on phantom models. Therefore, we designed an experimental set-up in order to track the guidewire movement inside the developed phantom.

A box model of the RCA made of PVA-H was used for the validation experiments (see Figure 4b). In order to record the trajectory of the guidewire during the experiment, three cameras (15 frames per second, 1920 × 1080 screen resolution) were positioned on three sides of the model. In addition, load cells (Kyowa Electronic Instruments Co., Ltd.) with an operating range of 10N were placed under the phantom model to measure the applied forces downward (in z-direction) to the phantom's wall. The motion, which could be translational and rotational and its pattern could change depending on the vascular geometry, was applied by a linear stage to the proximal side of the guidewire. In our experiments, the speed of the translational and rotational motion were 2 mm/s and 10 deg/s, respectively. The motion pattern could change depending on the vascular geometry.

Since the diameter of RCA ranges from less than 1 to 3 mm along the length, the use of 0.014-inch guidewires (0.36 mm) in combination with 5- or 6-Fr (approximately 2 mm) catheters were recommended in real intervention to not limit the coronary circulation [10]. Therefore, we used the same size guidewires in both simulation and experiments.

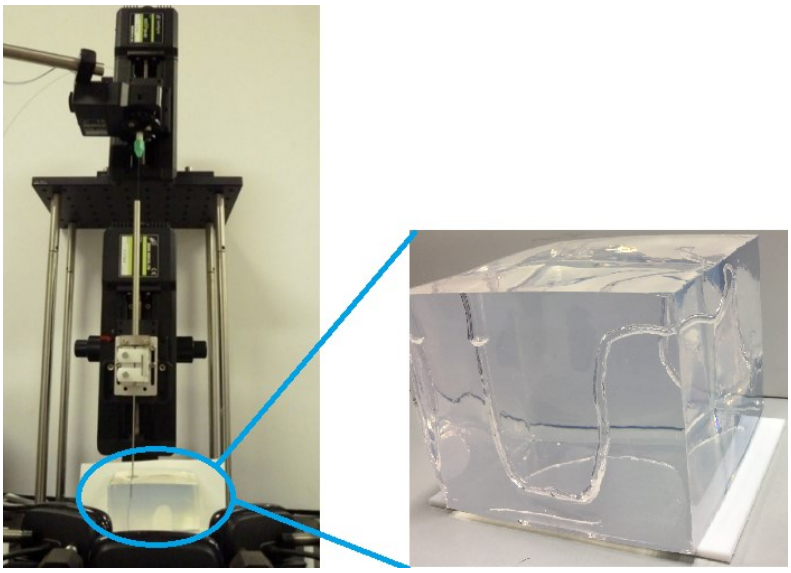

(a) (b)

Figure 6: a) Experiment setup which consists of a two-axis automatic stage (Sigma Koki Co., Ltd.,SGSP20-85(X), SGSP-40YAW) to insert the instrument into the phantom, b) box model of the RCA

Results

Table 2 shows a list of developed phantoms and achieved properties. Based on this information, we selected the P5 phantom which was made of a mixture of PVA-H and DSMO, and fulfilled most of our criteria.

Table 2: Phantom properties

Property / Phantom	Accurate geometry	Material properties	Simplicity	Transparent
P1	−	−	+	+
P2	+	−	+	+
P3	−	−	–+	–+
P4	+	+	−	–+
P5	+	+	–+	+

Figure 7 shows the process of extracting the position of guidewire's tip using the images acquired by the cameras. The image processing was done in collaboration with Takashima lab and detail information can be find in [11].

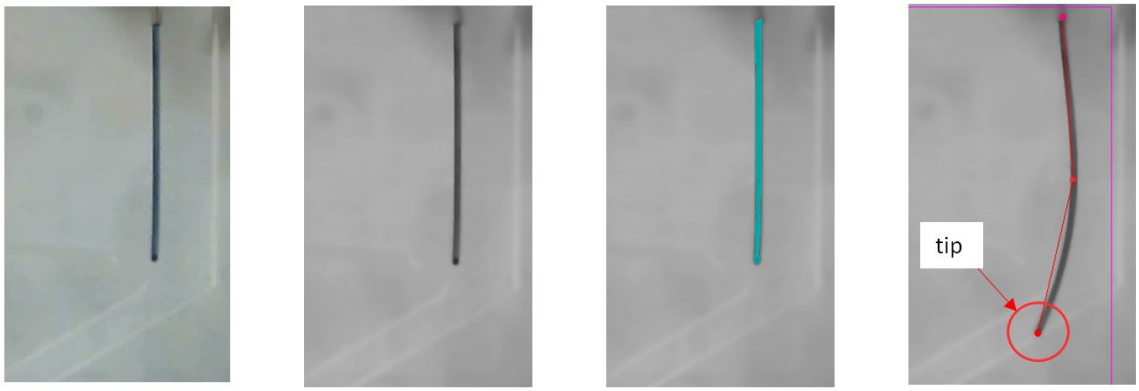

Figure 7: The process of tracking the tip of a guidewire in the images taken by the cameras

At the end, to examine the applicability of our developed phantom as well as the tracking set-up, we performed a few experiments and compared the outcomes with the simulation results. As an example, Figure 8 shows the tip trajectories of the two guidewires with different stiffness in the RCA artery, both in the simulation and the experiments. These results show how the flexibility of a guidewire impacts its behavior during advancement: higher flexibility, more fluctuations. Moreover, the simulation results show the trajectory of the stiffer guidewire deviated more from the experiments, and it can be explained by the fact that we used a discretized model of the guidewires in the simulation; when the guidewire is more stiff, the segments have to be smaller to be able to model the behavior more precisely [Chapter 5].

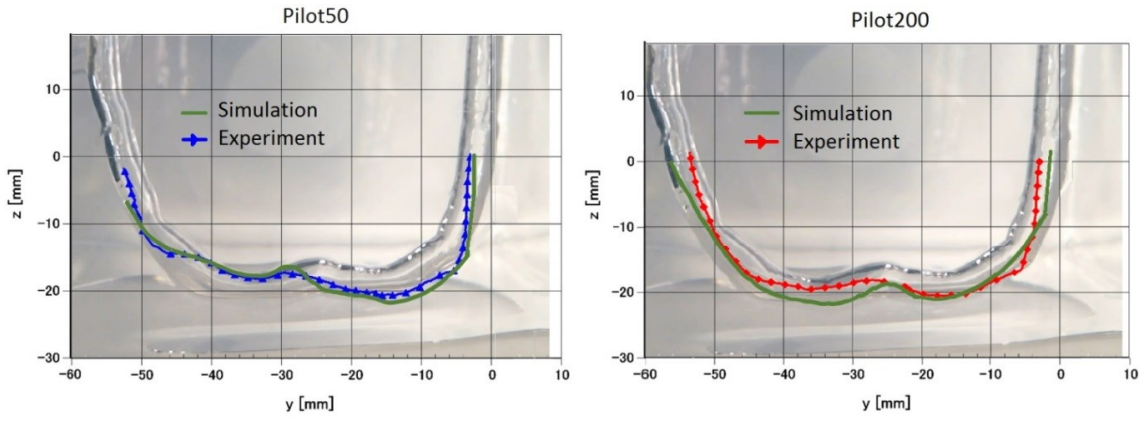

(a) (b)

Figure 8: Comparing the tip trajectory of two guidewires with curved tip inside the RCA: a) Pilot50, b) Pilot200

In the experimental set-up, the force sensors measure the amount of applied forces in z-direction. Figure 9 compares the total amount of applied forces to the artery's wall via each guidewire, in the simulation and validation experiments, while the guidewires were inserted into the RCA. The results show that as the stiffness of the guidewire increases, the guidewire applies more forces to the vascular wall. The differences between the experiments (Figure 9a) and simulations (Figure 9b) are mainly due to the force sensors used in the experiments; we used 5 and 10 N load cells for Pilot50 and Pilot200, respectively, while the amount of applied forces are in the range of mN.

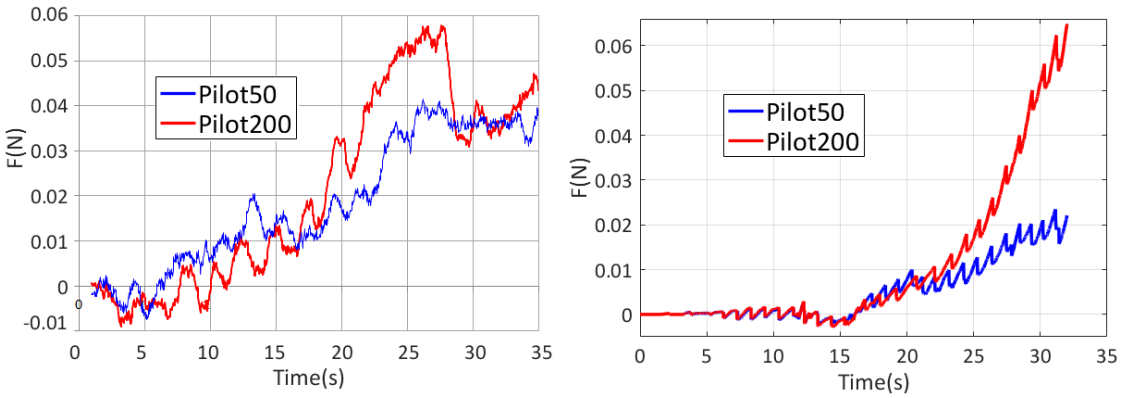

(a) (b)

Figure 9: Comparing the total amount of force applied by Pilot200 and Pilot50: a) experiment b) simulation

Discussion

We presented an overview of the developed phantoms. The phantoms consisted of different materials and were used in validation studies of the simulation model. Considering our design criteria, e.g., similar mechanical properties to vascular walls and being transparent for the purpose of video tracking, the phantom made of PVA-H and DSMO mixture was chosen to be used in our validation experiments.

Moreover, the preliminary results of the validation experiments were discussed. In the experiments, we used a linear stage to insert the guidewire into the phantom with fix speed motions. Although the simulation model is readily adoptable to either motion input or force input, the experimental-setup needs to be improved in a way to be able to apply forces instead of motion.

Reference

1. Clogenson, H. C. M. "MRI-Compatible Endovascular Instruments: Improved Maneuverability during Navigation." (2014).
2. Schaap, Michiel, Coert T. Metz, Theo van Walsum, Alina G. van der Giessen, Annick C. Weustink, Nico R. Mollet, Christian Bauer et al. "Standardized evaluation methodology and reference database for evaluating coronary artery centerline extraction algorithms." Medical image analysis 13, no. 5 (2009): 701-714.
3. K. Takashima, R. Shimomura, T. Kitou, H. Terada, K. Yoshinaka, and K. Ikeuchi, “Contact and friction between catheter and blood vessel,” Tribology International, vol. 40, no. 2, pp. 319–328, 2007.
4. H. E. Burton, J. M. Freij, and D. M. Espino, “Dynamic viscoelasticity and surface properties of porcine left anterior descending coronary arteries,” Cardiovascular engineering and technology, vol. 8, no. 1, pp. 41–56, 2017.
5. M. Ohta, A. Handa, H. Iwata, D. A. Rfenacht, and S. Tsutsumi, “Poly-vinyl alcohol hydrogel vascular models for in vitro aneurysm simulations: The key to low friction surfaces,” Technology and Health Care, vol. 12, no. 3, pp. 225–233, 2004.
6. Y.-b. WANG, Z.-x. HUANG, and L.-m. ZHANG, “Damping properties of silicone rubber/polyacrylate sequential interpenetrating networks,” Transactions of Nonferrous Metals Society of China, vol. 16, pp. s517–s520, 2006.
7. J. e. a. Winter, “The material properties of gelatin gels,” 1975.
8. J. Eysturskar, “Mechanical properties of gelatin gels; effect of molecular weight and molecular weight distribution,” Ph.D. dissertation, Norwegian University of Science and Technology, 2010.
9. YU, ChangHo, Hiroyuki KOSUKEGAWA, Keisuke MAMADA, Kanju KUROKI, Kazuto TAKASHIMA, Kiyoshi YOSHINAKA, and Makoto OHTA. "Development of an in vitro tracking system with poly (vinyl alcohol) hydrogel for catheter motion." Journal of Biomechanical Science and Engineering 5, no. 1 (2010): 11-17.
10. Schneider, Peter A. Endovascular skills: guidewire and catheter skills for endovascular surgery. New York, NY, USA: Informa Healthcare, 2009.
11. Takashima, Kazuto, Shotaro Tsuzuki, Atomu Ooike, Kiyoshi Yoshinaka, Kaihong Yu, Makoto Ohta, and Koji Mori. "Numerical analysis and experimental observation of guidewire motion in a blood vessel model." Medical engineering & physics 36, no. 12 (2014): 1672-1683.

Curriculum Vitae

Hoda Sharei-Amarghan

19 March 1986	Born in Mashhad, Iran.

Related experience

2014–2018	PhD candidate Department of biomechanical engineering, Delft university of technology, Delft, The Netherlands.
Nov–Dec 2016	Visiting researcher Kyushu Institute of Technology, Kitakyushu, Japan
Feb–March 2015	Visiting researcher Philips, Eindhoven, The Netherland
2012–2014:	Researcher Department of biomedical engineering, Liege university, Belgium
2009–2012:	Master of science Department of electrical and computer engineering Shiraz University, Shiraz, Iran
2008–2009:	Medical technology advisor Avicenna hospital, Shiraz, Iran.
2004–2008:	Bachelor of science Department of biomedical engineering Amirkabir University of Iran, Tehran

List of Publications and awards

- **Hoda Sharei**, Ronald Stoute, John J. van den Dobbelsteen, Maria Siebes, and Jenny Dankelman. “Data Communication Pathway for Sensing Guidewire at Proximal Side: A Review.” Journal of Medical Devices 11, no. 2 (2017): 024501.

- **Hoda Sharei**, Tanja Alderliesten, John J. van den Dobbelsteen, Jenny Dankelman, "Navigation of guidewires and catheters in the body during intervention procedures: a review of computer-based models," J. Med. Imag. 5(1), 010902 (2018), doi: 10.1117/1.JMI.5.1.010902.

- **Hoda Sharei**, Jeroen Kieft, Kazuto Takashima, Norihiro Hayashida, John J. van den Dobbelsteen, Jenny Dankelman, “A Multi-body Dynamic Model to Study the Translational motion of Guidewires based on their Mechanical Properties”, submitted.

- **Hoda Sharei**, Kazuto Takashima, John J. van den Dobbelsteen, Jenny Dankelman. “Interactive Manipulation of Guidewires and Catheters inside the Vascular System during Intervention”, submitted.

- **Hoda Sharei**, John J. van den Dobbelsteen, Jenny Dankelman. “Overview of State of the art: Guidewire's Proximal Connectors”, 5th Dutch Bio-Medical Engineering Conference, Egmond aan Zee, The Netherlands (2015).

- **Hoda Sharei**, John J. van den Dobbelsteen, Jenny Dankelman. “Guidewire Construction and its Characteristics for Use in Interventional Procedure: A Review of Contemporary Technology”, 27th International Conference of the Society for Medical innovation and Technology (SMIT), Brno, Czech Republic (2015).

- **Hoda Sharei**, John J. van den Dobbelsteen, Jenny Dankelman. “Guidewire Model Based on its Mechanical Properties”, 28th International Conference of the Society for Medical innovation and Technology (SMIT), Delft, The Netherlands (2016).

- **Hoda Sharei**, John J. van den Dobbelsteen, Jenny Dankelman. “3D Model of guidewire motion based on its mechanical properties”, 6th Dutch Bio-Medical Engineering Conference, Egmond aan Zee, The Netherlands (2017).

- **Hoda Sharei**, John J. van den Dobbelsteen, Jenny Dankelman. "Modelling the behavior of guidewire inside the vascular system and comparing the trajectory and the applied forces", Design of Medical Device Conference, Eindhoven, the Netherlands (2017).

- **Hoda Sharei**, John J. van den Dobbelsteen, Jenny Dankelman. "Prediction of Guidewire Trajectory inside the Vascular System: 3D Computer based Model", 29th International Conference of the Society for Medical innovation and Technology (SMIT), Turin, Italy (2017).

- **Hoda Sharei**, Kazuto Takashima, John J. van den Dobbelsteen, Jenny Dankelman. "Modelling and analysis of guidewire motion to evaluate the effect of bending stiffness", submitted.

- **Hoda Sharei**, John J. van den Dobbelsteen, Jenny Dankelman. "Modelling the behavior of guidewires: effect of angled-tip and rotation", 30th International Conference of the Society for Medical innovation and Technology (SMIT), Seoul, South Korea (2018).

- **Best poster award** (150 euro)- 3ME PhD day- Delft university of Technology.

- **Travel award** (700 dollars)- Smit2018- Seoul, South Korea.

Acknowledgements

"Our life is a constant journey, from birth to death. The landscape changes, the people change, our needs change, but the train keeps moving. Life is the train, not the station", Paulo Coelho.

The four years I spent completing my PhD was one of the most challenging stations, and it would have been impossible to pass without a number of people who accompanied me on this journey. Therefore, before moving to the next station, I want to thank them.

Firstly, I would like to thank my promotors **Jenny Dankelman** and **John van Dobbelsteen**. Jenny, thank you for your trust in me and for giving me the opportunity to be a part of your team. Thank you for your not only scientific but also emotional support during the last four years; there was always a sense of relief after talking with you. John, thank you for your guidance as I worked toward my PhD. Your broad knowledge and your out-of-the-box thinking were always admirable.

Secondly, thanks go out to the reading committee, for investing their time in reading and evaluating this thesis.

I am very thankful for the opportunities I received as a guest researcher. Working for two months at Philips in Eindhoven was a great opportunity to get to know the industrial environment; I thank **Ronald Dekker** for hosting me in his group. At the same time, I would like to thank **Ronald Status**, my project-mate, not only for being my guide at Philips but also for helping me to start my PhD, reading my draft, and giving me confidence with his encouraging words. Thank you, Ronald, for trusting me to present your work at the EMBC conference when I had just started my PhD; your trust made me feel more confident. Moreover, I had the pleasure of working in the Takashima lab at the Kyushu Institute of Technology, Japan, for two months. I would like to thank **Kazuto Takashima** and his students for their hospitality. I would also like to thank **Theo van Walsum** from Erasmus MC for supporting me with patient data.

Besides all the scientific help, doing a PhD is not possible without wonderful friends and colleagues to have fun with during coffee and lunch breaks. My officemates, **Ronald**, **Xavier**, **Paulos**, **Federico**, and **Bram**, thank you all for creating a nice office atmosphere! I learned a lot from each one of you and enjoyed every second of being in the office with you guys. I missed you a great deal when you left one by one, and I wish you all the best. I also thank **Dick Plettenburg** just because of his smiling face and warm "good morning" every day when I passed his office. **Marco,** thank you for spending quality time on reading my first paper, it was a great help. **Germa en Mats,** hartelijk bedankt voor het vertalen van mijn samenvatting in het Nederlands.

Moving to MISIT lab had the advantage of allowing me not only to practice my Dutch but also to make new friends. **John, Tonke, Roos, Jullie, Marit, Nick, Arjo, Arjan, Linda, Tim, Jan**, heel veel bedankt voor jullie geduld en steun. Ik heb heel veel plezier gehad in MISIT lab in de laatste jaar van mijn PhD. Mijn speciale dank gaat naar **Tonke** – Lieve Tonke, ik kan niet je genoeg bedanken voor jouw open, lief en behulpzaam houding, bedankt voor welkomen me in MISIT lab.

And of course my life outside the university was filled with the love and support of my friends and family, whom I would like to name and acknowledge here. Firstly, I would like to thank **Janny** – lieve Janny, je was niet alleen mijn Nederlandse docent maar ook een echte vriendin! Ik kan nooit jouw genoeg bedanken voor alle liefde en steun die heb ik altijd van jouw gekregen zowel voor mijn taalvaardigheid als in mijn gewoon leven, hartelijk bedankt! Next, I would like to thank my special friends who were with me from the beginning of my PhD journey (and even before), and who never hesitate to offer me any help I need: **Tricia**, I had so much fun with you in our day-out trips and in our spontaneous trip to Sardinia – thank you for reading my paper and correcting my English! **Somaye**, my smiley face friend, thank you for reminding me how much more appealing is the life with flowers! **Farahnaz**, my beautiful friend, it is always enjoyable to have a break with you, and to chat and share and listen to each other's thoughts and forget about time! **Ahmad**, thank you for always being up for any adventure, either skydiving or just having a dinner in a noisy bar while you really wish for a quiet place!

Many thanks to all my family in Iran, specially my dear sister, **Zari**, thank you simply for being in my life! Thank you for all the messages and calls from so far away, and for trying hard to cheer me up any time I needed it! Thank you for your lifelong support!

And the last one, **Bijan**, the love of my life: I can't describe your love and support during the last 14 years, and especially during the last 4 years! Without your words of encouragement, your confidence in me, and your efforts to make me relax, it would have been impossible to finish this book – thank you for moving from Maastricht to Delft, in the middle of your own PhD, just to make me feel more comfortable in my new job… thank you for your undying love and devotion to me.

Hoda Sharei
Delft, January 2019